An analysis of the dynamic performance of D.C. machines with thyristor assisted commutation

Moore, J. R.

An Analysis of the Dynamic Performance

of

D.C. Machines

with thyristor assisted commutation

by

J.R. Moore, B.Sc.

Thesis submitted for the degree of Doctor
of Philosophy in the Faculty of Science
in the University of Durham

May 1972

Abstract

The thesis presents a method of analysis of direct current machines using thyristor assisted commutation. The method is based upon the General Machine Theory and the formulation of voltage and torque equations from the theory is shown to be successful. These equations have predicted the performance of the machine over a wide range of operating conditions. A computer programme has been developed to deal with the most complex operating conditions and, by suitable simplifications, the programme is readily adaptable to compute steady state characteristics.

A subsidary theme of the thesis is to show how the output of thyristor assisted machines may be controlled by an electronic method of rocking the brushes. The method is simply demonstrated on no load or light load conditions but loading effects produce some limitations. Sufficient experimental results are given to illustrate the method.

Table of Contents

List of Symbols and Abbreviations

(* denotes that letter is usually a subscript)

Roman Alphabet

a	*	main armature coil during commutation
A	*	armature coil during slip ring period
A		unit of current, ampere
AT		ampere turn
b		brush arc
B		flux density, Tesla
c	*	shorted armature coil during commutation
d		direct axis of machine
e		base of natural logarithms
f	*	field winding
H		unit of inductance, henry
i	*	interpole winding
ia	*	series connection of interpole and main armature windings
iA	*	series connection of interpole and armature windings
I		current
J		inertia
K		constant
l		length
L		self inductance
M		mutual inductance
m		unit of length, metre
N		unit of force, newton
p		differential operator (d/dt)
P		power
q		quadrature axis of machine
r		radian
R		resistance

s	segment arc
S	unit of time, second
t	time
T	torque
v	velocity
V	unit of voltage, volt
V	voltage
x	ratio

Greek Alphabet

β	beta	coefficent in differential equation
γ	gamma	damping factor
δ	delta	commutation angle
θ	theta	angle between armature and neutral axes
φ	phi	angle at which commutation starts
ψ	psi	voltage integral
ω	omega	rotational speed, radians per second

Abbreviations

a.c.	alternating current
d.a.c.	diode assisted commutation
d.c.	direct current
e.b.s.	electronic brush shift
f.s.d.	full scale deflection
p.u.	per unit
t.a.c.	thyristor assisted commutation

Other symbols and abbreviations as defined in the text.

Chapter 1 Introduction

1.1 Object of Thesis

The general object of the work was to consider methods of analysing the performance of direct current machines with thyristor assisted commutation (t.a.c. machines). Eventually, the method of analysis should enable the characteristics of a machine at the design stage to be calculated and corrections made to obtain the best performance. For standard d.c. machines many years of experience have produced well defined procedures which are based upon essentially steady state methods. For conventional machines this is valid because the mmfs and fluxes are relatively fixed. T.A.C. machines have a wide commutating zone and the mmfs and fluxes are variable over a wide range. Consequently, a dynamic type of analysis was thought to be more applicable to the t.a.c. machine and a method based upon the general machine theory was used. Such a method depends upon the knowledge of inductance parameters and there are considerable problems in calculating them.

To test the validity of the method of analysis, the inductances were measured on an experimental machine. If the measured values gave accurate predictions of the performance of the machine when used with the general theory, then a further stage in the analysis is to consider how they may be calculated from design criteria. Until the validity of the method has been tested, there is little point in attempting the calculations. During the work, the analysis and experimental work showed that the speed of the motor could oscillate under certain operating conditions. Although it is more important to be able to calculate the standard characteristics such as speed torque, the prediction of such phenomena provided a very good test.

The main theme of the thesis is to present a method of analysis of the experimental machine based upon the general machine theory. The formulation of equations from the general theory has been successful and these equations have predicted the the performance of the machine over a wide range of operating conditions. A computer programme has been developed to deal with the most complex operating conditions and by suitable simplifications, the programme is readily adaptable to compute the steady state characteristics.

A subsidary theme is to show how the output of t.a.c. machines may be controlled by an electronic method of rocking the brushes. The method is simply demonstrated under light or no load conditions but loading effects produce some limitations. The concept is interesting and some experimental results are given but the method has by no means been investigated fully.

1.2 Historical Background

Early analyses and practical experience had shown that commutation problems were responsible for many of the difficulties found in d.c. machines. Improvements in the form of interpoles and compensating windings had helped but significant improvements could only be achieved by a removal or modification of the commutator and commutation process.

With the introduction of semiconductors many papers were published on the control of d.c. machines by using these devices. In general, these methods incorporated some form of armature voltage control; they did not remove or modify the commutator. Ideas of using thyristors and diodes to assist the commutation process were published [1.1] and it was thought that the switched winding or armature would be better placed on the stator with the field winding

on the rotor. In 1964, a practical design for a d.c. motor with assisted commutation was described by Bates, Sridhar and Tustin [1.2] and the results of tests on a small machine were given a year or so later [1.3]. Bates et al. showed that once the commutation process was no longer dependent upon the carbon brush for the successful reversal of current in the armature, it was possible to get a much improved performance from the machine. This additional performance for a given frame size well justified the cost of the extra equipment. Recent machines have been built up to power levels of 400 hp [1.4].

Other schemes also exist for assisting the commutation process. Andrews [1.5] suggested the use of a laminated brush consisting of four or more slices insulated from each other. A thyristor was connected to each slice and, by suitable arrangements, the current can be transferred from slice to slice without the slice actually making or breaking contact with a commutator bar while it is still carrying current. Other methods usually involve turning the machine inside out, putting the field system on the rotor and the armature winding around the stator [1.6].

Each method offers advantages over the conventional machine. In general, these new methods remove some of the more restrictive commutation problems and allow more power to be obtained from a given frame size. The disadvantages are usually those of additional equipment with their extra cost.

1.3 Theory of Operation of T.A.C. Machines

The t.a.c. machine uses a conventional armature winding but instead of a single commutator, there are two part commutators. Each part commutator has only eight or so segments and the tappings from the armature winding are connected to alternate segments. Four

brushes feed current into the armature and are arranged in two pairs. Each pair is connected in parallel and to the thyristor. The thyristor is triggered by a contact operated from a synchronising ring on the shaft. Figure 1.1 shows the schematic arrangement.

Commutation of the current in the armature winding takes place as follows. Assume initially that thyristor T2 is conducting and that the current is flowing into the armature via brush b22 and segment S21 as shown in Figure 1.1. When brush b11 is just fully on S12, T1 is fired into conduction. Commutation now proceeds under the action of the interpole induced voltage in the closed circuit formed by T1, b11, S12, the coil C12, S21, b22 and T2. The polarity of the voltage is such that the current through T2 tends to reduce; that through T1 to increase. As long as the current through T2 is reduced to zero before b22 leaves S21, the brush will leave the segment carrying no current and there must be no sparking. All the current now enters through T1. As the brushes move, b12 will take over the current from b11 and eventually, b21 will just be on S23. The commutation process repeats as T2 is fired. This time T1 goes 'off' while T2 comes 'on'. The process repeats each time the leading brushes are just completely on the beginning of an active segment.

Three points are worthy of note. Firstly, as long as the current through a trailing brush is brought to zero before the brush leaves the segment, no sparking will occur. This implies that there is a minimum value for the interpolar induced flux but no maximum. There appears to be no reason why the interpole cannot be made much stronger than necessary so that commutation will be complete well before the brush reaches the end of the segment. While this would give the machine a degree of protection against shock loadings, it is possible for the t.a.c. motor speed to oscillate continuously when using an

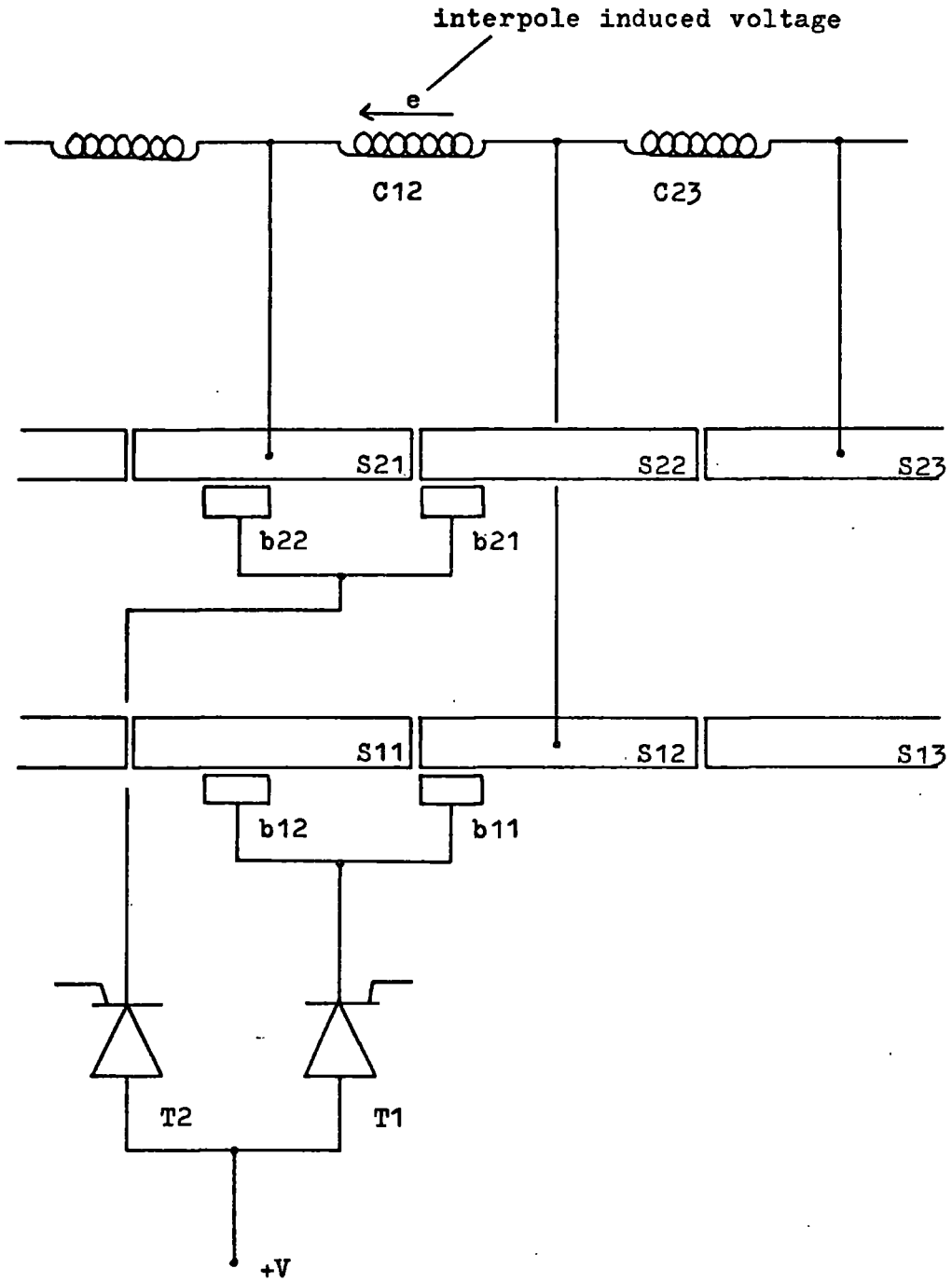

Fig. 1.1 Schematic Diagram of Thyristor assisted Commutation

overwound, series connected interpole winding. This oscillatory nature is shown and discussed in later chapters.

The second point is that at no time does the brush bring about commutation. They act only as a sliding contact between the armature winding and the external circuit. The switching of currents is done entirely by the thyristors. The firing of a thyristor is always carried out when the brush is sitting completely on a segment - never when it is bridging two segments. This eliminates the possibility of uncertain contact between the brush and segment.

The third point follows from the second. As commutation is not started until a brush is completely on a segment and must be finished before the brush on the other part commutator leaves the segment, commutation takes place in discrete intervals and not continuously as in conventional d.c. machines. The interval is determined by the brush and segment geometry and by the strength of the interpole flux. Between these intervals there is no commutation and the machine acts as a slip ring machine. T.A.C. machines, therefore, operate with two zones. A commutation zone is followed by the slip ring zone and the relative times of each zone obviously depend upon the time of commutation.

1.4 Introduction to the Thesis

The use of conventional machine analysis allows the steady state characteristics of a machine to be easily calculated but does not generally permit detailed information to be obtained under changing or transient conditions. For standard machines, the mmfs and fluxes are relatively fixed owing to the small commutating zone of about $\pm 2^{\circ}$. The commutation zone in t.a.c. machines is not small (i.e. 32° in the experimental machine) and the commutation process

is not continuous. At the end of each zone there is a large change in the armature axis position and so the mmfs and fluxes are continually moving. The method of analysis was based upon a general type in which the dynamics are included from the start, Such a method is the general machine theory and the starting point for the analysis is the voltage and torque equations for four mutually coupled coils. In chapter 2, these relationships are formulated into dynamic equations which take account of the differences between conventional and t.a.c. machines. These differences include the two zones of operation, the large angles over which the armature axis can move and the presence of thyristors in the armature circuit.

The method of analysis requires the variation of the inductances with rotor angle to be known and while these variations are easy to measure it would be difficult to calculate them. If, however, by using the measured values, the characteristics can be accurately predicted then the validity of the method will be confirmed. The next stage in the analysis would be to consider methods of calculating the inductances from the physical and electrical parameters of the machine. It is first necessary to prove the method and the inductances were measured on a small experimental machine. The results are given in chapter 3 and the method of measurement in Appendix A.

Using the equations and the variation of inductance, the analysis is continued in two ways. First, a formal method using differential equations is used to show the form of behaviour under various operating conditions and this method is shown in chapter 4. The second method uses the equations as the foundation for a computer programme to accurately predict the performance of the machine. The computer programme and detailed comparisons between the predicted and actual behaviour of the t.a.c. machine are given in chapter 5. The

computer programme is fully described in Appendix B. In both the formal and computer analyses and also in the experimental machine, the steady state characteristics of the series connected interpole motor would degenerate into a continuous speed and current oscillation under certain field current and load torque conditions. Although such oscillations are of little practical use, their accurate prediction enables the analysis to be used with greater confidence. The oscillations and methods of prevention are discussed in chapter 6.

Since commutation is no longer performed by the brushes but rather controlled by the thyristors, the commutation zone is not limited to a small zone about the interpolar axis. By using a small commutating zone, the average position of the armature axis may be adjusted and an effect obtained which is similar to rocking the brushes in a conventional d.c. machine. To move the armature axis, a control unit was constructed which electronically rocked the brushes by delaying the thyristor firing pulses. The concept is explained in chapter 7 and the method amply illustrated by the machine's performance on light and no loads. Loading effects create some further limitations and widespread application of the method may not be possible. The results show the scope of the method but it has by no means been fully investigated.

Practical details of the machine and the electrical and electronic circuits are to be found in chapter 8 with further detail on certain points given in Appendix C. ~~Future work using the experimental machine to investigate flux pulsations is indicated in chapter 9 and~~ The thesis is concluded by the comments and recommendations which are given, along with the general conclusion, in chapter ~~10~~ 9.

Chapter 2 Derivation of Machine Equations

2.1 The General Machine Theory

The d.c. machine may be represented by four windings two of which are on the stator and two on the rotor. The stator windings consist of the field and interpole windings which lie along the direct and quadrature axes respectively. The rotor windings are part of one complete coil but it is convenient to separate the winding into two parts. The current flowing in those turns which are shorted by the brushes will not, in general, be the same as in the rest of the armature. By the action of the commutator the axis of the short circuited turns is constrained to lie along the d axis. Figure 2.1 shows the position of the windings; the axis of the shorted turns being displaced by an angle (θ) from the d axis.

In the t.a.c. machine there is a period when none of the armature coils is shorted by the brushes and thyristors. During this period the machine operates as a slip ring machine - there being no commutation of current in the armature winding. The coils 'a' and 'c' of Figure 2.1 may be replaced by a single armature coil - coil 'A' - whose axis lies along the quadrature axis. It can be shown that there is a displacement of $\frac{1}{2}s^{o}$ between the axes of the two armature coils 'a' and 'A' with respect to the rotor shaft. (s^{o} is the commutator segment arc).

2.2 The Voltage Equation

The voltage equation for the four coils shown in Figure 2.1 may be written in the matrix form of

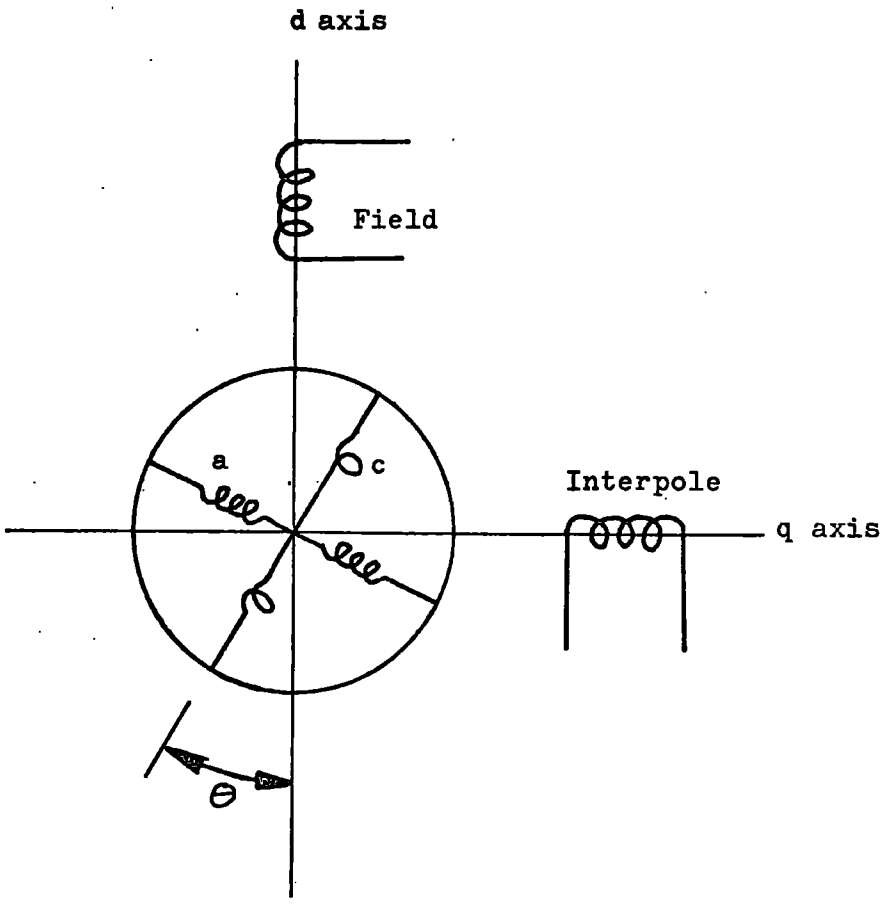

Fig. 2.1 Four Winding representation of a D.C. Machine

$$\begin{vmatrix} V_f \\ V_i \\ V_a \\ V_c \end{vmatrix} = \begin{vmatrix} R_f + pL_f & pM_{fi} & pM_{fa} & pM_{fc} \\ pM_{if} & R_i + pL_i & pM_{ia} & pM_{ic} \\ pM_{af} & pM_{ai} & R_a + pL_a & pM_{ac} \\ pM_{cf} & pM_{ci} & pM_{ca} & R_c + pL_c \end{vmatrix} \times \begin{vmatrix} I_f \\ I_i \\ I_a \\ I_c \end{vmatrix}$$

where p is the differential operator d/dt.

The general term $pM_{xy}.I_y$ may be expanded to obtain

$$pM_{xy}.I_y = M_{xy}.pI_y + I_y.pM_{xy}$$

which may be rewritten as

$$pM_{xy}.I_y = M_{xy}.pI_y + I_y.\omega.d(M_{xy})/d\theta$$

where ω is the rotational speed in radians per second.
To solve the above matrix equation, the value of $d(M_{xy})/d\theta$ is required. That is, the variation of M_{xy} with the angle θ must be obtained.

2.3 The Nature of the Inductances

The self inductance of each winding and the mutual inductance between pairs of windings were measured and the results are given in detail in Chapter 3. In this section, only the form of the inductances are indicated so that the derivation of the machine equations may be continued for the t.a.c. machine.

The stator self inductances were independent of rotor angle but dependent upon the coil current. All the inductances were affected by saturation and care must be taken to ensure that saturation effects

are included in the analysis. The rotor self inductances were dependent upon rotor angle at low currents but at rated field and interpole current the effects of rotor angle were negligable. The mutual inductances were very dependent upon rotor angle, the variation of inductance being of a sine or cosine function. Table 2.1 gives the form of the inductance waveforms, their values and derivitives around the commutating zone.

2.4 The Action of the Commutator

In a conventional machine the commutator limits the variation of θ to a small range $\pm\frac{1}{2}\delta$ about the position $\theta = 0^{\circ}$. δ is the angle of commutation and has a typical value of 5°. With this small angle ($\pm 2\frac{1}{2}^{\circ}$) any cosine function may be assumed to remain at its maximum value throughout commutation and, also, the mean value of any sine function to be zero. This assumption is not valid in the t.a.c. machine since the commutation angle is not small and, except in the special case of commutation taking all the available angle, the average armature axis position will not lie along the quadrature axis ($\theta = 0^{\circ}$).

To simplify the initial analysis the assumption that any cosine type of function will remain at its maximum value is used. This introduces a maximum error of 4% when commutation occurs very rapidly but under more normal conditions, the error is typically 1.5%. Sine functions are included as such and are not approximated to zero.

2.5 The Commutator and Slip Ring Voltage Equations

The voltage equation of section 2.2 may be expanded to give the commutator and slip ring voltage equations for the t.a.c. machine. For the commutation period, the voltage equation is

Inductance	Type of Waveform	Value around $\theta = 0^{\circ}$	Value of derivative around $\theta = 0^{\circ}$
Self			
L_f	--	$\hat{L}_f$	0
L_i	--	$\hat{L}_i$	0
L_a	--	$\hat{L}_a$	0
L_c	--	$\hat{L}_c$	0
L_A	--	$\hat{L}_A$	0
Mutual			
$M_{f.i}$	--	0	0
$M_{f.a}$	sine	$\hat{M}_{f.a}.\sin(\theta)$	$\hat{M}_{f.a}$
$M_{f.A}$	sine	$\hat{M}_{f.A}.\sin(\theta)$	$\hat{M}_{f.A}$
$M_{f.c}$	cosine	$\hat{M}_{f.c}$	$-\hat{M}_{f.c}.\sin(\theta)$
$M_{i.a}$	cosine	$\hat{M}_{i.a}$	$-\hat{M}_{i.a}.\sin(\theta)$
$M_{i.A}$	cosine	$\hat{M}_{i.A}$	$-\hat{M}_{i.A}.\sin(\theta)$
$M_{i.c}$	sine	$\hat{M}_{i.c}.\sin(\theta)$	$\hat{M}_{i.c}$
$M_{a.c}$	sine	$\hat{M}_{a.c}.\sin(2\theta)$	$2\hat{M}_{a.c}$

Table 2.1 Values of Inductances and Derivatives

$$
\begin{vmatrix} V_f \\ V_i \\ V_a \\ V_c \end{vmatrix} = \begin{vmatrix} R_f + \hat{L}_f \cdot p & - & -\hat{M}_{fa} \cdot \sin\theta \cdot p \; -\hat{M}_{fa} \cdot \omega & -\hat{M}_{fc} \cdot \sin\theta \cdot \omega \; \hat{M}_{fc} \cdot p \\ - & R_i + \hat{L}_i \cdot p & -\hat{M}_{ia} \cdot \sin\theta \cdot \omega \; \hat{M}_{ia} \cdot p & \hat{M}_{ic} \cdot \sin\theta \cdot p \; \hat{M}_{ic} \cdot \omega \\ -\hat{M}_{fa} \cdot \sin\theta \cdot p \; -\hat{M}_{fa} \cdot \omega & -\hat{M}_{ia} \cdot \sin\theta \cdot \omega \; \hat{M}_{ia} \cdot p & R_a + \hat{L}_a \cdot p & \hat{M}_{ac} \cdot \sin 2\theta \cdot p \; 2 \cdot \hat{M}_{ac} \cdot \omega \\ -\hat{M}_{fc} \cdot \sin\theta \cdot \omega \; \hat{M}_{fc} \cdot p & \hat{M}_{ic} \cdot \sin\theta \cdot p \; \hat{M}_{ic} \cdot \omega & \hat{M}_{ac} \cdot \sin 2\theta \cdot p \; 2 \cdot \hat{M}_{ac} \cdot \omega & R_c + \hat{L}_c \cdot p \end{vmatrix} \times \begin{vmatrix} I_f \\ I_i \\ I_a \\ I_c \end{vmatrix}
$$

where $\hat{M}_{xy}$ represents the maximum value of the inductance M_{xy}.
In t.a.c. machines, as in conventional d.c. machines, the interpole winding may be connected in series opposition to the armature winding and the voltage equation may be rewritten as

$$
\begin{vmatrix} V_f \\ V_{ia} \\ V_c \end{vmatrix} = \begin{vmatrix} R_f + \hat{L}_f \cdot p & -\hat{M}_{fa} \cdot \sin\theta \cdot p \; -\hat{M}_{fa} \cdot \omega & -\hat{M}_{fc} \cdot \sin\theta \cdot \omega \; \hat{M}_{fc} \cdot p \\ -\hat{M}_{fa} \cdot \sin\theta \cdot p \; -\hat{M}_{fa} \cdot \omega & R_i + p\hat{L}_i \; R_a + p\hat{L}_a \; -2 \cdot \hat{M}_{ia} \cdot p \; +2 \cdot \hat{M}_{ia} \cdot \sin\theta \cdot \omega & -\hat{M}_{ic} \cdot \sin\theta \cdot p \; -\hat{M}_{ic} \cdot \omega \; \hat{M}_{ac} \cdot \sin 2\theta \cdot p \; \hat{M}_{ac} \cdot \omega \\ -\hat{M}_{fc} \cdot \sin\theta \cdot \omega \; \hat{M}_{fc} \cdot p & -\hat{M}_{ic} \cdot \sin\theta \cdot p \; -\hat{M}_{ic} \cdot \omega + 2\hat{M}_{ac} \cdot \omega \; \hat{M}_{ac} \cdot \sin 2\theta \cdot p & R_c + \hat{L}_c \cdot p \end{vmatrix} \times \begin{vmatrix} I_f \\ I_{ia} \\ I_c \end{vmatrix}
$$

where V_{ia} is the voltage across the series connected interpole and armature windings and I_{ia} is the current through them.

During the slip ring period the short circuited coils become electrically part of the armature winding and the slip ring voltage equation, for series connected interpoles, is

$$\begin{vmatrix} V_f \\ V_{iA} \end{vmatrix} = \begin{vmatrix} R_f + \hat{L}_f \cdot p & -\hat{M}_{fA} \cdot \sin\theta \cdot p \\ & -\hat{M}_{fA} \cdot \omega \\ -\hat{M}_{fA} \cdot \sin\theta \cdot p & R_i + \hat{L}_i \cdot p \\ -\hat{M}_{fA} \cdot \omega & R_A + \hat{L}_A \cdot p \\ & -2\hat{M}_{iA} \cdot p \\ & 2\hat{M}_{iA} \cdot \sin\theta \cdot \omega \end{vmatrix} \times \begin{vmatrix} I_f \\ I_{iA} \end{vmatrix}$$

For series connected interpoles, the resistance and inductance of the armature and interpole windings may be denoted by R_{ia} and L_{ia} in the commutator equations and by R_{iA} and L_{iA} in the slip ring equations. Therefore

$$R_{ia} = R_i + R_a$$

and $$L_{ia} = L_i + L_a - 2M_{ia}$$

and similarly for R_{iA} and L_{iA}. Since $d(L_i)/dt$ and $d(L_a)/dt$ were found to be zero,

$$pL_{ia} \cdot I_{ia} = L_i \cdot pI_{ia} + L_a \cdot pI_{ia} - 2M_{ia} \cdot pI_{ia} + 2M_{ia} \cdot \omega \cdot \sin(\theta) \cdot I_{ia}$$

which is consistent with the voltage equations above.

2.6 Average Values

The voltages and currents in the machine obviously depend upon both the commutator and slip ring equations. The overall equation relating voltage and current is therefore lengthy and rather cumbersome. The above equations are correct for either instantaneous or average values of θ but if only the average values are required some simplification of the equations may be made. For example, the average value of the current in the short circuited armature winding is zero and so any term containing I_c will also be zero and may be deleted from the equations.

For average values only the following assumption was made. The mean value of a machine parameter is the sum of x times its commutator value and (1-x) times its slip ring value. x is defined as the ratio of the commutation time to the sum of the commutation and slip ring times.

2.7 Power and Torque Equations

The power input to a circuit containing resistance and self and mutual inductance is

$$v.i = i^2.r + i.p(L.i) + i.p(M.i_1)$$

which may be expanded to give

$$v.i = i^2.r + i^2.pL + L.i.pi + i.i_1.pM + i.M.pi_1$$

However,

$$d(\tfrac{1}{2}L.i^2) / dt = \tfrac{1}{2}i^2.pL + L.i.pi$$

so

$$v.i = i^2.r + p(\tfrac{1}{2}L.i^2) + \tfrac{1}{2}i^2.pL + i.i_1.pM + i.M.pi_1$$

If there is no rotary motion then pL = pM = 0 and all the power supplied to the circuit is either dissipated as heat or used to increase the energy stored in the self and mutual fields. If rotary motion does occur, then the powers associated with the terms pL and pM must provide the power for that motion. The power converted to mechanical power must therefore be

$$P = \tfrac{1}{2}\cdot i^2\cdot pL + i\cdot i_1\cdot pM$$

$$= \tfrac{1}{2}\cdot i^2\cdot\omega\ {}^{dL}/_{d\theta} + i\cdot i_1\cdot\omega\cdot\ {}^{dM}/_{d\theta}$$

From the previous voltage equations the power converted during the commutation period is

$$P_{comm} = -\hat{M}_{fa}\cdot\omega.I_f.I_{ia} + \hat{M}_{ia}\cdot\sin\theta\cdot\omega\cdot I_{ia}^2$$
$$-\hat{M}_{ic}\cdot\omega.I_c.I_{ia} + 2\hat{M}_{ac}\cdot\omega.I_c.I_{ia}$$

and this may be simplified to

$$P_{comm} = -\hat{M}_{fa} \cdot \omega \cdot I_f \cdot I_{ia} + \hat{M}_{ia} \cdot \sin\Theta \cdot \omega \cdot I_{ia}^2$$

if only the average power converted is required since, as previously stated, the mean value of I_c is zero. The power converted during the slip ring period is given by

$$P_{slip} = -\hat{M}_{fA} \cdot \omega \cdot I_f \cdot I_{iA} + \hat{M}_{iA} \cdot \sin\Theta \cdot \omega \cdot I_{iA}^2$$

The total average power converted from electrical to mechanical power or vice versa is

$$P = x.P_{comm} + (1-x).P_{slip}$$

The converted power provides a torque which overcomes friction and drives the load - any excess accelerates the system. The total mechanical power requirement is

$$\text{Power} = \text{Torque} \cdot \text{speed}$$

$$P = (T + J.d\omega/dt) \cdot \omega$$

The total electrical and mechanical powers may be equated to obtain

$$x.P_{comm} + (1-x).P_{slip} = (T + J.d\omega/dt).\omega$$

This is an expression which links the electrical and mechanical parameters of the machine and together with the voltage equations may be used to analyse the performance of the t.a.c. machine.

Chapter 3 The Self and Mutual Inductance Parameters

3.1 Measurement of Self and Mutual Inductance

During the derivation of the voltage equations the variations of the inductance parameters with rotor angle were required. The form of the variations, i.e. sine or cosine functions, were given in Table 2.1 and in this chapter the detailed waveforms are shown and discussed.

The inductances were measured using the direct current inductance bridge developed independently by Jones [3.1] and Prescott and El-Karashi [3.2]. Details of the theory, the operation and practical difficulties in using the bridge are given in Appendix A. The measurement of the inductances was done using currents in the range 0.05 to 2.0 of the rated value for that coil. Initially, much smaller currents (typically 0.001 A.) were used but these produced misleading results due to leakage effects. The effects of hysteris were minimised by taking the average of two readings using equal current flow in opposite directions.

3.2 Self Inductances

The self inductances of the field and interpole windings were independent of rotor position but dependent upon the value of the current flowing in the coil. There was little cross saturation: a change in the field current from zero to rated value produced a 14% reduction in the field self inductance but only a 3% change in the interpole self inductance. The variation of the self inductances of the field and interpole windings are shown in Figure 3.1 (a) and (b) respectively.

The rotor self inductances were dependent upon both rotor position and the field and interpole currents - i.e. upon the d and q axes

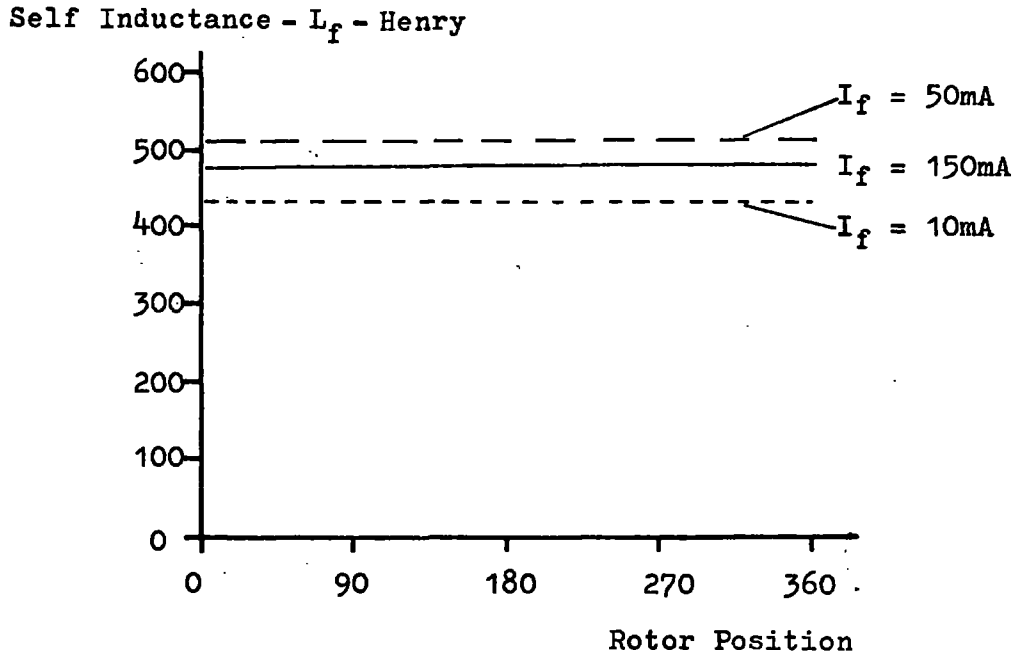

(a) Field Self Inductance - L_f

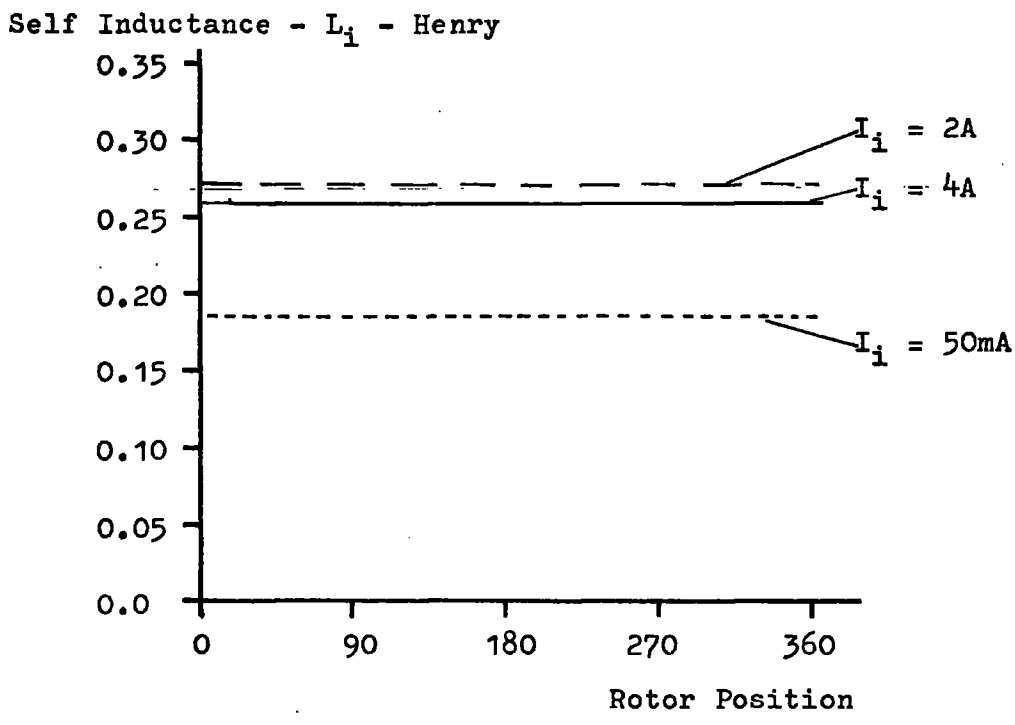

(b) Interpole Self Inductance - L_i

Fig. 3.1 (a,b) Variation of Self Inductance

(c) Main Armature Self Inductance - L_a , L_A

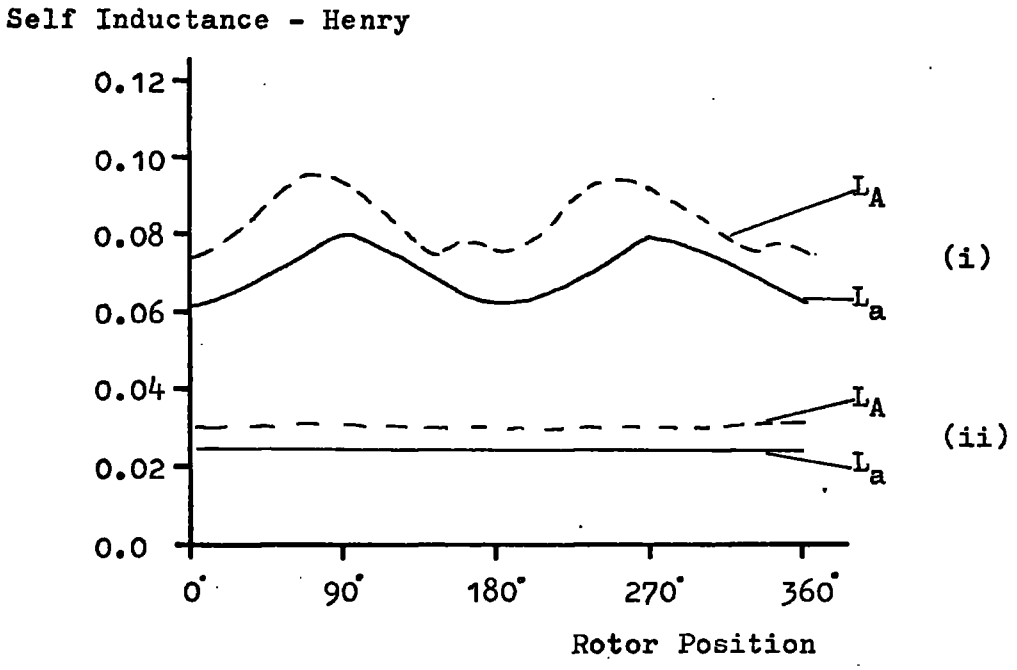

Conditions - (i) I_f = 0.0A I_i = 0A

(ii) I_f = 0.3A I_i = 10A

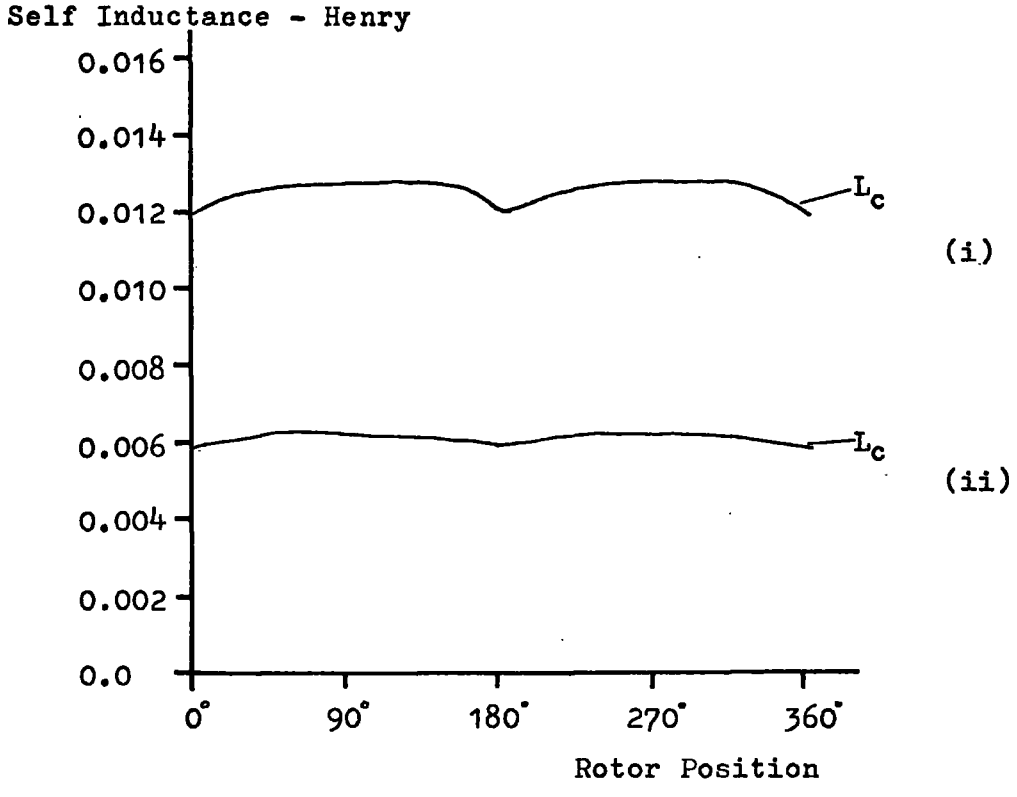

(d) Armature Shorted Turns Self Inductance - L_c

Fig. 3.1 (c,d) Variation of Self Inductance

saturation levels. At and around the rated values of these currents the effect of rotor angle was negligable, The variation of the self inductances of the main armature (L_a) and the total armature (L_A) windings are shown in Figure 3.1 (c) while that of the short circuit turns (L_c) is shown in Figure 3.1 (d).

3.3 Mutual Inductances

The mutual inductance between the field coil and the main armature windings (M_{fa} and M_{fA}) changed appreciably with rotor angle - the variation being of a modified sine wave - Figure 3.2 (a). The variation of the mutual inductance between the field and the armature shorted turns (M_{fc}) was that of a cosine function - Figure 3.2 (b). The variation of the interpole - armature inductances followed a cosine wave - Figure 3.2 (c) whilst that of the interpole - shorted turns was a very modified type of sine wave - Figure 3.2 (d).

The variation of the main armature - shorted turns mutual inductance (M_{ac}) with rotor angle was a sine wave of double the frequency of the other mutual inductances. The magnitude of M_{ac} was very dependent upon the d and q axes saturation levels and at rated currents in the stator coils, the magnitude of M_{ac} was almost negligable - Figure 3.2 (e).

Lastly, the variation of the mutual inductance between the field and the interpole coils at different rotor angles was measured, Figure 3.2 (f). Since the two windings are in space quadrature there should be no mutual inductance between them. A slight variation was recorded and this may be attributed to positioning errors of the rotor, interpole or the main field poles.

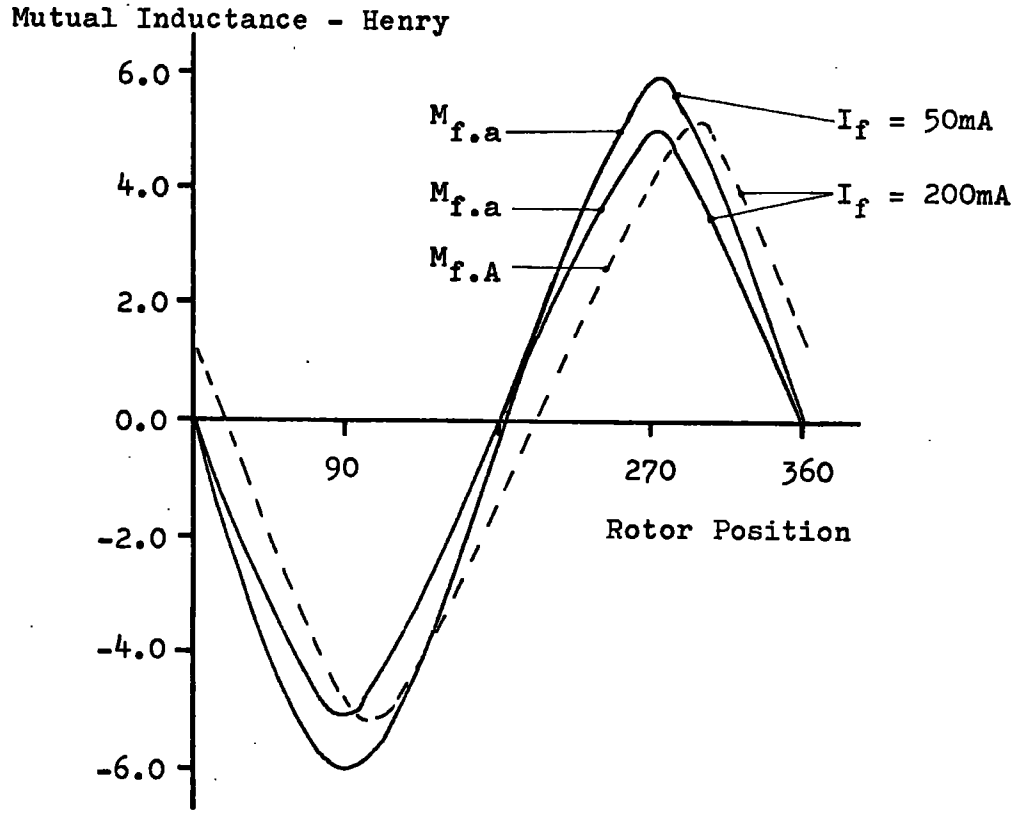

(a) Field - Armature Mutual Inductance - $M_{f.a}$, $M_{f.A}$

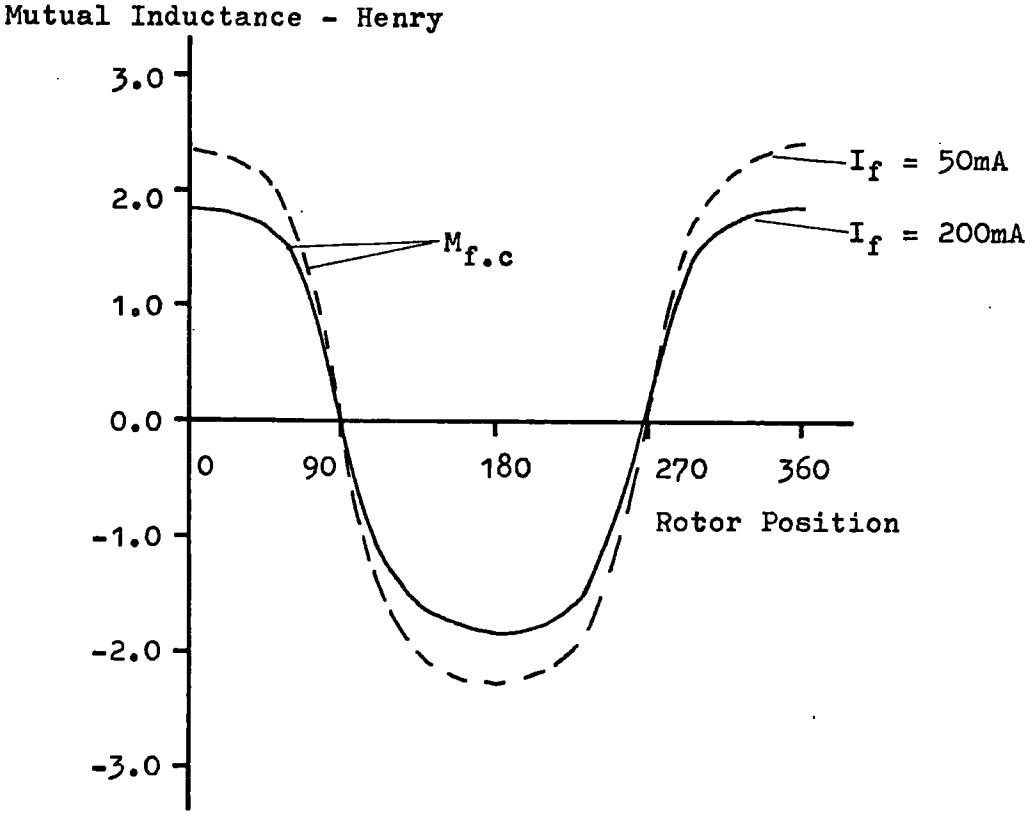

(b) Field - Shorted Turns Mutual Inductance - $M_{f.c}$

Fig. 3.2 (a,b) Variation of Mutual Inductance

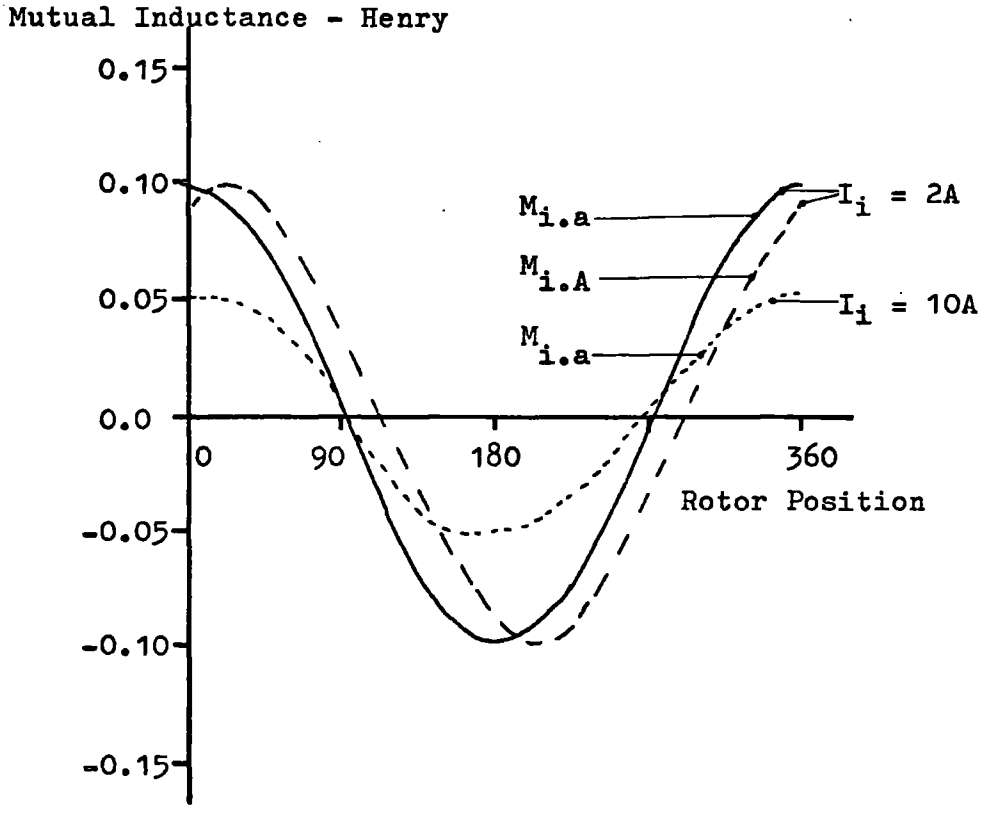

(c) Interpole - Armature Mutual Inductance - $M_{i.a}$, $M_{i.A}$

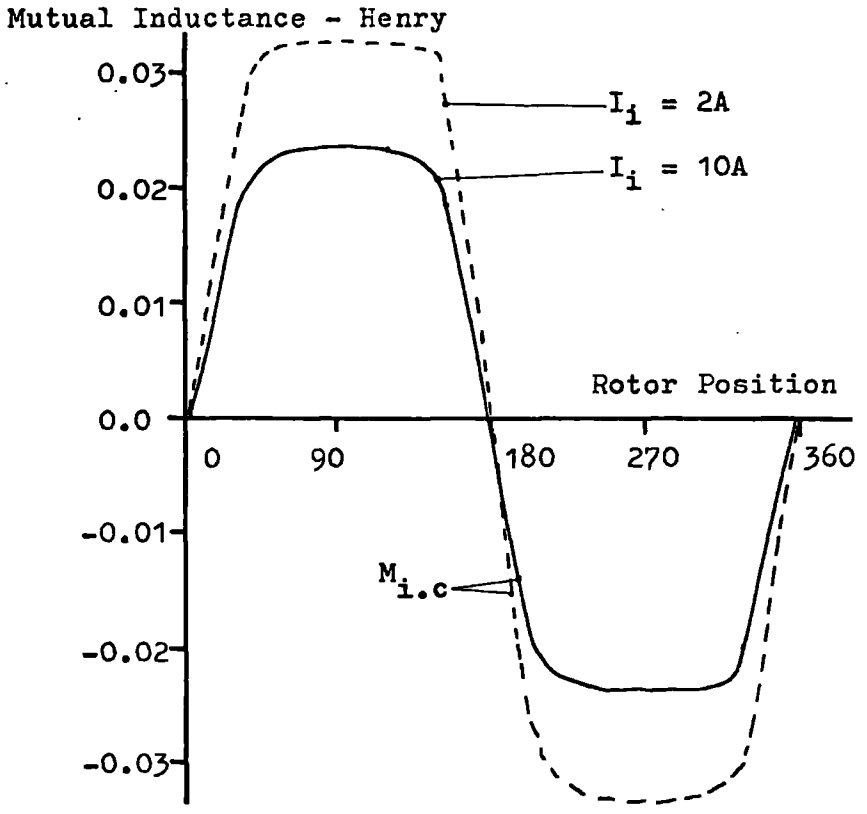

(d) Interpole - Shorted Turns Mutual Inductance - $M_{i.c}$

Fig. 3.2 (c,d) Variation of Mutual Inductance

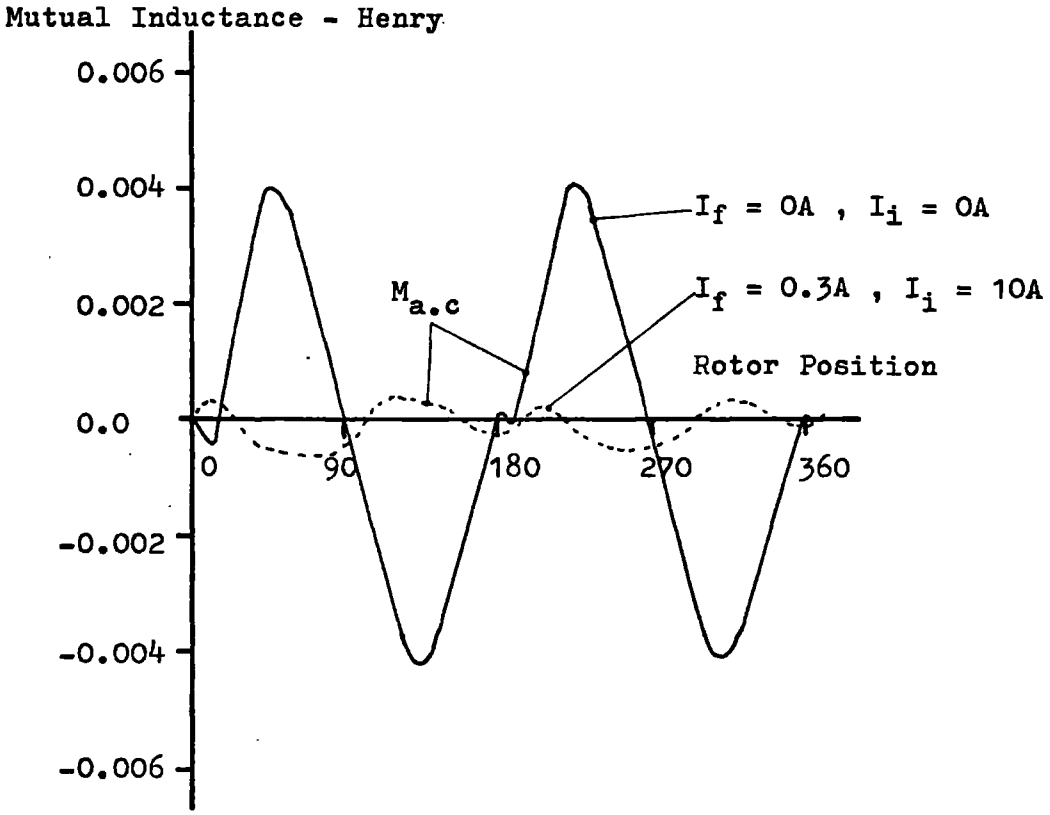

(e) Armature - Shorted Turns Mutual Inductance - $M_{a.c}$

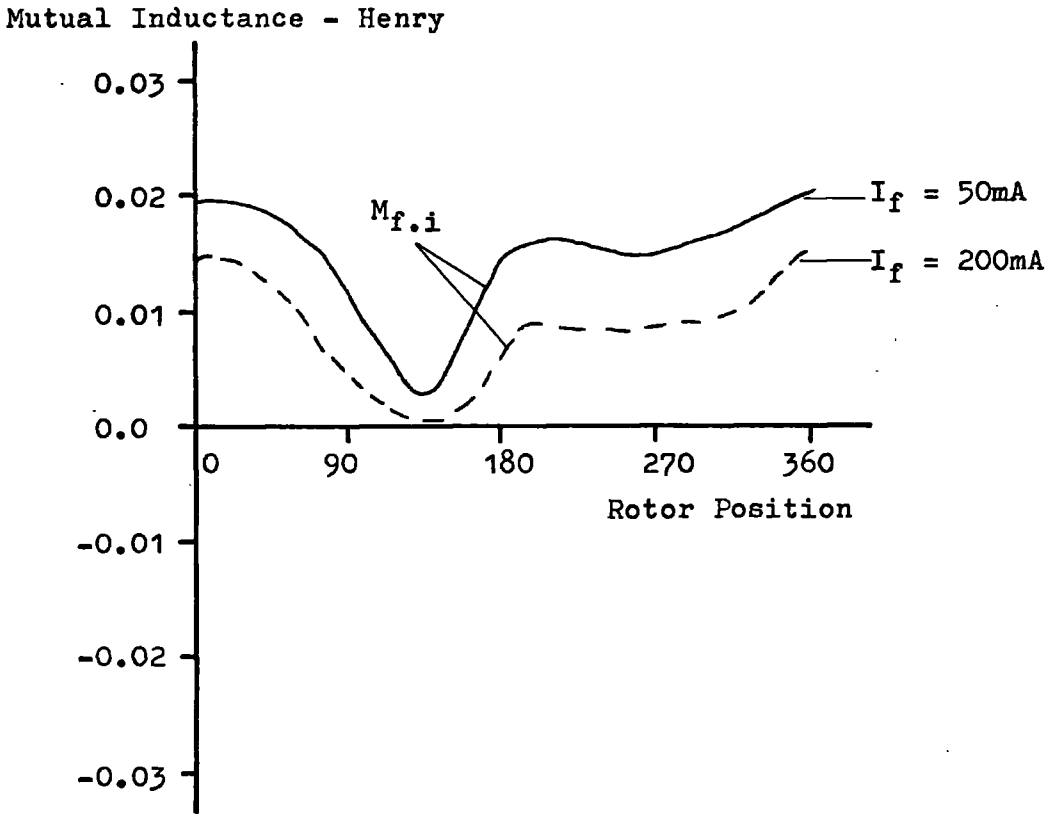

(f) Field - Interpole Mutual Inductance - $M_{f.i}$

Fig. 3.2 (e,f) Variation of Mutual Inductance

3.4 Saturation

Throughout the above figures the effect of saturation may be observed in changing the values of the mutual inductances. For two of these inductances, the maximum value of that inductance was measured over a range of exciting currents. Figure 3.3 (a) shows the change of $\hat{M}_{fa}$ with field current I_f. The value increased to a maximum at around 0.05 A. and then began to fall owing to saturation in the direct axis. A similar situation existed in the q axis and Figure 3.3 (b) gives the change of $\hat{M}_{ia}$ with interpole current I_i. The effect of saturation is very evident, the maximum value of M_{ia} being almost halved as the interpole current was increased from 2 to 10 amperes.

3.5 Derivative or Slope?

In the voltage equations, it is the derivative $d(M_{xy}) / d\theta$ which is required around the position $\theta=0^{\circ}$. However, it has been found by trial that the value of the slope $\Delta M_{xy} / \Delta\theta$ around the position $\theta=0^{\circ}$ gave better results than did the differential values. This is to be expected as the variations of inductance with angle were not pure sine or cosine functions but contained higher harmonics. As an example, the differential value of M_{fa} was 12% higher than that calculated from the slope $\Delta M_{fa} / \Delta\theta$. This latter value differed by less than 3% from that obtained experimentally from the open circuit characteristic of the t.a.c. generator.

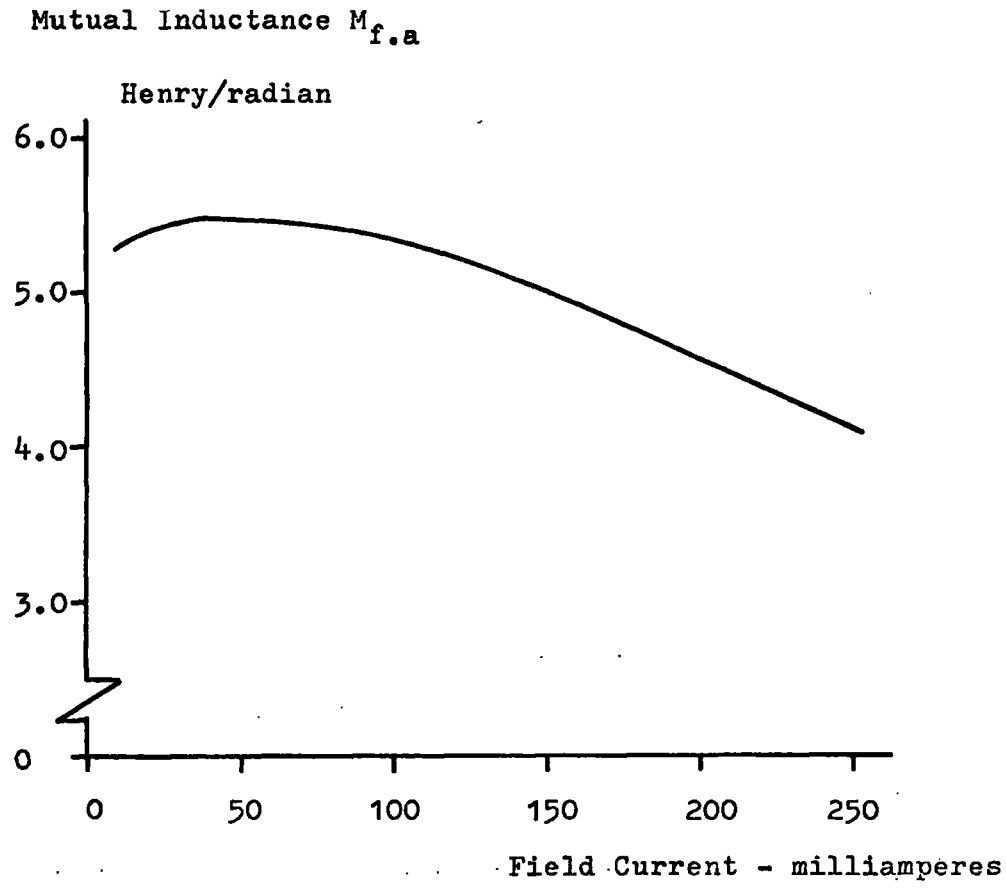

Fig. 3.3 a Direct Axis Saturation

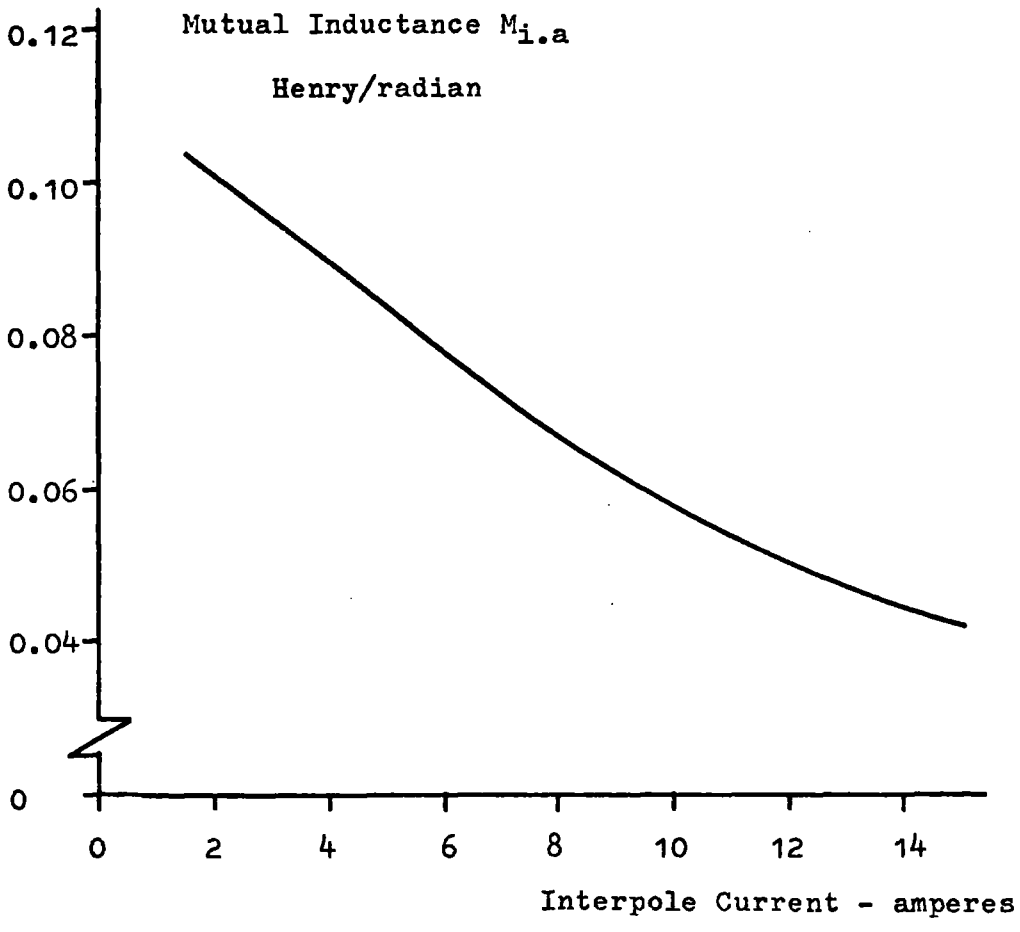

Fig. 3.3 b Quadrature Axis Saturation

Chapter 4 The Analytical Solution

4.1 Differential Equation for Series Interpole Machines

An accurate formal solution of the equations of the t.a.c. machine would be extremely complicated because of factors such as saturation which affect the values of the inductance coefficients. By simplifications and approximations involving errors of not more than 10% the forms of the solution of the differential equations may be shown. A computer programme is later developed to give a more accurate prediction of the machine's performance.

If $\hat{M}_{fa}$ is assumed to be equal to $\hat{M}_{fA}$ then from the power equations

$$\left(-\hat{M}_{fA} \cdot I_f + \hat{M}_{iA} \cdot \sin\theta \cdot I_{iA}\right) I_{iA} = T + J \cdot d\omega/dt$$

or, by rearranging

$$\hat{M}_{iA} \cdot \sin\theta \cdot I_{iA}^2 - \hat{M}_{fA} \cdot I_f \cdot I_{iA} - T - J \cdot d\omega/dt = 0$$

which is a quadratic equation in I_{iA}. If commutation takes all the available angle then the average value of θ is zero and a unique solution exists for I_{iA}, viz

$$I_{iA} = \left(T + J\, d\omega/dt\right) \Big/ \left(-\hat{M}_{fA} \cdot I_f\right)$$

For all other cases, θ will not be zero and I_{iA} will be given by

$$I_{iA} = \frac{\hat{M}_{fA} \cdot I_f}{2 \cdot M_{iA} \cdot \sin\theta} \pm \frac{\hat{M}_{fA} \cdot I_f}{2 M_{iA} \cdot \sin\theta} \left[1 + \frac{4\, \hat{M}_{iA} \sin\theta \left(T + J\, d\omega/dt\right)}{\left(\hat{M}_{fA} \cdot I_f\right)^2}\right]^{1/2}$$

The binomial expansion

$$(1+y)^p = 1 + p \cdot y + \frac{p(p-1)\, y^2}{2.1} + \frac{p(p-1)(p-2)\, y^3}{3.2.1} + \cdots$$

may be used to obtain

$$I_{iA} = \frac{\hat{M}_{fA} \cdot I_f}{2 \cdot \hat{M}_{iA} \cdot \sin\theta} \pm \left[\frac{\hat{M}_{fA} \cdot I_f}{2 \hat{M}_{iA} \cdot \sin\theta} + \frac{T + J \cdot d\omega/dt}{\hat{M}_{fA} \cdot I_f} - \frac{\hat{M}_{iA} \cdot \sin\theta \cdot \left(T + J \cdot d\omega/dt\right)^2}{\left(\hat{M}_{fA} \cdot I_f\right)^3} + \cdots\right.$$

which, on taking the negative sign and setting $\theta = 0^0$, reduces to the simple expression for I_{iA} as above.

Using the values given in Table 4.1 which gives typical values of the machine parameters it can be shown that the last term in the above equation is small - less than 10% - compared to the other terms. Taking the negative sign, the expression reduces to

$$I_{iA} = -\frac{T + J.\,d\omega/dt}{\hat{M}_{fA}.I_f} + \frac{\hat{M}_{iA}.\sin\theta.(T + J.\,d\omega/dt)}{(\hat{M}_{fA}.I_f)^2}$$

This expression may be differentiated with respect to time to give

$$pI_{iA} = -\frac{J}{\hat{M}_{fA}.I_f}\left[\frac{d^2\omega}{dt^2} - \frac{2\,\hat{M}_{iA}.\sin\theta.(T + J.\,d\omega/dt)}{(\hat{M}_{fA}.I_f)^2}\right]$$

Having obtained expressions for I_{iA} and pI_{iA}, these may be substituted into the armature voltage equations that were derived in Chapter 2. In the slip ring voltage equation

$$V_{iA} = -\hat{M}_{fA}.\sin\theta.pI_f - \hat{M}_{fA}.\omega.I_f + R_{iA}.I_{iA} + L_{iA}.pI_{iA} + 2\hat{M}_{iA}.\sin\theta.\omega.I_{iA}$$

the first term, i.e. that containing pI_f, may be neglected since later computer studies indicate that the magnitude of this term is some three orders smaller than the other terms in the same equation.

After substitution the following non linear, second order differential equation is obtained.

$$\frac{L_{iA}.J}{\hat{M}_{fA}.I_f}\left[\frac{d^2\omega}{dt^2} - \frac{2.\hat{M}_{iA}.\sin\theta.(T + J.\,d\omega/dt)}{(\hat{M}_{fA}.I_f)^2}\right]$$

$$+ \frac{R_{iA}.J}{\hat{M}_{fA}.I_f}\left[1 - \frac{2.\hat{M}_{iA}.\sin\theta.T}{(\hat{M}_{fA}.I_f)^2} - \frac{\hat{M}_{iA}.\sin\theta.J.\,d\omega/dt}{(\hat{M}_{fA}.I_f)^2}\right]\frac{d\omega}{dt}$$

$$+ \frac{2.\hat{M}_{iA}.\sin\theta.J}{\hat{M}_{fA}.I_f}\left[1 - \frac{2\hat{M}_{iA}.\sin\theta.T}{(\hat{M}_{fA}.I_f)^2} - \frac{\hat{M}_{iA}.\sin\theta.J.\,d\omega/dt}{(\hat{M}_{fA}.I_f)^2}\right]\frac{\omega.d\omega}{dt}$$

$$+ \left[\hat{M}_{fA}.I_f + \frac{2\,\hat{M}_{iA}.\sin\theta.T}{\hat{M}_{fA}.I_f}\right].\omega$$

$$= -\left[V_{iA} + \frac{R_{iA}.T}{\hat{M}_{fA}.I_f}\right]$$

Typical Motor Parameter Values

Parameter	Symbol	Value
Voltage	V_{ia}, V_{iA}	200 volts
Voltage	V_f	200 volts
Current	I_f	250 mA
Current	I_{ia}, I_{iA}	3 amperes no-load
Resistance	R_{ia}	2.6 ohms
Resistance	R_{iA}	2.9 ohms
Inductance	$\hat{L}_{ia}$, $\hat{L}_{iA}$	0.1 henry unsaturated
Inductance	$\hat{M}_{i.a}$, $\hat{M}_{i.A}$	0.1 henry "
Inductance	$\hat{M}_{f.a}$, $\hat{M}_{f.A}$	5 henry "
Inertia	J	0.5 Nm sec^2 incl. dynamometer
Torque	T_f	3 Nm " "
Speed	w	1800 rev/min
Angle	θ	-7^o

Table 4.1 Typical Motor Parameter Values

This equation is probably only soluble by numerical means because the values of the terms are not constant but depend upon many factors such as speed and satuation. Again by reference to Table 4.1, those terms which are dominant in the above equation can be used to show the forms of the solution. Using only the dominant terms, the equation reduces to

$$\frac{L_{iA} \cdot J}{\hat{M}_{fA} \cdot I_f} \cdot \frac{d^2\omega}{dt^2} + \left[\frac{R_{iA} \cdot J}{\hat{M}_{fA} \cdot I_f} + \frac{2\hat{M}_{iA} \cdot \sin\theta \cdot \omega \cdot J}{\hat{M}_{fA} \cdot I_f}\right] \frac{d\omega}{dt} + \hat{M}_{fA} \cdot I_f \cdot \omega$$

$$= -\left[V_{iA} + \frac{R_{iA} \cdot T}{\hat{M}_{fA} \cdot I_f}\right]$$

4.2 Forms of Solution

If the commutation process is allowed to take all the available angle the average value of θ is zero. The differential equation then becomes

$$\frac{d^2\omega}{dt^2} + \frac{R_{iA}}{L_{iA}} \cdot \frac{d\omega}{dt} + \frac{(M_{fA} \cdot I_f)^2}{L_{iA} \cdot J} \cdot \omega = -\frac{V_{iA} \cdot \hat{M}_{fA} \cdot I_f}{L_{iA} \cdot J} - \frac{R_{iA} \cdot T}{L_{iA} \cdot J}$$

This is a second order, differential equation and, if the coefficients are considered constant, the auxiliary equation has the solution

$$\omega = e^{-15t} \cdot \left(k_1 \cdot \cosh(13t) + k_2 \sinh(13t)\right)$$

and the particular solution is

$$\omega_o = -\frac{V_{iA} \cdot \hat{M}_{fA} \cdot I_f - R_{iA} \cdot J}{(\hat{M}_{fA} \cdot I_f)^2}$$

The response of the motor speed to a change of say, supply voltage is a stable, well damped response of the type shown in Figure 4.1 (a).

If the commutation process does not take all the available angle then the value of θ is no longer zero. The differential equation

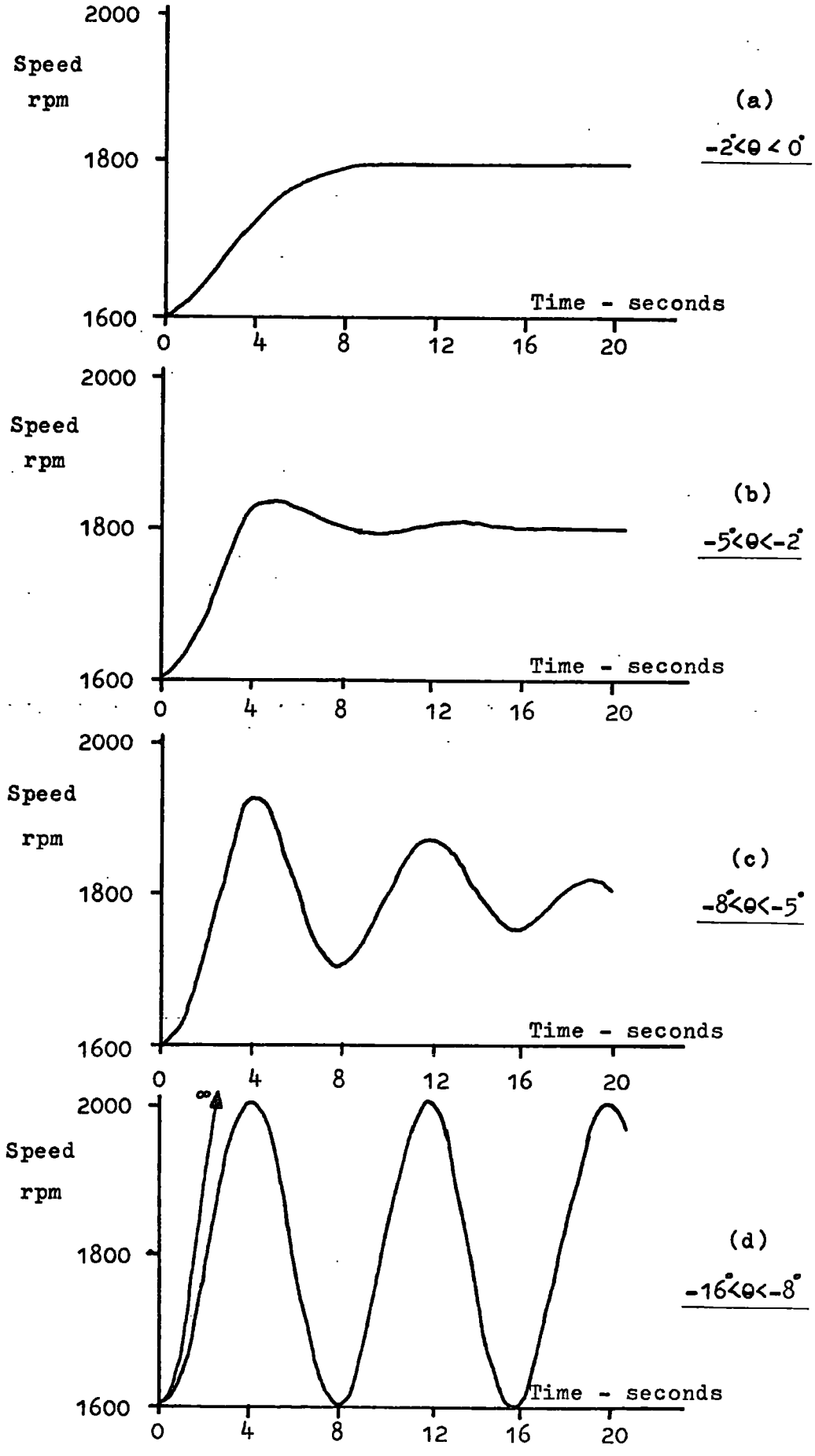

Fig. 4.1 Forms of Speed Response at different Armature Axis Positions

$$\frac{d^2\omega}{dt^2} + \frac{R_{iA} + 2\cdot\hat{M}_{iA}\cdot\sin\Theta\cdot\omega}{L_{iA}}\cdot\frac{d\omega}{dt} + \frac{(\hat{M}_{fA}\cdot I_f)^2}{L_{iA}\cdot J}\cdot\omega = \frac{-V_{iA}\cdot\hat{M}_{fA}\cdot I_f - R_{iA}\cdot J}{L_{iA}\cdot J}$$

may be written in the form

$$(D^2 + 2\cdot\gamma\cdot D + \beta)\,\omega = k$$

Unfortunately, this equation is still non linear because of the $\omega.d\omega/dt$ term and because the coefficients themselves depend upon saturation. However, it is the general form of solution that is required, not the detailed solution for which the computer model is to be used. It may be noted that the change in speed is small - less than 10% of the mean speed and so, to an approximation, the term

$$(R_{iA} + 2\cdot\hat{M}_{iA}\cdot\sin\Theta\cdot\omega)/L_{iA}$$

may be regarded as being a constant coefficient of $d\omega/dt$. Therefore

$$\gamma = (R_{iA} + 2\hat{M}_{iA}\cdot\sin\Theta\cdot\omega)/2\cdot L_{iA}$$

$$\beta = (M_{fA}\,I_f)^2/(L_{iA}\cdot J)$$

The auxiliary equation

$$m^2 + 2\cdot\gamma\cdot m + \beta = 0$$

has roots of

$$m_1, m_2 = -\gamma \pm \sqrt{\gamma^2-\beta}$$

and the solution is

$$\omega = e^{-\gamma t}\cdot\left[k_3\cdot e^{\sqrt{\gamma^2-\beta}\cdot t} + k_4\cdot e^{-\sqrt{\gamma^2-\beta}\cdot t}\right]$$

The response of the system will depend upon the value of the damping term γ.

Under conditions of rapid commutation the average value of Θ is negative: the more rapidly commutation takes place, the larger is the negative value of Θ. The damping term γ will decrease in value as Θ increases negatively. It is possible for the value of

θ to have a negative value and any disturbance will not produce a steady state result - the machine will be unstable.

If the response of the motor to a step change of armature voltage is calculated using the above equation then, as the value of θ becomes more negative, the response changes from being over to under damped and eventually completely unstable. Figures 4.1 (a) to (d) show the typical forms of the response to a constant step change of armature supply voltage at different angles of commutation. In Figure 4.1 (a) commutation takes all the available angle; in Figure 4.1 (d) commutation is completed in about 5 to 10% of the maximum available angle.

From the above approximate analytical solution and using typical numerical values for the inductance parameters, etc., the frequency of oscillation should be about 0.7 Hz. The frequency of the speed oscillation as measured experimentally was 0.4 to 0.5 Hz; an error of some 25%. To obtain a greater accuracy, more terms must be included in the equations which then become quite lengthy and difficult to manipulate. For the moment, it is sufficient to accept this error and to note that the response of the motor may, in certain conditions, become oscillatory or unstable. The performance predicted by the analytical solution was, in general, observed on the t.a.c. motor.

4.3 Comparison of Analytical Solution with Experimental Motor

As the angle of commutation is reduced the response becomes more underdamped until eventually a point of no damping is reached. Any parameter change tending to increase the speed would, from the equations, cause the speed to increase indefinitely. The experimental motor does exhibit these types of response but the speed does not increase ad infinitum. Consider the case when, according to the

analytical solution, the speed should increase without limit after a change of say, supply voltage.

For the speed to rise an accelerating torque must be provided by an increase in the armature current. This increase, through saturation, reduces the value of $\hat{M}_{iA}$. As the value of $\hat{M}_{iA}$ falls, the damping term (δ) changes from a negative to a small, positive amount and the motor speed begins to oscillate as a highly underdamped system. The speed and current then fall; the value of $\hat{M}_{iA}$ rising as the current falls. The damping term once again becomes negative and the speed and current try to reach $-\infty$. The current is limited by the diode action of the thyristors to be always positive or zero and therefore the current reduces only to zero. The speed then falls owing to the load and frictional torques until the thyristors become forward biased allowing armature current to flow once again. The damping term is initially negative and the speed and current immediately attempt to reach $+\infty$. The cycle repeats as the effects of saturation restrict the range over which negative damping can occur. Outside this range the damping is small but positive and the responses of the speed and current of the t.a.c. motor under conditions of rapid commutation are similar to those of a highly underdamped system.

Two points are worthy of note. First, that the diode action is not essential in preventing the speed and current from reaching $-\infty$. Saturation effects occur in both directions of current flow and would prevent excessive speeds. Secondly, computer studies have confirmed that saturation is indeed responsible for preventing excessive speeds and currents. If saturation is neglected, both speed and current attempt to reach very high values (i.e. greater than 100 times rated).

4.4 Differential Equation for Separately Excited Interpoles

The analytical method for the t.a.c. motor which uses a separate, constant interpole current is very similar in outline to that for series interpole excitation. The simplifications that are used are those that were stated during the previous analysis and are not, therefore, repeated.

Starting from the power equation for the motor

$$\left(T + J \cdot {}^{d\omega}/_{dt}\right) \cdot \omega = -\hat{M}_{fA} \cdot I_f \cdot I_A \cdot \omega - \hat{M}_{iA} \cdot \sin\Theta \cdot \omega \cdot I_i \cdot I_A$$

an expression for I_A may be obtained

$$I_A = -\left(T + J\,{}^{d\omega}/_{dt}\right) \Big/ \left(\hat{M}_{fA} \cdot I_f + \hat{M}_{iA} \cdot \sin\Theta \cdot I_i\right)$$

which is then differentiated to obtain pI_A as

$$pI_A = -\left(J \cdot {}^{d^2\omega}/_{dt^2}\right) \Big/ \left(\hat{M}_{fA} \cdot I_f + \hat{M}_{iA} \cdot \sin\Theta \cdot I_i\right)$$

These expressions may be substituted into the voltage equation.

$$V_A = -\hat{M}_{fA} \cdot \omega \cdot I_f - \hat{M}_{fA} \cdot \sin\Theta \cdot pI_f - \hat{M}_{iA} \cdot \sin\Theta \cdot \omega \cdot I_i + M_{iA} \cdot pI_i + R_A \cdot I_A + L_A \cdot pI_A$$

to obtain a differential equation as before

$$-\frac{L_A \cdot J}{\hat{M}_{fA} I_f + \hat{M}_{iA} \sin\Theta I_i} \cdot \frac{d^2\omega}{dt^2} - \frac{R_A \cdot J}{\hat{M}_{fA} \cdot I_f + \hat{M}_{iA} \sin\Theta I_i} \cdot \frac{d\omega}{dt} - \hat{M}_{fA} \cdot I_f \cdot \omega$$

$$-\hat{M}_{iA} \cdot \sin\Theta \cdot \omega I_i = V_A + \frac{R_A \cdot T}{\hat{M}_{fA} \cdot I_f + \hat{M}_{iA} \cdot \sin\Theta \cdot I_i} + \hat{M}_{fA} \cdot \sin\Theta \cdot pI_f + \hat{M}_{iA} \cdot pI_i$$

Since the interpole current is constant, and the rate of change of I_f small, the differential equation may be simplified to

$$\frac{d^2\omega}{dt^2} + \frac{R_A}{L_A} \cdot \frac{d\omega}{dt} + \frac{\left(\hat{M}_{fA} \cdot I_f + \hat{M}_{iA} \cdot \sin\Theta \cdot I_i\right) M_{fA} \cdot I_f}{L_A \cdot J} \cdot \omega$$

$$+ \frac{\left(\hat{M}_{fA} \cdot I_f + \hat{M}_{iA} \cdot \sin\Theta \cdot I_i\right) \cdot \hat{M}_{iA} \sin\Theta \cdot I_i}{L_A \cdot J} \cdot \omega$$

$$= -\frac{V_A \left(\hat{M}_{fA} \cdot I_f + \hat{M}_{iA} \cdot \sin\Theta \cdot I_i\right)}{L_A \cdot J} - \frac{R_A \cdot T}{L_A \cdot J}$$

This is a differential equation of the form

$$\left(D^2 + 2 \cdot \gamma_1 \cdot D + \beta_1\right) \omega = k_r$$

where

$$\gamma_1 = R_a / 2 \cdot L_a$$

and it is noted that the damping term depends only upon the resistance and inductance of the armature circuit. It does not depend upon the mutual coupling between the interpole and armature windings, the speed or the angle by which the average armature axis position is displaced from the quadrature axis. To any particular parameter change, the motor speed will have a final steady state value. The degree of damping will however depend upon the other terms in the above differential equation.

Chapter 5 Comparison of Computed and Experimental Characteristics

5.1 The Computer Programme

The programme uses the voltage and power equations which were developed in Chapter 2. In outline, the programme first calculates the saturation effects of the various currents flowing in the coils and adjusts the values of the self and mutual inductances accordingly. Using the equation for the short circuited coil the time of commutation is obtained which, together with the speed of rotation, enables the average value of e to be calculated. The voltage and power equations are rewritten in the form

$$d(z) / dt = \text{function (voltage, current, speed, etc.)}$$

and the rates of change of current and speed are evaluated. From the present values and the rates of change, an integration method can compute new values of current and speed. These values are then used to obtain new rates of change. By repeating the process, the machine's performance may be calculated.

The accuracy of the simulation depends, obviously, upon the accuracy of the numerical values used for the parameters of the machine. It also depends upon the type of integration proceedure. A simple slope method using a large step length will not be as accurate as say, a fourth or fifth order, variable step method that contains an error checking routine. The computing time required for the simulation will be greatly affected by the type of integration method that is used.

The programme was written to be run under the control of CSMP - Continuous Systems Modelling Program - which is a general programme developed specifically for the dynamic modelling of systems.

5.2 Steady State Comparisons

The generator characteristics were calculated from a programme similar to that descibed in Appendix B. The predicted open circuit characteristic was about 3% higher than that measured on the t.a.c. machine - Figure 5.1. The shape of the computed and measured curves were extremely similar. Also very similar were the computed and measured regulation curves of the generator as shown in Figure 5.2. The predicted curve was again 3% higher than the measured characteristic.

The 3% error may be attributed to the approximations made during the derivation of the voltage and power equations. The values of the slope of the inductance coefficients were measured or calculated at the position $\theta=0^{\circ}$. At different values of θ, the slope may change slightly. For example, the voltage waveform during the periods of commutation and slip ring operation predicted by the computer were more peaked than those observed on the experimental machine. In Figure 5.3 waveform (a) shows the experimental machine voltage waveform and (b) is the waveform from the computer. The average value of the computed curve is some 4% higher than that observed. If the variation of the slope over the range of θ is used and not just its average value at $\theta=0^{\circ}$, then the computed waveform becomes less peaked and its average value is within 1% of the experimental curve - Figure 5.3 (c). Unfortunately, to include this kind of detail in the computer programme would significantly increase the computing time necessary to perform the simulation of the machine's performance.

It must be remembered that all the inductances were measured with the rotor stationary and it is only to be expected that some modification of the inductance waveforms would occur when the armature is rotating under normal operating conditions. With these facts in

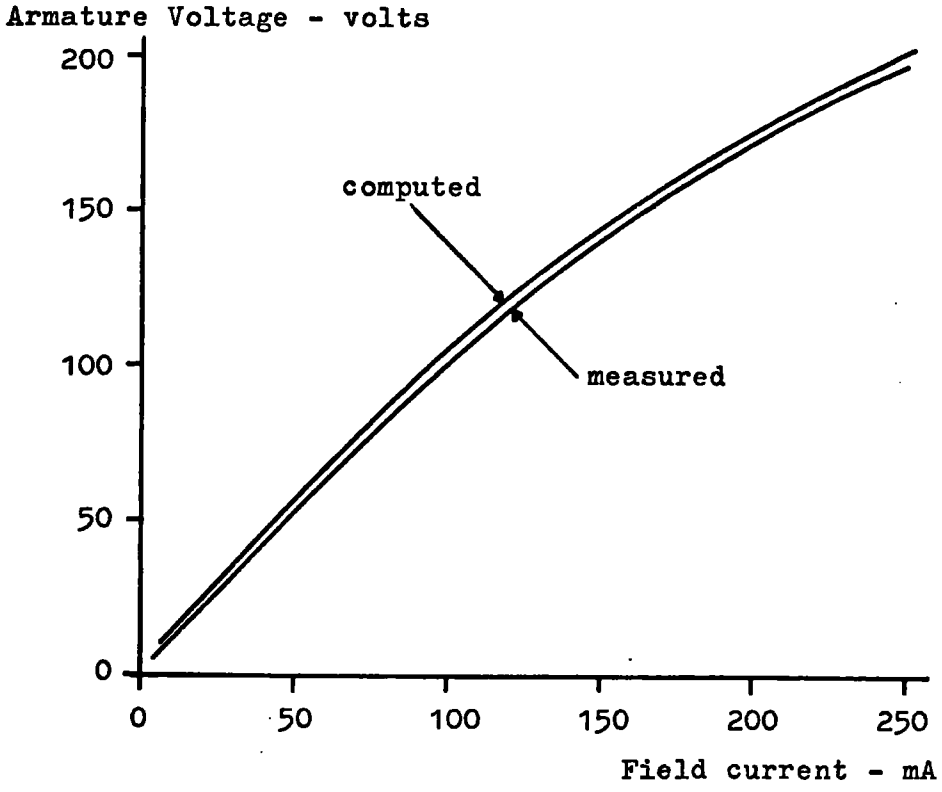

Fig. 5.1 Open Circuit Characteristic of Generator

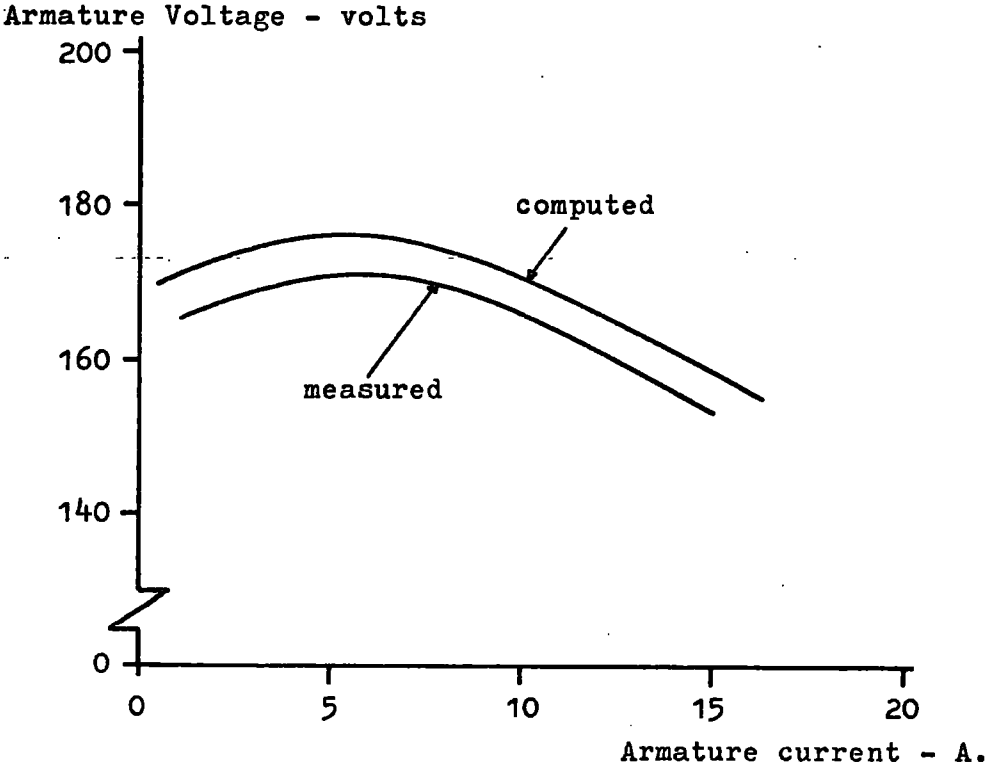

Fig. 5.2 Regulation Characteristic of Generator

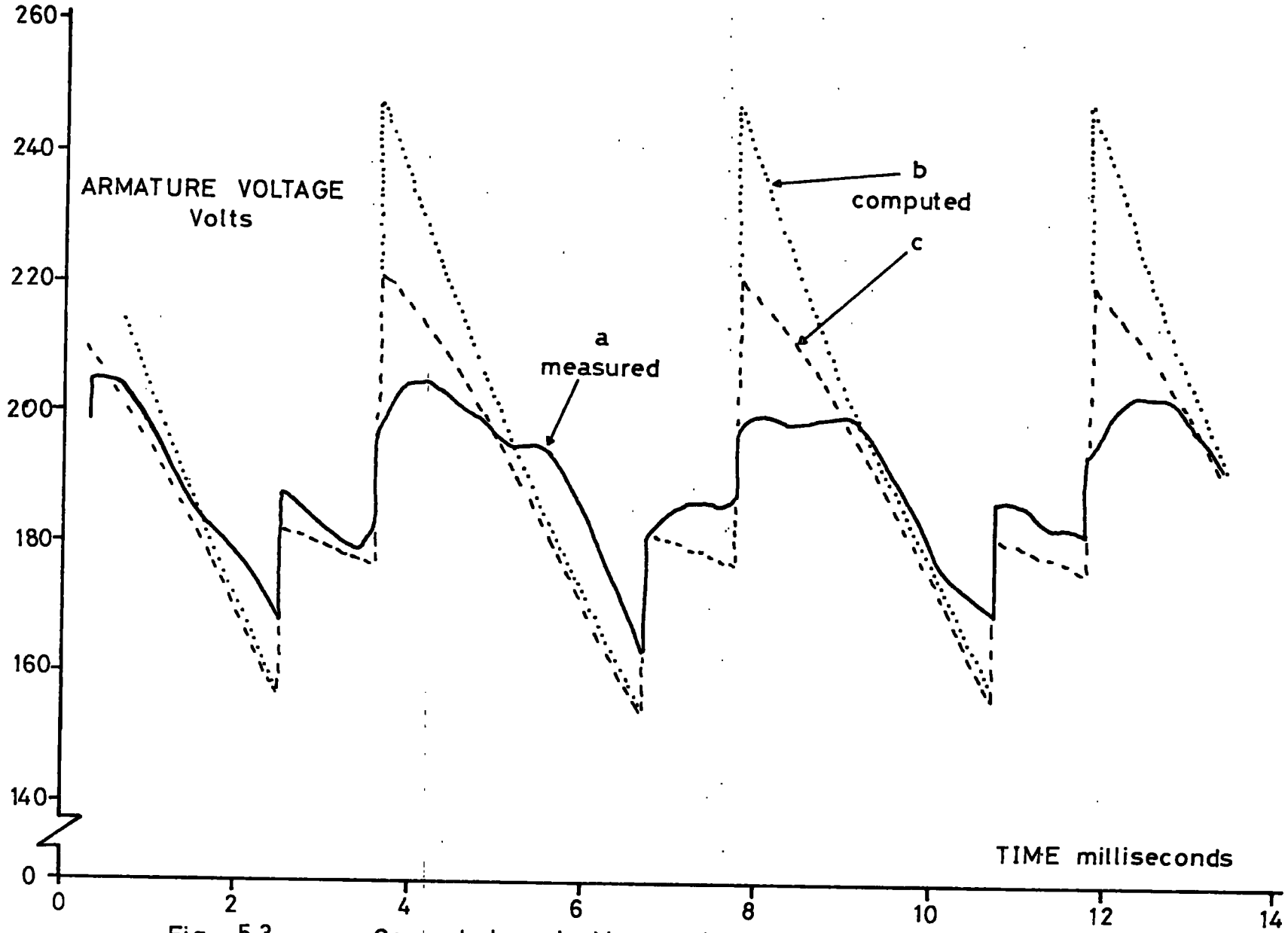

Fig. 5.3 Computed and Measured Voltage Waveforms

mind, the accuracy with which the computer model predicted the generator characteristics is considered sufficient for the model to be used to study the transient behaviour of the t.a.c. motor.

The steady state characteristics of the motor were calculated and compared to those obtained experimentally. The speed - field current characteristic for the series interpole machine is shown in Figure 5.4: curve (a) being experimental, curve (b) computed. The speed-load current characteristic is given in Figure 5.5: again (a) is experimental and curve (b) computed. The 3% difference between the computed and experimental characteristics is again apparent but of more importance is the great similarity between them. Under weak field and light load conditions both the computer model and the experimental motor exhibit the same kind of oscillatory performance.

5.3 Transient Comparisons

As a test of the model under changing conditions the self excitation curve of the generator and the starting performance of the motor were simulated. Figure 5.6 gives the measured and computed self excitation curve and, to within 4%, the computer has successfully predicted the output voltage. The starting performance of the motor is shown in Figure 5.7 and again the computer has simulated the machine fairly accurately. Below a speed of 60 rps the results are not totally valid because of the method of determining the time of commutation. This method is discussed in Appendix B. Nevertheless, the model predicted the motor speed to within 5% of the measured values over the speed range of 0 to 120 rps.

The responses of the motor to a step change in one of the parameters were recorded on the experimental machine and then compared to a simulation of the same change. The step disturbance applied to

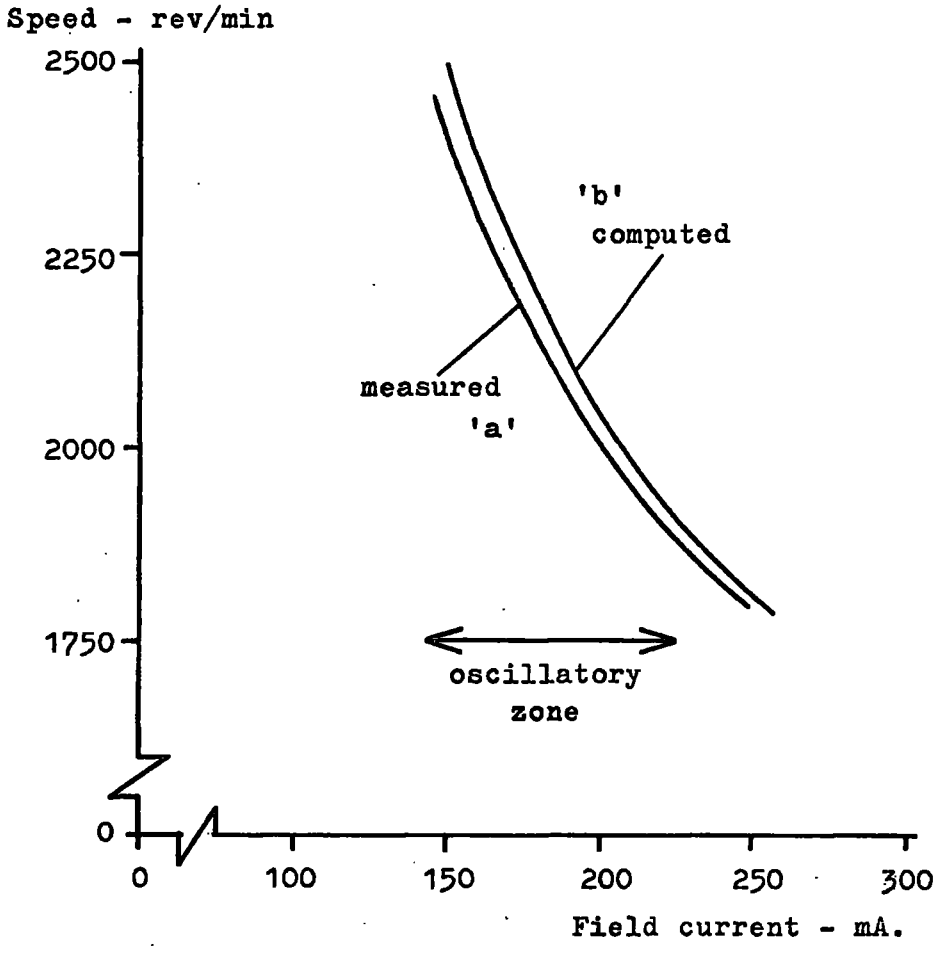

Fig. 5.4 Speed - Field Current Characteristic of Motor

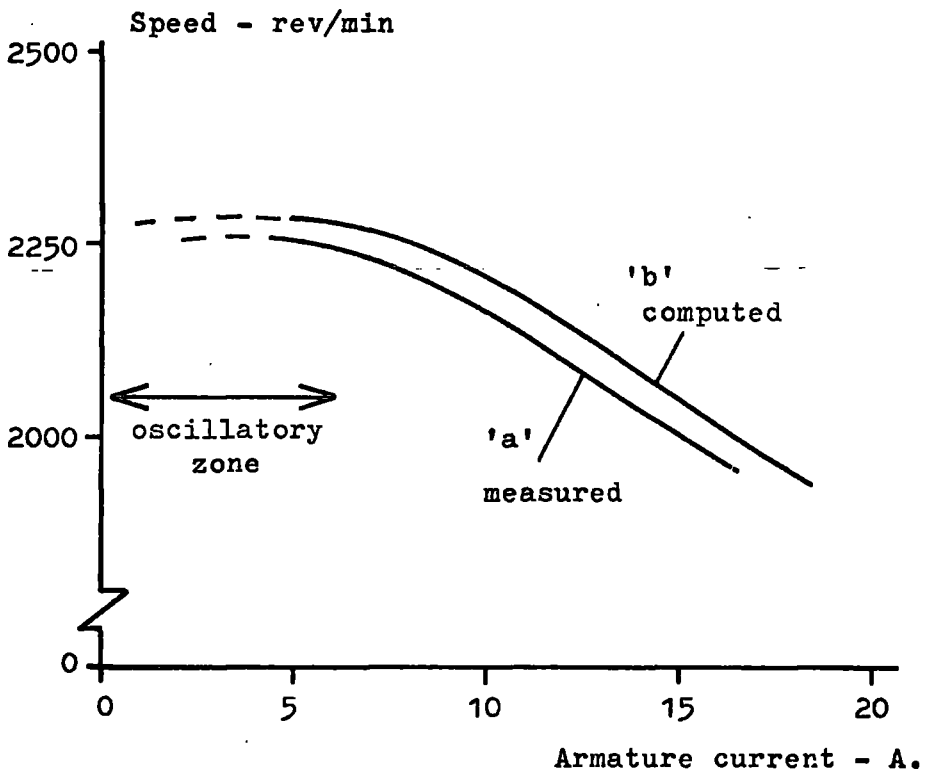

Fig. 5.5 Speed - Armature Current Characteristic of Motor

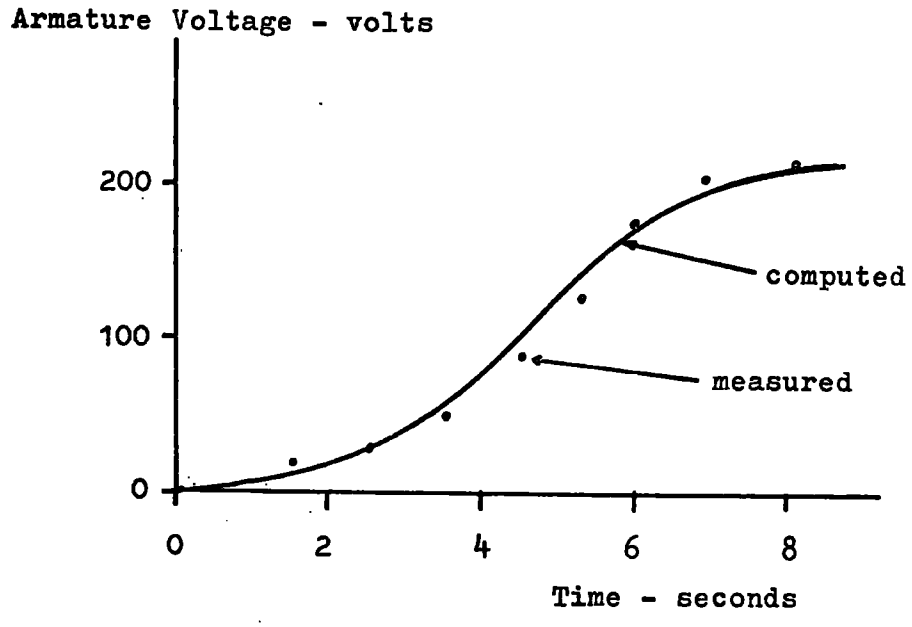

Fig. 5.6 Self excitation Characteristic of Generator

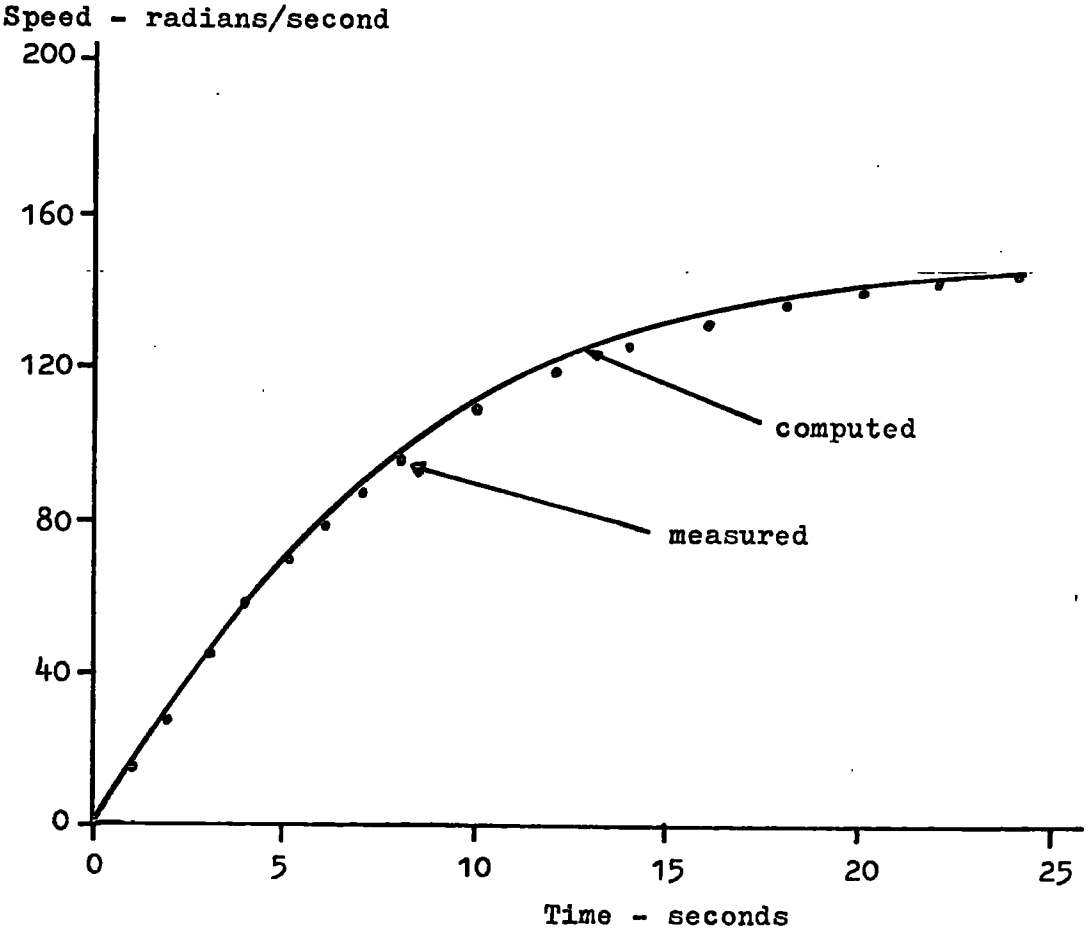

Fig. 5.7 Speed Run-up of T.A.C. Motor

both the machine and model was that of switching out a resistor of 3 ohms in the armature circuit. Under light running conditions the armature current was nominally 2.5 A so that 7.5 V were dropped across the resistor. Shorting out the resistor causes the armature to see a step increase of 7.5 volts.

The response of the machine speed and armature current to the above change was recorded at four different levels of field current. In each case the interpole winding was series connected with the armature and the t.a.c. machine was mechanically coupled to the dynamometer. At maximum field current (i.e. minimum speed) the response was that of a well damped system - Figure 5.8 (a). The computer simulation for the same conditions gave a more rapid initial increase in the current waveform but after 0.2 seconds, the waveforms matched closely - generally to within $\pm 3\%$. As the field current was reduced and the nominal motor speed increased, the responses of both the motor and model became underdamped and eventually, continuous speed oscillations were obtained. Figures 5.8 (b) to (d) show typical responses as the field current is reduced. Only the current waveforms are shown as these gave a more critical test of matching.

Before discussing these results, two more tests of the machine and model are given. The first is the response to the above step change of voltage but with the armature current at its rated value - Figure 5.9 (a). Secondly, the response of the motor to the removal of a load torque is given in Figure 5.9 (b). Around the rated current the responses were stable but oscillations were again produced when the load torque was removed and the motor left to run under light load conditions. The computer simulations agreed closely with the experimental measurements.

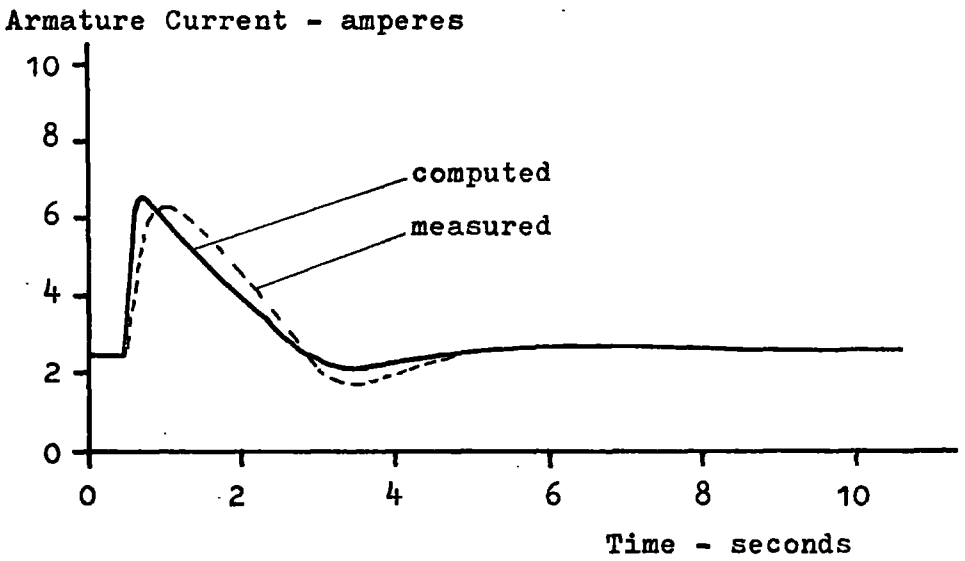

(a) Motor Current Response - I_f = 0.250 ampere

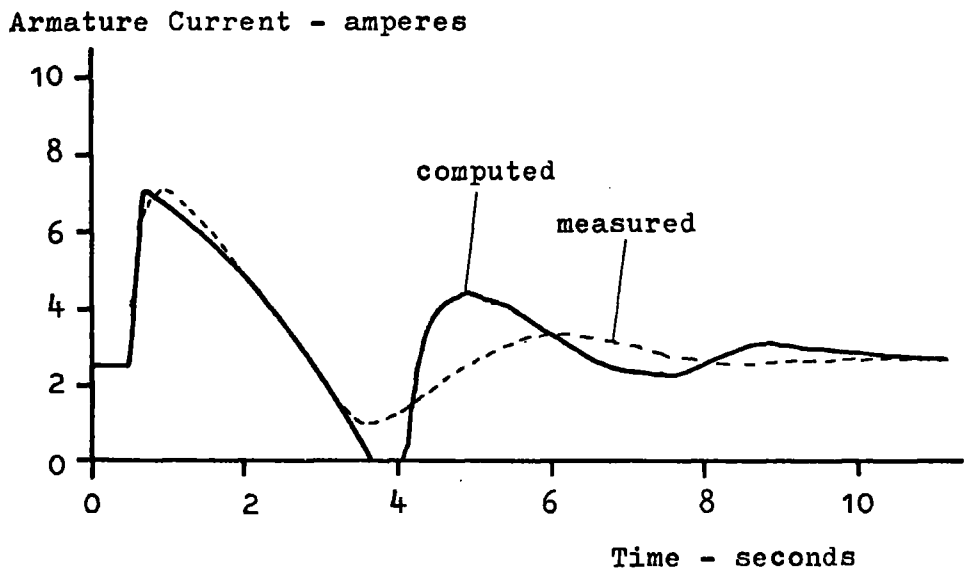

(b) Motor Current Response - I_f = 0.225 ampere

Fig. 5.8 (a,b) Motor Current Responses

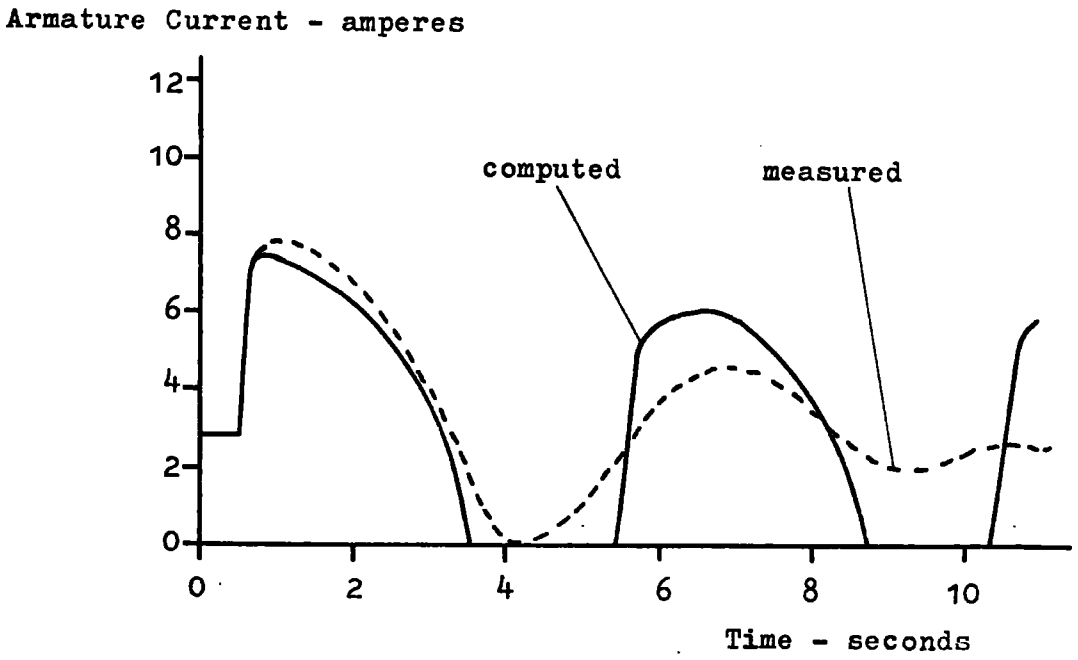

(c) Motor Current Response - I_f = 0.200 ampere

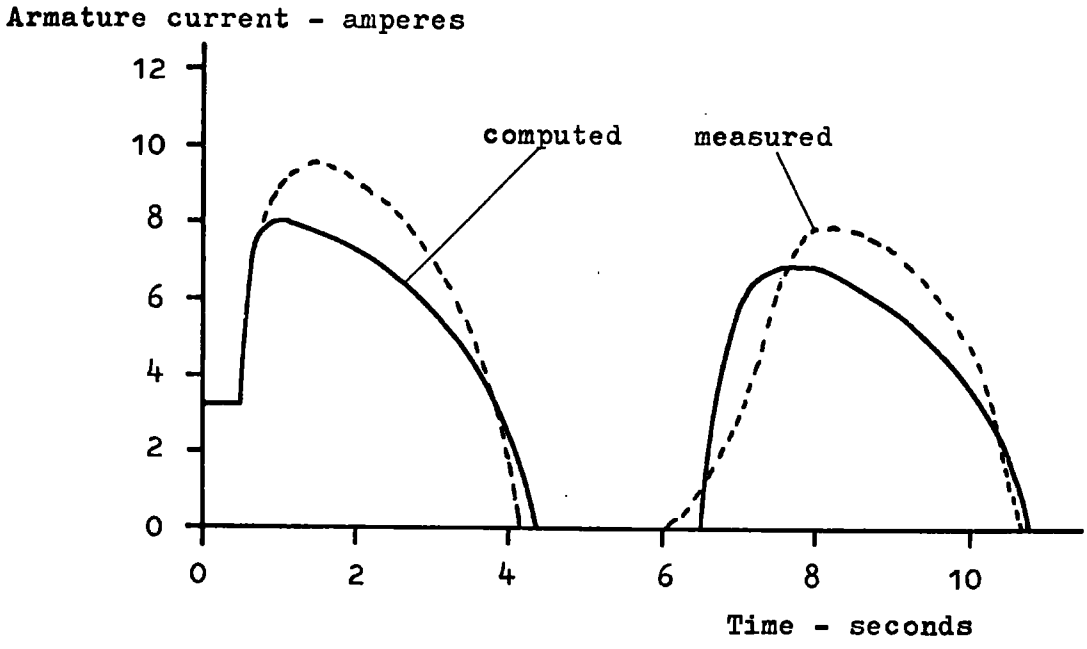

(d) Motor Current Response - I_f = 0.175 ampere

Fig. 5.8 (c,d) Motor Current Responses

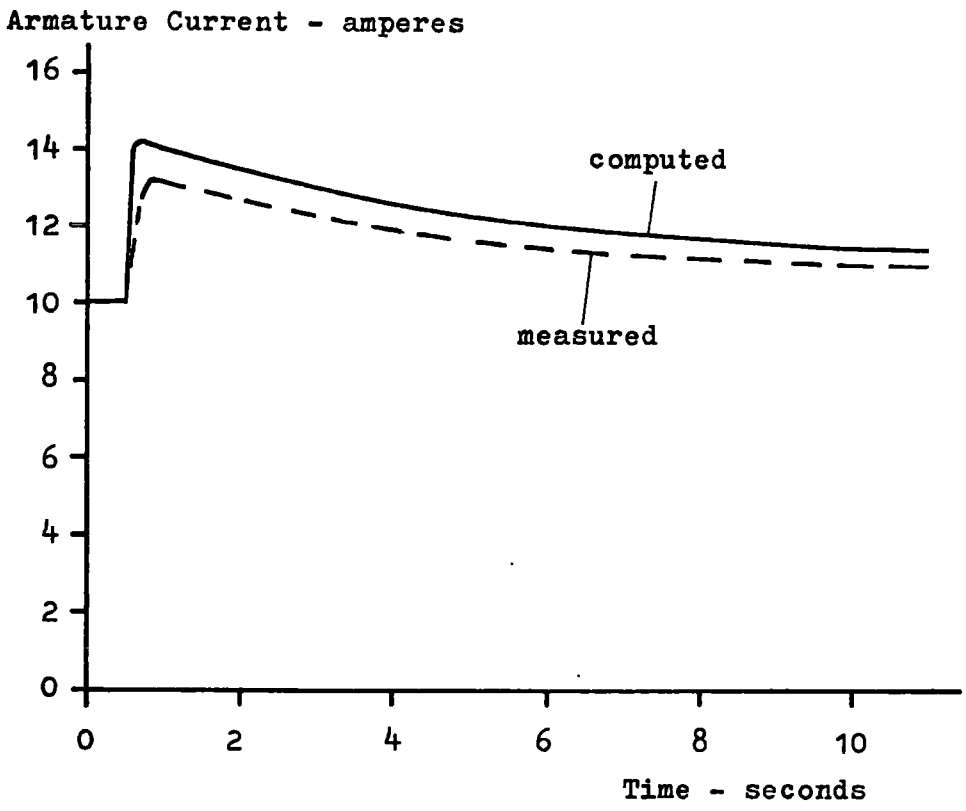

(a) Motor Current Response - I_f = 0.175ampere

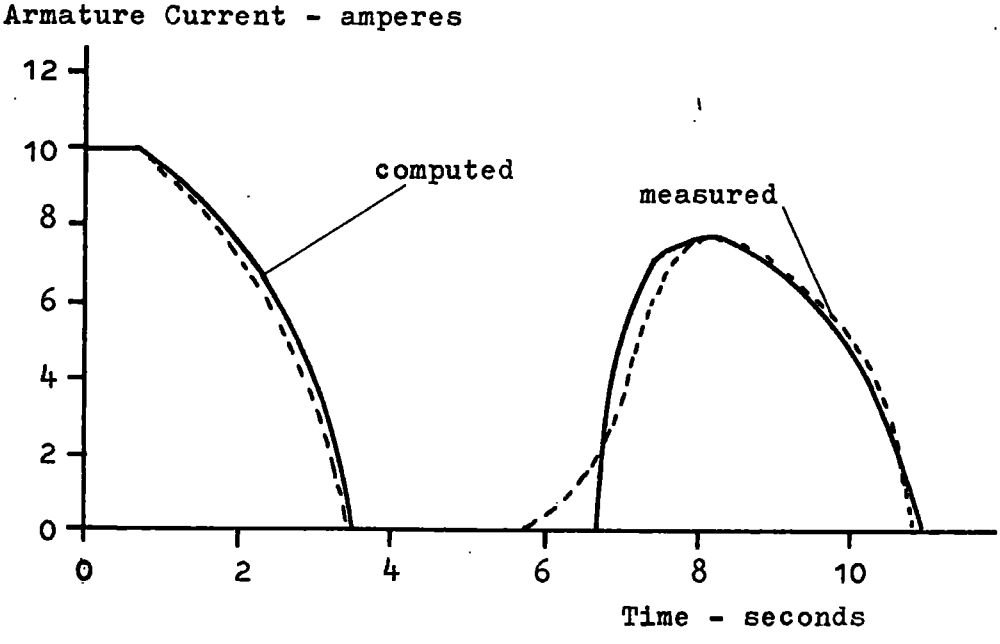

(b) Motor Current Response - I_f = 0.175 ampere

Fig. 5.9 Motor Current Responses

5.4 Discussion on the Computer Model

The voltage and power equations have been satisfactorily developed into a computer programme capable of predicting the performance of the machine over a wide range of steady state and transient conditions. The computer model does in some cases predict that the motor will oscillate continuously whereas the experimental motor does have a final steady speed. Computer studies have shown that the response of the motor is particularly sensitive to changes of angle and saturation criteria. A difference of 2° can significantly alter the form of response as is shown in Figure 5.10. At an angle of $\theta=-8^{\circ}$ the response is underdamped and oscillatory but at $\theta=-6^{\circ}$, the response is critically damped. A change in the starting position of commutation by as little as 1° can alter the matching of the results. At 1800 rev/min, a time delay of 0.1 mS was equivalent to the rotor moving through an angle of 1°. The design of the first triggering circuit was such that time delays of this magnitude were feasible. Saturation effects may also prevent accurate matching and as a test of the sensitivity of the model, a simulation was repeated using different saturation criteria. The effect of a $\pm$5% change in the maximum value of $\hat{M}_{iA}$ (at I_{iA} = 2 A.) can be clearly seen in Figure 5.11. Curve (c) was obtained using the saturation curve of Figure 3.3 (b) while curves (f) and (g) were produced by the above +5% and -5% displacements respectively. Curve (f) is oscillatory but curve (g) is overdamped.

Nevertheless, the model may be used to distinguish those areas of operation in which the performance of the motor is undesirable from the point of view of stability. The model can predict the performance of the t.a.c. machine with sufficient accuracy over a wide range of operating conditions.

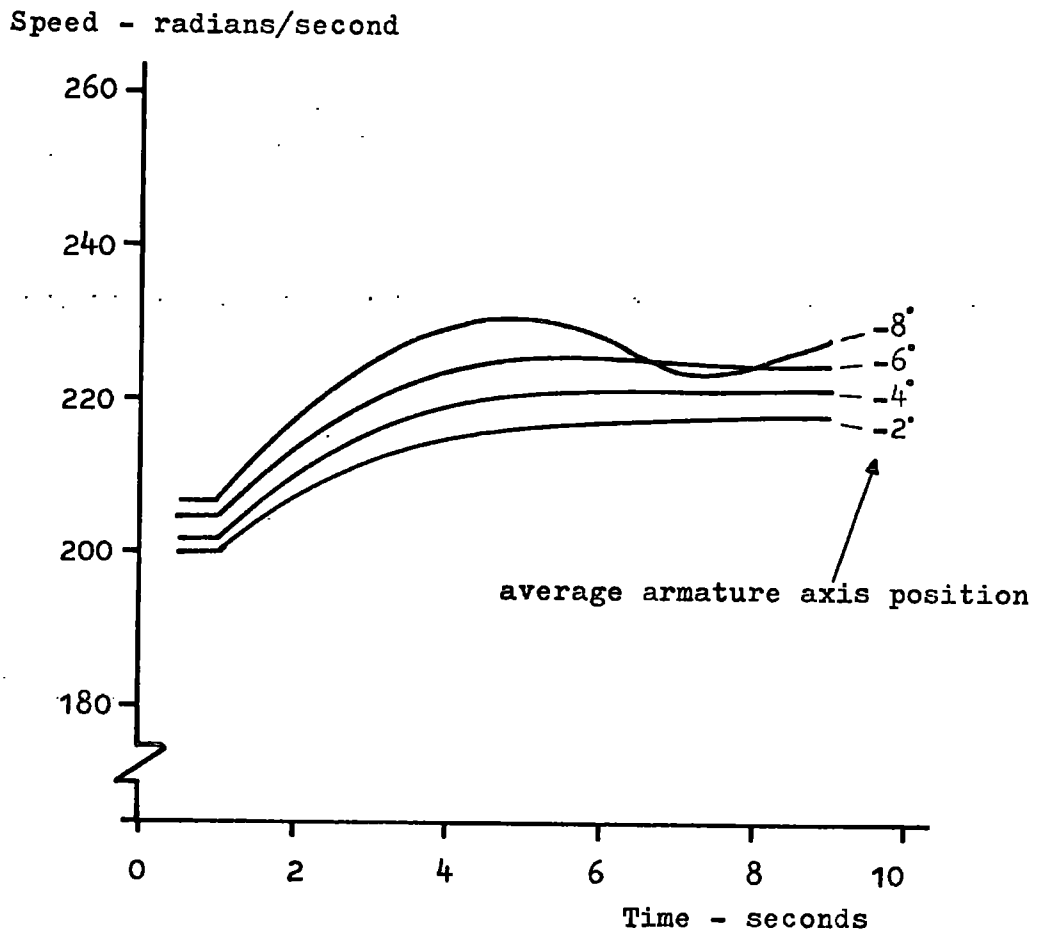

Fig. 5.10 Motor Speed Responses - Critical damping

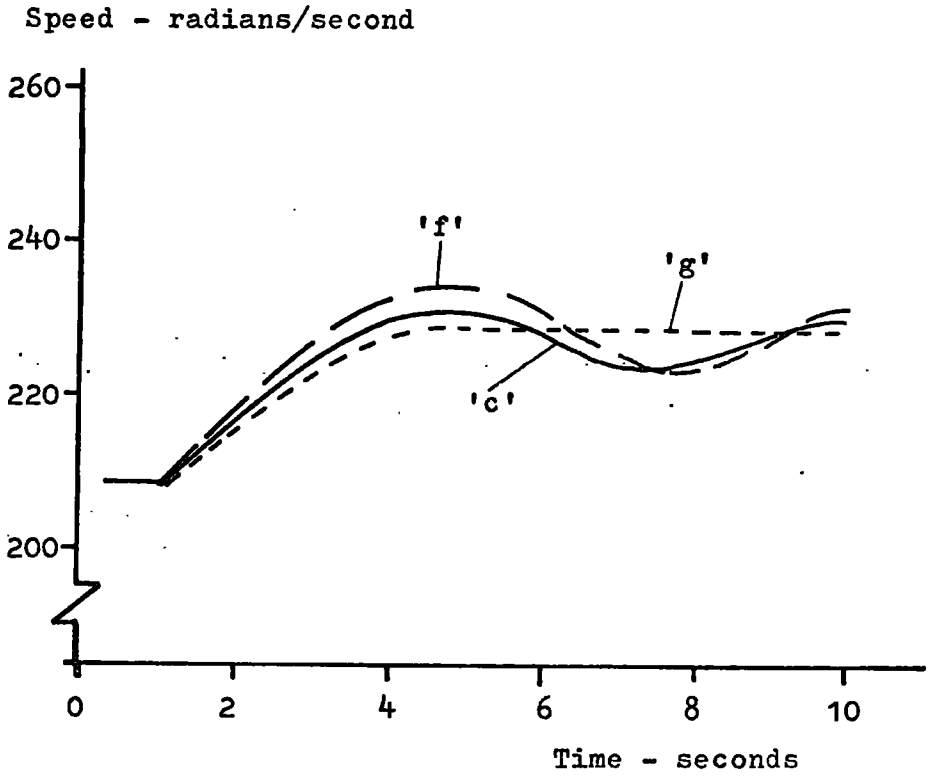

Fig. 5.11 Motor Speed Responses - Small Saturation Changes

5.5 Commutating Ability of Machine

At low speeds (below 50 rev/min) and at starting the interpole induced voltage is insufficient to ensure complete commutation of the armature current. Commutation is completed by the brushes as in a conventional d.c. machine. During this period the commutation process is usually accompanied by slight sparking at the trailing edge of the brushes. To determine the speed range over which the t.a.c. machine can operate it is necessary to be able to compute the commutating ability of the machine. That is, to be able to compute the range over which the interpole induced voltage is always sufficient to commutate the current in the armature before the brush leaves the segment.

This range may be calculated by using the voltage equation for the armature shorted turns -

$$V_c = \hat{M}_{fc} \cdot pI_f - \hat{M}_{ic} \cdot \omega \cdot I_{ia} + 2\hat{M}_{ac} \cdot \omega \cdot I_{ia} + R_c \cdot I_c + \hat{L}_c \cdot pI_c$$

(series interpole excitation)

The time required for the reversal of the armature current is evaluated and compared to the time between the start of each commutation period. The maximum ratio of these two times depends upon the brush - segment geometry and is given by (s-2b)/s where s is the segment arc and b the brush arc.

The commutating ability of the experimental machine was computed from the above equation and is given in Figure 5.12 for two values of armature current. The maximum ratio is 0.71 for the machine and from the curves, the machine should be able to commutate satisfactorily down to about 35 rev/min. In practice, slight sparking was observed up to about 40 - 45 rev/min.

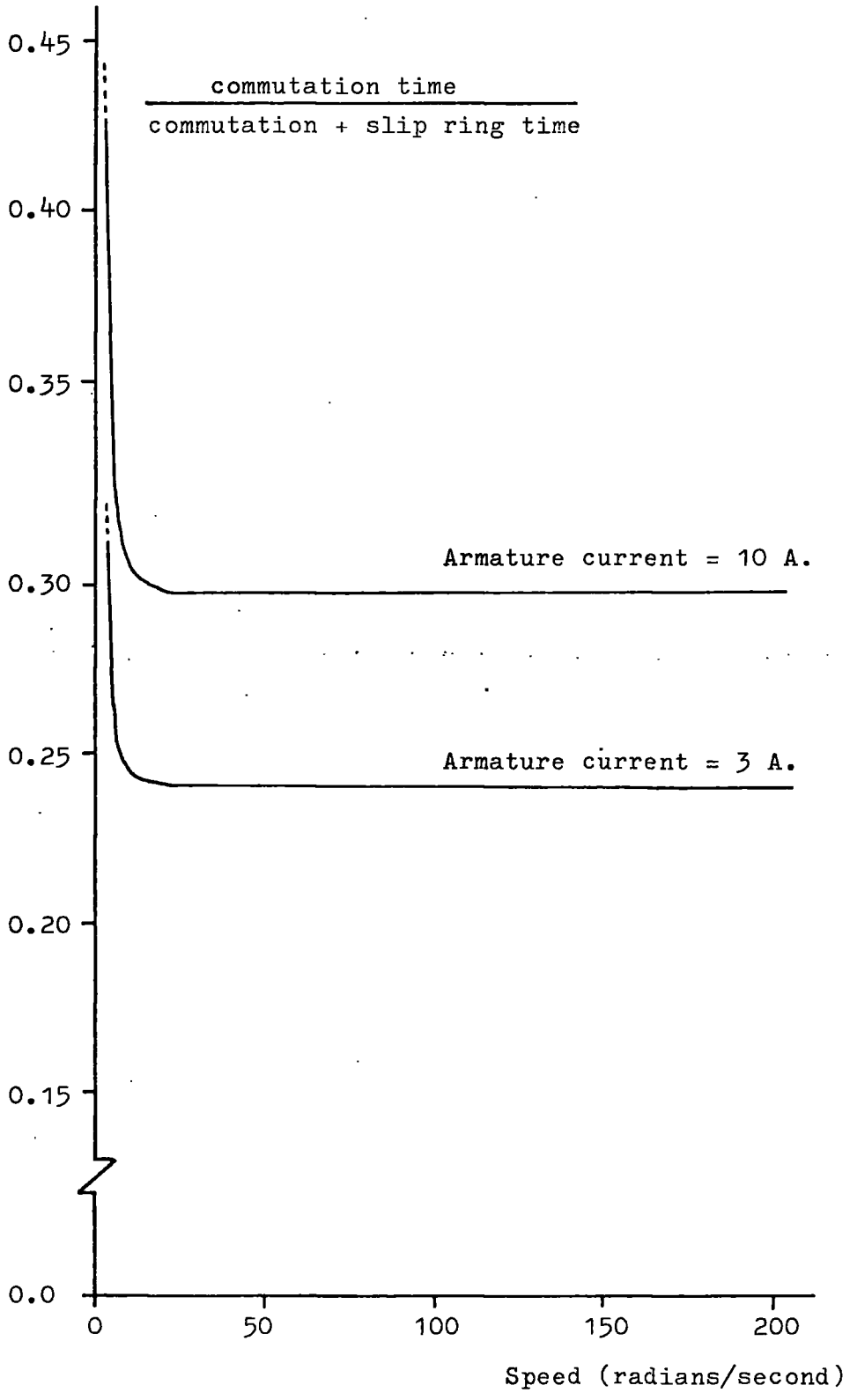

Fig. 5.12 Computed Commutating Ability of Motor

(series interpole)

Chapter 6 Discussion on the Speed Oscillations

6.1 Comparison with Conventional Machines

Moullin [6.1] discusses the possibility of speed oscillations occuring in conventional d.c. machines and shows that a prime cause is the demagnetising effect of the armature mmf. This causes the motor speed to rise with increasing armature current if the machine is operating under such conditions that the speed rises with decreasing field flux. The motor thus has a rising speed characteristic. Should the armature current increase for any reason, the torque developed will be in excess of the load requirement and the system will be accelerated. This increase of speed causes more armature current to flow which, in turn, increases the speed still further. The speed and current tend to rise towards infinity until the motor protecting devices (e.g. fuse) prevent any further increase. However, if the load torque also increases with speed it will tend to counteract the rising nature and it is feasible for the motor to hunt about a fixed speed. The hunting is clearly dependent upon the motor and load torque characteristics and a rising characteristic is necessary.

In the t.a.c. machine, the armature axis may be considerably displaced from the neutral axis and the demagnetising effect of the armature mmf will be considerably larger. With the axis displaced from the neutral axis speed and current oscillations were recorded in the experimental machine with series connected interpoles. Hunting could occur for the same reasons as above but in the experimental motor it was saturation and not load torque requirements that prevented excessive speeds and currents. Initially, the speed and current rise as described above but eventually saturation prevents the armature mmf from any further proportional increase and the current begins

to fall as the speed approaches the value set by the overall flux. As the current falls, the demagnetising mmf becomes smaller tending to slow the motor. The motor thus requires less current. The process is cumulative and the speed and current reduce still further. Eventually the current falls to zero where it is prevented from going negative by the diode action of the thyristors. The speed falls due to load and frictional torques until the thyristors become forward biased and the cycle repeats.

The cause of hunting is similar in the t.a.c. machine and in conventional machines and is due to a rising speed-torque characteristic produced by the demagnetising effect of the armature mmf. The effects are likely to be more pronounced in the t.a.c. machine because of the greater displacement between the armature and neutral axes.

6.2 Methods of Prevention of Speed Oscillation

The demagnetising effects of the armature mmf may be compensated by including an extra winding on the field system of a conventional machine. This winding is series connected with the armature and produces a magnetising flux that just counteracts the demagnetising amature flux. The rising characteristic does not then occur and hunting is prevented. Such a winding may also be used in the t.a.c. machine but, for exact compensation, the strength of the compensating winding would be dependent upon the relative position of the armature axis. Although this winding could be designed to prevent oscillation of the motor speed it could also produce a severe droop in the speed torque curve if the armature axis position was behind the neutral axis. Such a method is hardly satisfactory and other methods of preventing oscillations were considered.

In Chapter 4 the equation of motion of the t.a.c. motor using overwound, series excited interpoles had the approximate form

$$\frac{d^2\omega}{dt^2} + \frac{R_{iA} + 2\cdot\hat{M}_{iA}\cdot\sin\theta\cdot\omega}{\hat{L}_{iA}}\cdot\frac{d\omega}{dt} + \frac{(M_{fA}\cdot I_f)^2}{L_{iA}\cdot J}\cdot\omega$$

$$= \left(-V_{iA} - \frac{R_{iA}\cdot T}{I_f\cdot\hat{M}_{fA}}\right)\cdot\frac{\hat{M}_{fA}\cdot I_f}{\hat{L}_{iA}\cdot J}$$

or

$$\left(D^2 + 2\cdot\gamma\cdot D + \beta\right)\cdot\omega = k$$

where γ is the damping factor and is

$$\gamma = \left(R_{iA} + 2\cdot\hat{M}_{iA}\cdot\sin\theta\cdot\omega\right) \Big/ 2\cdot\hat{L}_{iA}$$

The response of the motor depends upon the numerical value of γ and as long as γ has a positive value, no matter how small, a steady state result will always be obtained. The first condition for a final steady state speed is

$$R_{iA} + 2\cdot\hat{M}_{iA}\cdot\sin\theta\cdot\omega > 0$$

If $\gamma \gg 0$, the response is very overdamped and as γ is reduced the response becomes progressively less damped until, at $\theta = 0$, continuous oscillations will occur - there being no damping present. Taking as the limiting case $\theta = 0$, the variation of speed with angular displacement (θ) of the armature and neutral axes was of the form of a rectangular hyperbola - Figure 6.1. The limiting boundary depended upon the magnitude of the armature resistance and the armature and interpole current. Stable operation was obtained if the operating point lay below the respective boundary. For stablity at high speeds a low value of θ was required and vice versa.

The condition for stability as given by the above expression

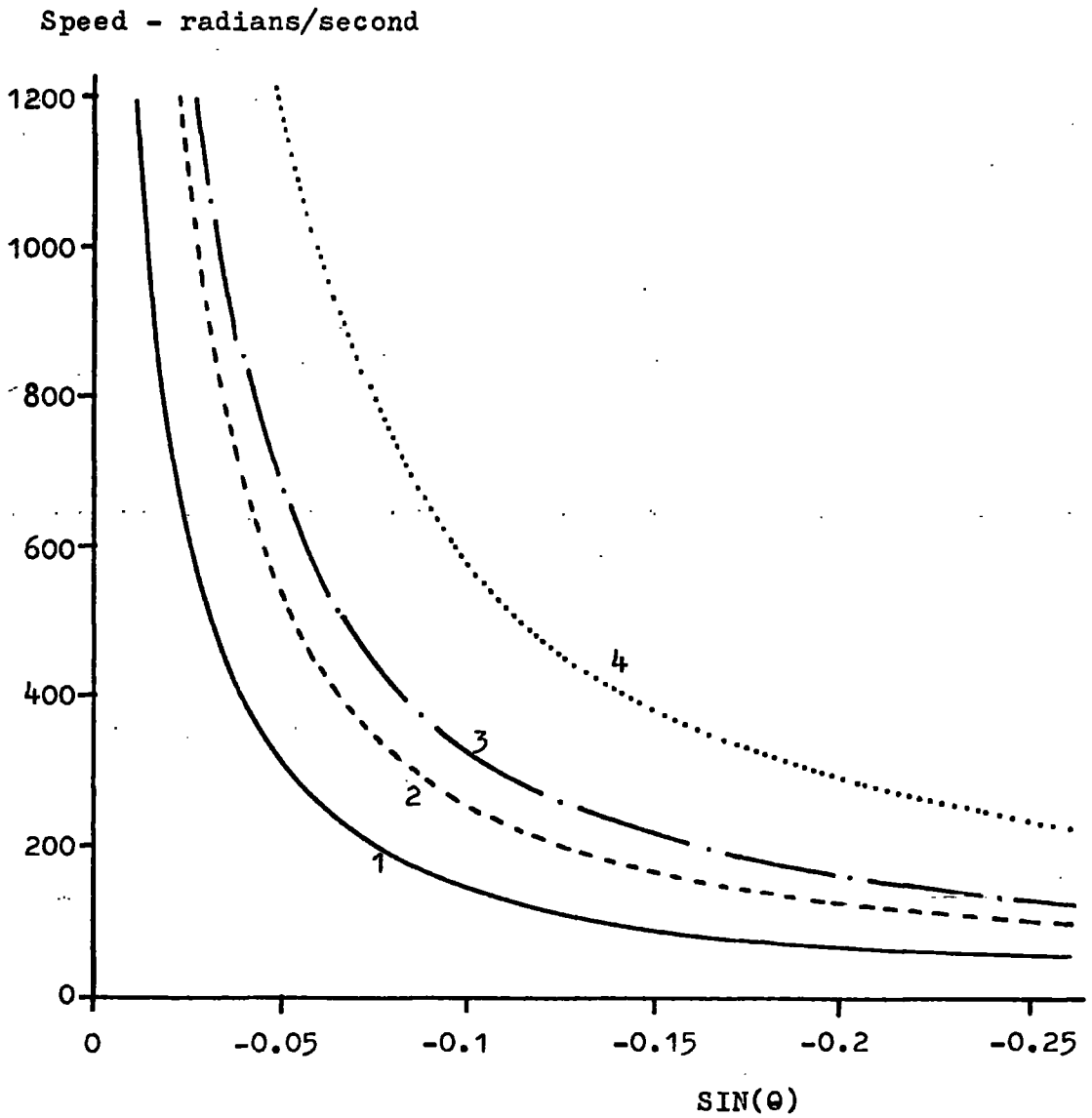

1 armature resistance 2.6 ohms, armature current 2 A

2 armature resistance 2.6 ohms, armature current 10A

3 armature resistance 6.0 ohms, armature current 2 A

4 armature resistance 6.0 ohms, armature current 10 A

Fig. 6.1 Limiting Speeds for non-oscillatory responses

may be plotted as a single straight line boundary as shown as line 'a' in Figure 6.2. Stable operating points lie above and to the left of this line; unstable points to the right and below the line. The degree of stability of an operating point may be judged by its distance from the line. A very overdamped stable response will be in the upper left of the figure whereas a damped but oscillatory response will be just above the line.

Typical loci of stable responses - loci 'e' and 'f' - and of unstable or oscillatory responses - loci 'r' and 's' - were plotted on Figure 6.2. The stable responses crossed the boundary into the unstable region as given by the expressions above. It is possible to construct a modified boundary - line 'b' - such that stable points existed only to the left of this new line while the loci of unstable or oscillatory responses existed in both regions. The modified boundary always lies to the right of, and below that given by the damping term in the approximate equation of motion. It is only possible to construct the modified boundary from the results of either practical measurements or from a simulation of the motor.

6.3 Discussion of the Stability Criteria

The inclusion of more terms into the equation of motion of the motor would tend to move the modified boundary nearer to that predicted by the theory. The approximate equation does not account for interaction between the voltages and currents of the field and armature circuits. For example, there is a slight transformer coupling between the field and armature which imparts to the motor a better performance than that that would be predicted by the simple equation. The effect of this coupling may be observed by simulating on the computer model the responses of the motor with and without this

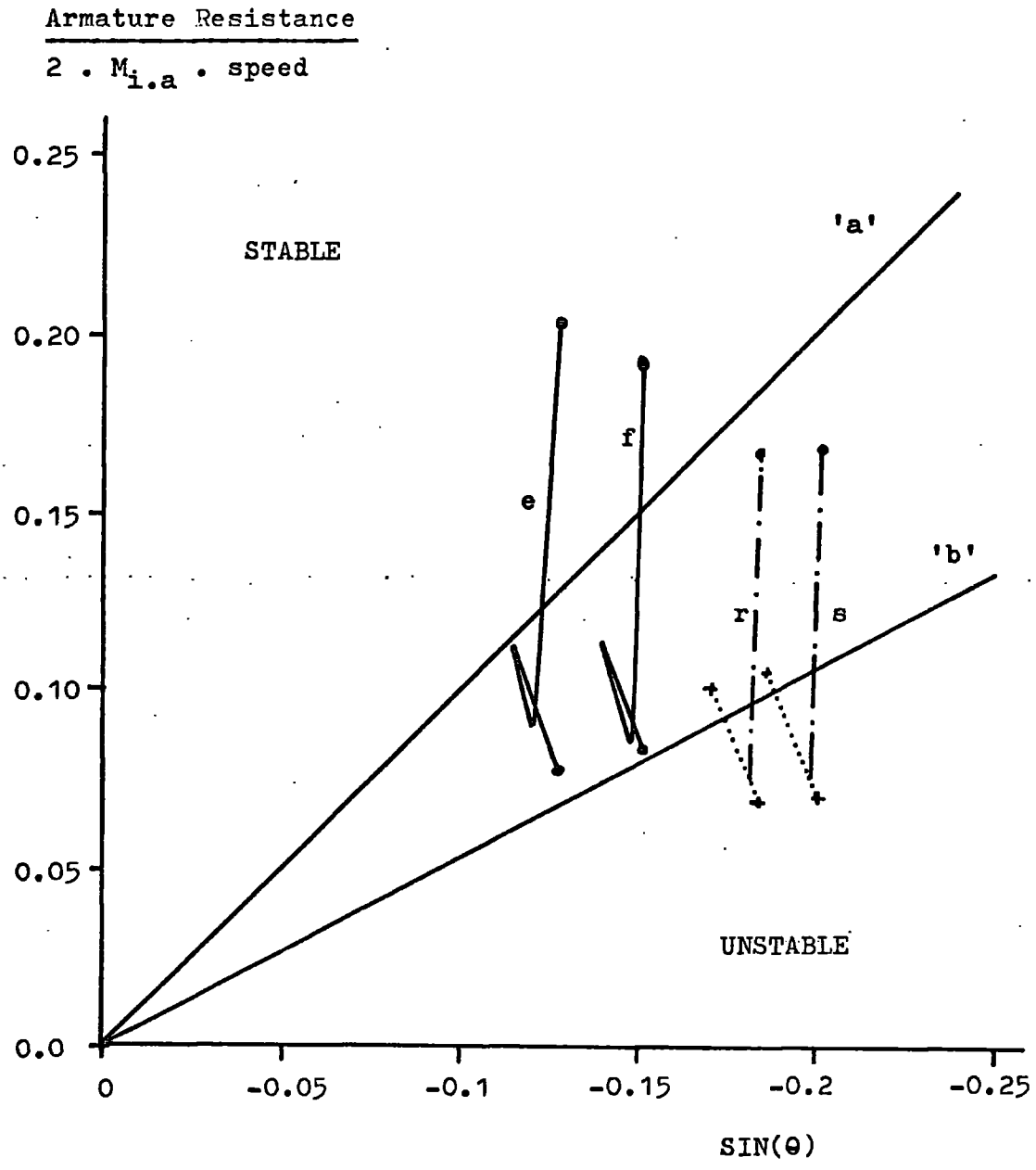

e, f loci of stable responses

r, s loci of unstable responses

Fig. 6.2 Stable and Unstable Operating Zones

coupling term included. Without the term the oscillations were of a higher frequency and of a different waveshape compared to those obtained with the term included. In Figure 6.3 the inclusion of this term predicts that a steady state result will eventually be obtained whereas without it, the model predicts that the motor speed will continuously oscillate.

There are other terms that are not included in the simple differential equation and which also affect the overall response. Nevertheless, the use of this simple equation and of the average values of the motor parameters can give an indication of the liklihood of stable operation.

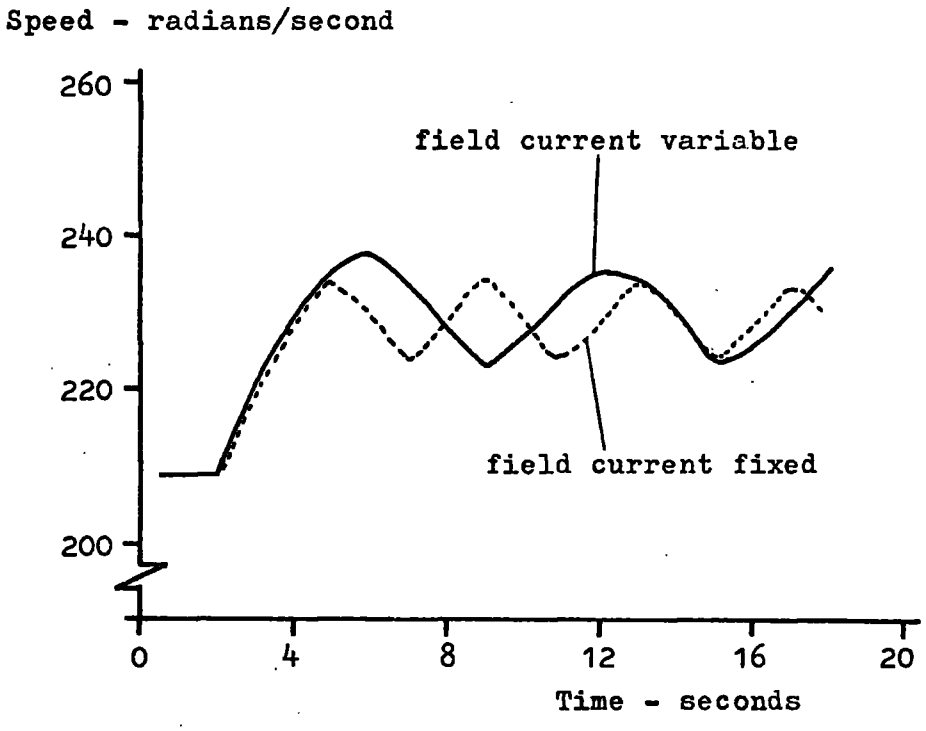

(a)

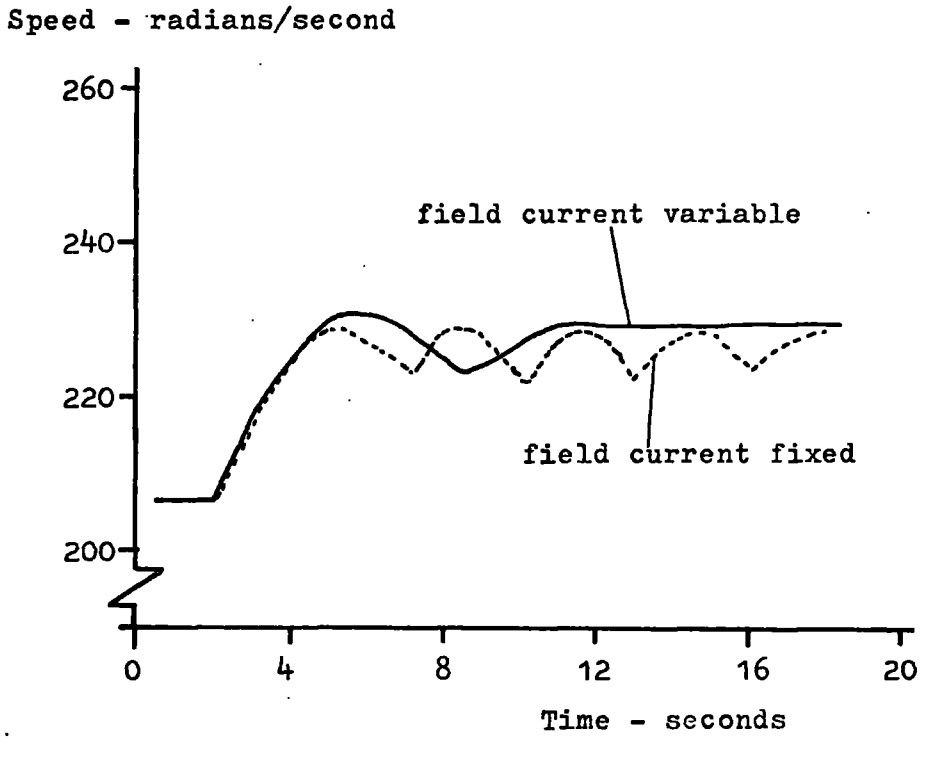

(b)

Fig. 6.3 Motor Speed Responses - Effect of Coupling Term between armature and field windings

Chapter 7 Control of the T.A.C. Machine by Delayed Thyristor Firing

7.1 Effect of Delayed Thyristor Firing

For all commutator machines it is a general rule that the direction of the armature mmf and flux is determined by the position of the brushes on the commutator. If the brushes are displaced from the neutral axis by an angle θ, the armature axis would also be displaced by this angle. The total flux now acting on the armature is a combination of the field and the interpole fluxes. Depending upon the positions of the brushes and the mode of operation of the machine, the interpole flux contribution may assist or detract from the main polar flux. In conventional machines it is the commutation process that dictates that the brush positions be restrained close to the neutral or quadrature axis.

With thyristor assisted commutation, the commutation process is not performed by the brushes. These only act as a means of passing current into and out of the armature winding. As long as the current in part of the armature is reversed before the brush leaves an active segment, there will be no sparking at the brushes. The use of an overwound interpole, a separately excited interpole or even part of the main field pole can all bring about commutation. There is, therefore, no reason why the output of the machine cannot be controlled, at least over a limited range, by shifting the position of the armature axis away from the neutral axis.

7.2 Practical Method of Moving Axis

The displacement of the armature axis from the neutral axis may be achieved in one of two ways. The first is to alter the time of

commutation and the second is to change the angle at which the commutation process starts. If the time of commutation is made variable by altering the strength of the interpole current then it is not possible for the average armature axis position to be behind the neutral axis. By definition, commutation is deemed to be taking the whole of the available angle when the average axis position lies along the neutral axis. For the axis to be behind the neutral axis commutation must be taking more than the available angle and sparking at the brushes will, most certainly, be seen.

If the angle of commutation is made small (20% of the maximum angle) then by controlling the start of this small commutation band the average armature axis position can vary over a fairly wide range about the neutral axis. Since the band is small, sparking will not occur unless the start of the band is so near the end of a segment that commutation is not completed before the brush leaves the segment. With a series connected interpole the degree of overwinding was not sufficient to make the angle of commutation very small. By using a constant, separate interpole excitation a small commutation band could be obtained for light loads (0.4 rated and below) thus enabling a preliminary investigation of the method to be made. The limitations caused by loading effects are discussed in a later section.

A practical method of shifting the armature axis is to use rapid commutation and to adjust the starting position of the commutation process. The brushes were left physically along the neutral axis but, by triggering the thyristors only a variable time delay, their effective positions could be readily changed. The armature axis position is being changed by electronically rocking the brushes by delayed thyristor firing.

7.3 Motor Characteristics - Light Loadings

For steady state, light load conditions the speed - field current characteristics are shown in Figure 7.1. Figure 7.1 (a) is for series excited interpoles and at low field currents, the steady state speed with minimum delay time degenerates in to a continuous oscillation about a mean value. The speed response of the motor depended upon both the delay time and the value of the field current. The delay time alters the relative position of the armature axis and the kind of speed responses are very similar to those shown and discussed in chapters 4 and 5.

Figure 7.1 (b) shows the speed - field current response for the motor with a separately excited interpole (I_i = 10 A). The range of control was much greater than that obtainable with series excitation but this must be qualified by the effects of loading which will be discussed in the next section. The speed response of the motor with separate excitation was overdamped for all values of delay time. Unfortunately, with separate excitation, the maximum armature current is limited to a value some 1.4 times the interpole current. To exceed this value would cause sparking owing to commutation failure. To keep within this figure large step changes must be made in two steps and the response time becomes much longer.

The linearity between the input voltage to the thyristor delay control unit (chapter 8) is given in Figure 7.2. Over the range indicated in the figure, a linearity of 2% or better was obtained using separate interpole excitation but of only 5% using series interpole excitation. A reason for this is the much smaller and more well defined zone of commutation obtained by using separate excitation.

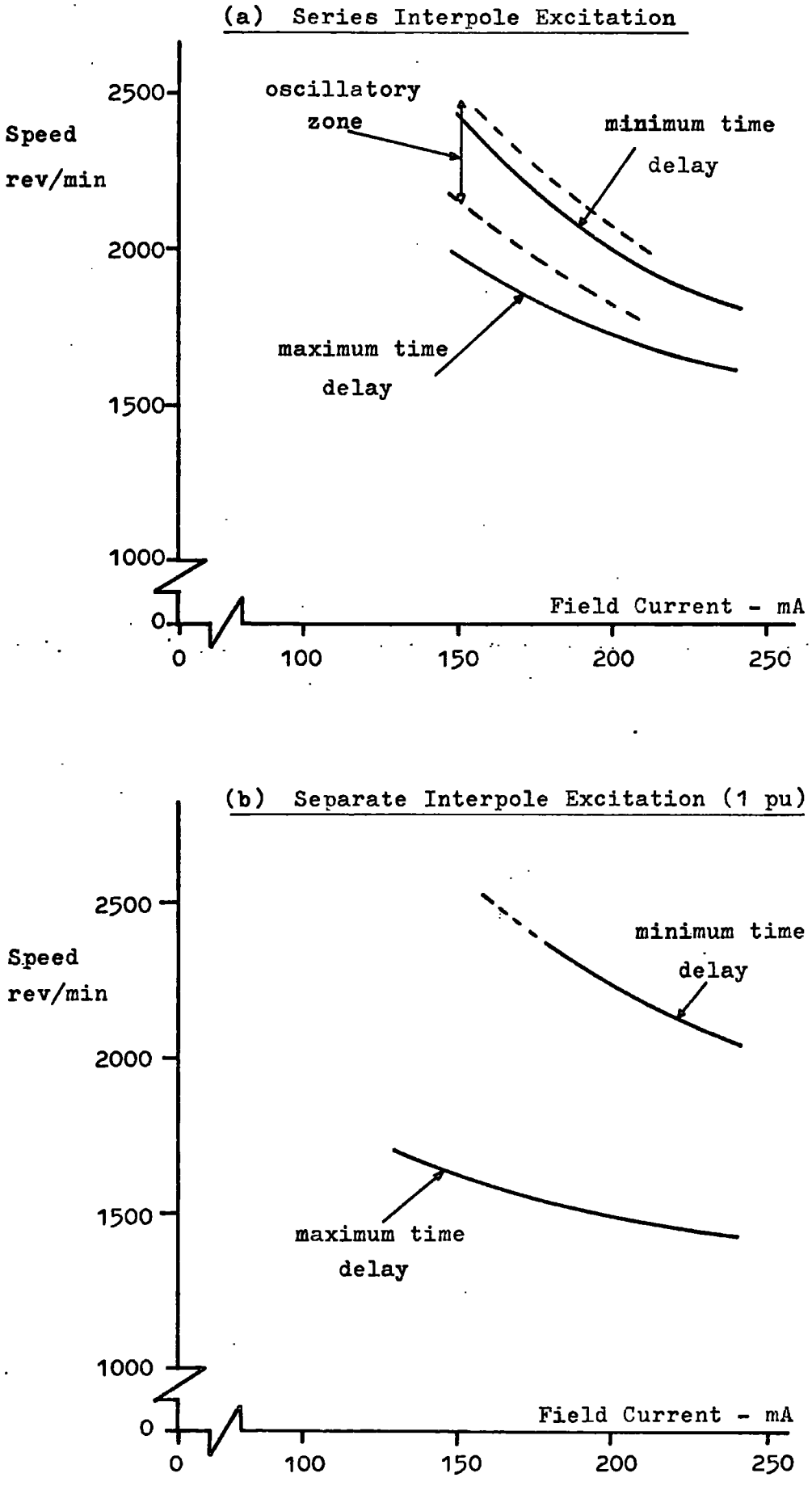

Fig. 7.1 Speed - Field Current Characteristic of Motor

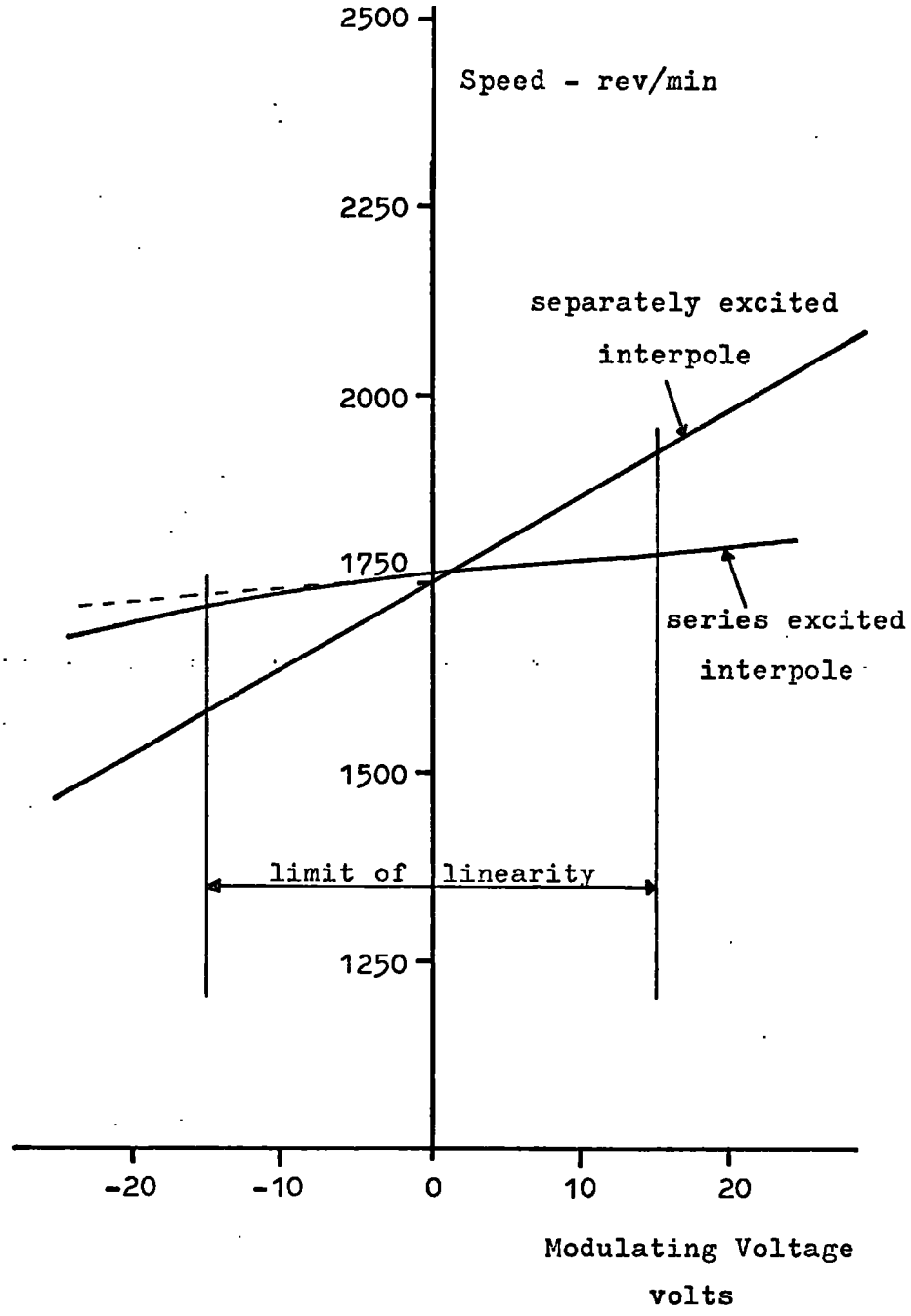

Fig. 7.2 Linearity of T.A.C. Motor Control

7.4 Effects of Loading on Motor Control

7.4.1 Commutation Angles

The previous sections indicated the range of control possible with separate interpole excitation when the motor was running on light loads. This range cannot be obtained with greater loadings because of the limitations imposed by the commutation of the higher currents and by the overall speed-torque characteristics of the motor. Figure 7.3 shows the measured commutation angle as a function of the armature current for a constant interpole current of 10 amperes. The commutation angle was measured with minimum and maximum firing delay times. Minimum delay corresponds to the thyristors being fired as soon as the brush is fully on the segment while maximum delay means that the firing is delayed so that commutation just finishes before any part of the brush leaves the segment. The points for maximum and minimum delay all lie about the same curve and by extrapolating the curve, the maximum commutable current is about 16.5 A. This value has been confirmed by experiment. The commutation angle is independent of delay time but very dependent upon the armature current. For small loads (say 3 A) commutation is completed in 2^{o} allowing the axis to lie within the range $\pm 15^{o}$ around the neutral axis. At rated current this range is reduced to $\pm 11^{o}$ and above the rated current, the range falls rapidly to zero for a current of 16.5 A.

7.4.2 Speed - Torque Characteristics

From the machine equations the steady state voltage and torque for the experimental machine are

$$V_A = \hat{M}_{fA} \cdot \omega \cdot I_f + R_A \cdot I_A + \hat{M}_{iA} \cdot \sin\Theta \cdot \omega \cdot I_I$$

$$T_{orque} = \hat{M}_{fA} \cdot I_f \cdot I_A + \hat{M}_{iA} \cdot \sin\Theta \cdot I_I \cdot I_A$$

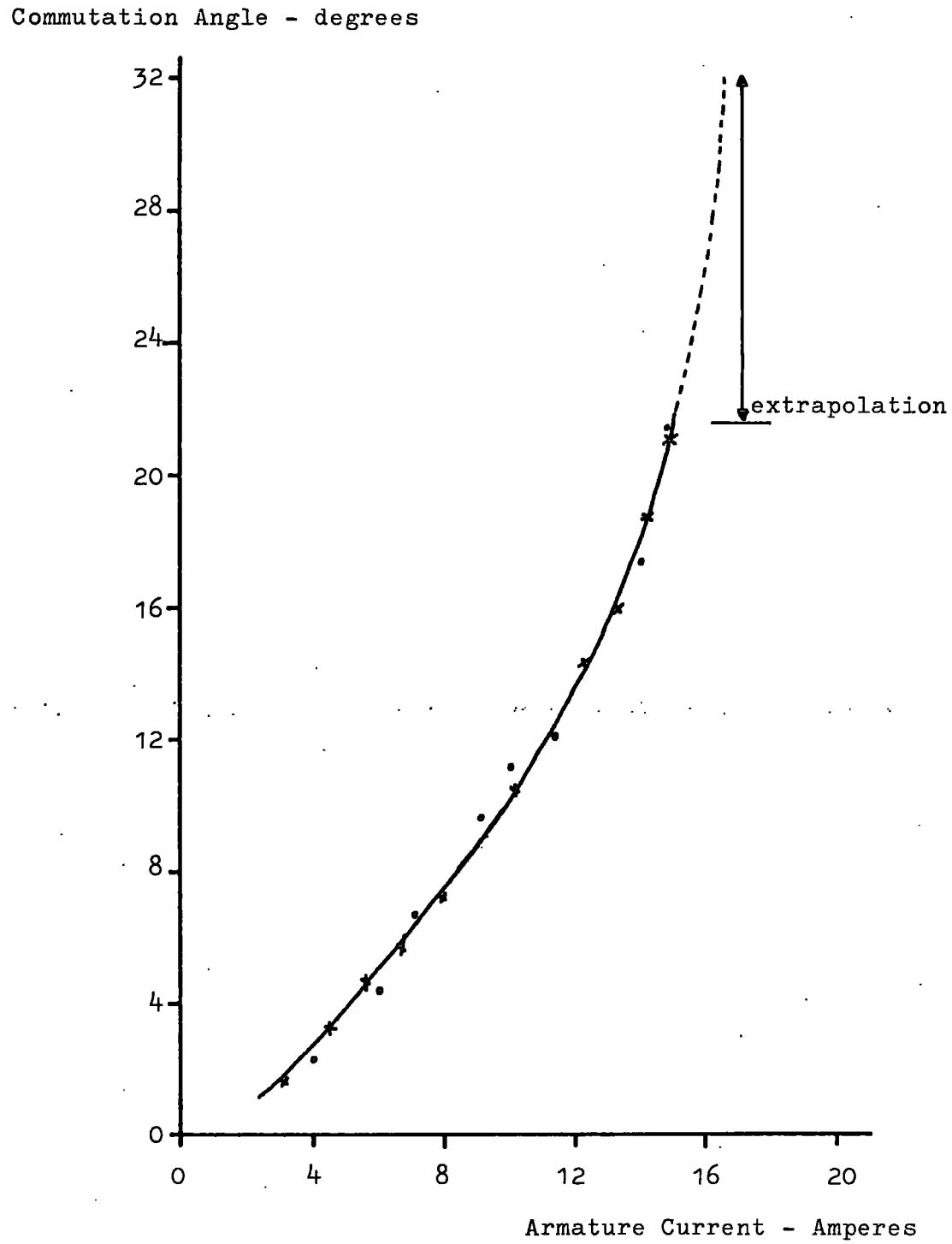

Fig. 7.3 Commutation Angle - Separate Interpole Excitation

With $\theta=0^{\circ}$, the speed - field current characteristics for a range of torque may be computed. Neglecting for the moment the restriction that only currents below 16.5 A can be commutated, Figure 7.4 shows the speed - field current characteristics using typical values of the machine's parameters. At high torques (>60 Nm) the speed falls as the field current is reduced while at lower torques and high field currents the characteristics have a rising nature. Also shown on the figure is the constant current line of 16.5 A i.e. the maximum current that can be commutated. For the experimental machine, its speed - field current characteristic is of a rising nature over its normal operating range.

Considering only this range the effect of introducing the maximum variation of the armature axis position was computed. The maximum variation is, of course, reduced at the higher torques in accordance with the curve shown in Figure 7.3. Figure 7.5 gives the computed speed - field current characteristics for constant torques of 0, 5 and 10 Nm. Figure 7.6 gives the speed - torque characteristics for constant field currents of 0.125 and 0.275 A. From these figures, the range over which the motor speed may be controlled depends upon both the load torque required and upon the field current. The available speed range at rated output is 50 to 70% of that at light or no-loads for the experimental machine.

Of particular note is the large speed reduction with load torque using minimum delay and the small change with maximum delay. This occurs since the commutation angle increases at the higher currents and the mean armature axis moves towards the neutral axis. The speed torque characteristics for minimum and maximum delay thus approach those for the 'normal' machine. This can be clearly seen in Figure 7.6.

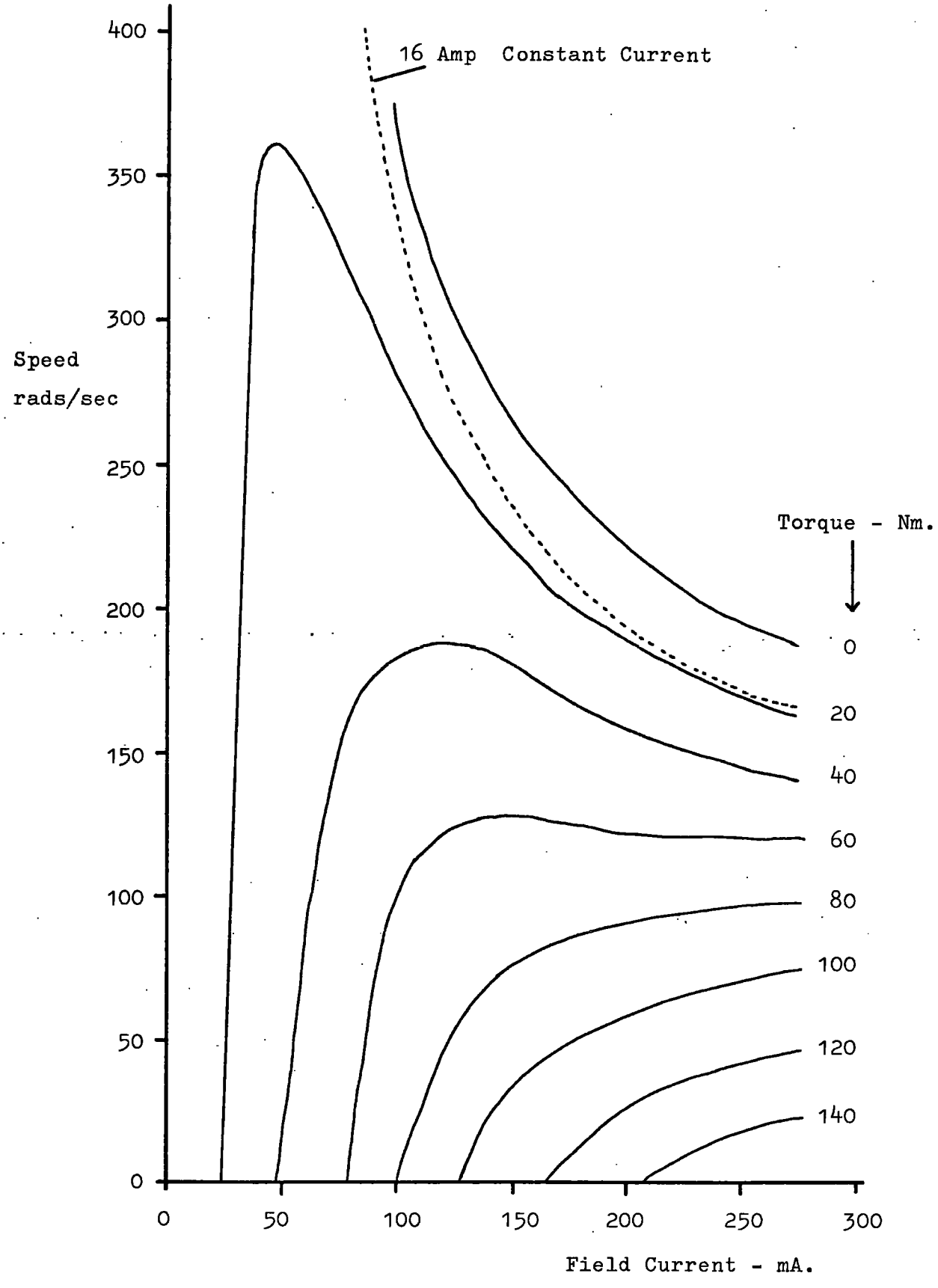

Fig. 7.4 Speed - Field Current Characteristics of Motor

(Separate Interpole Excitation)

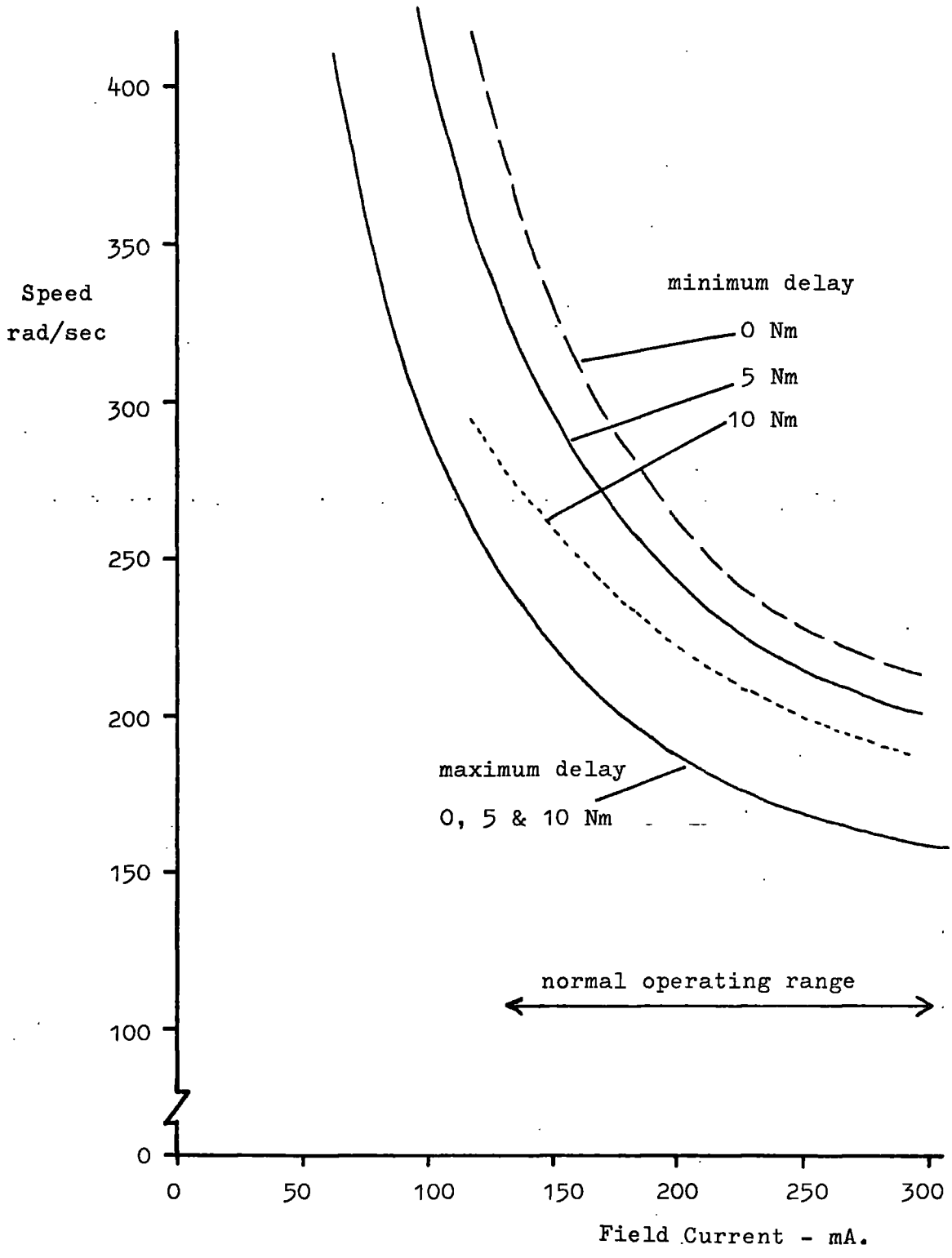

Fig. 7.5 Speed - Field Current Characteristic of Motor

(Separate Interpole Excitation)

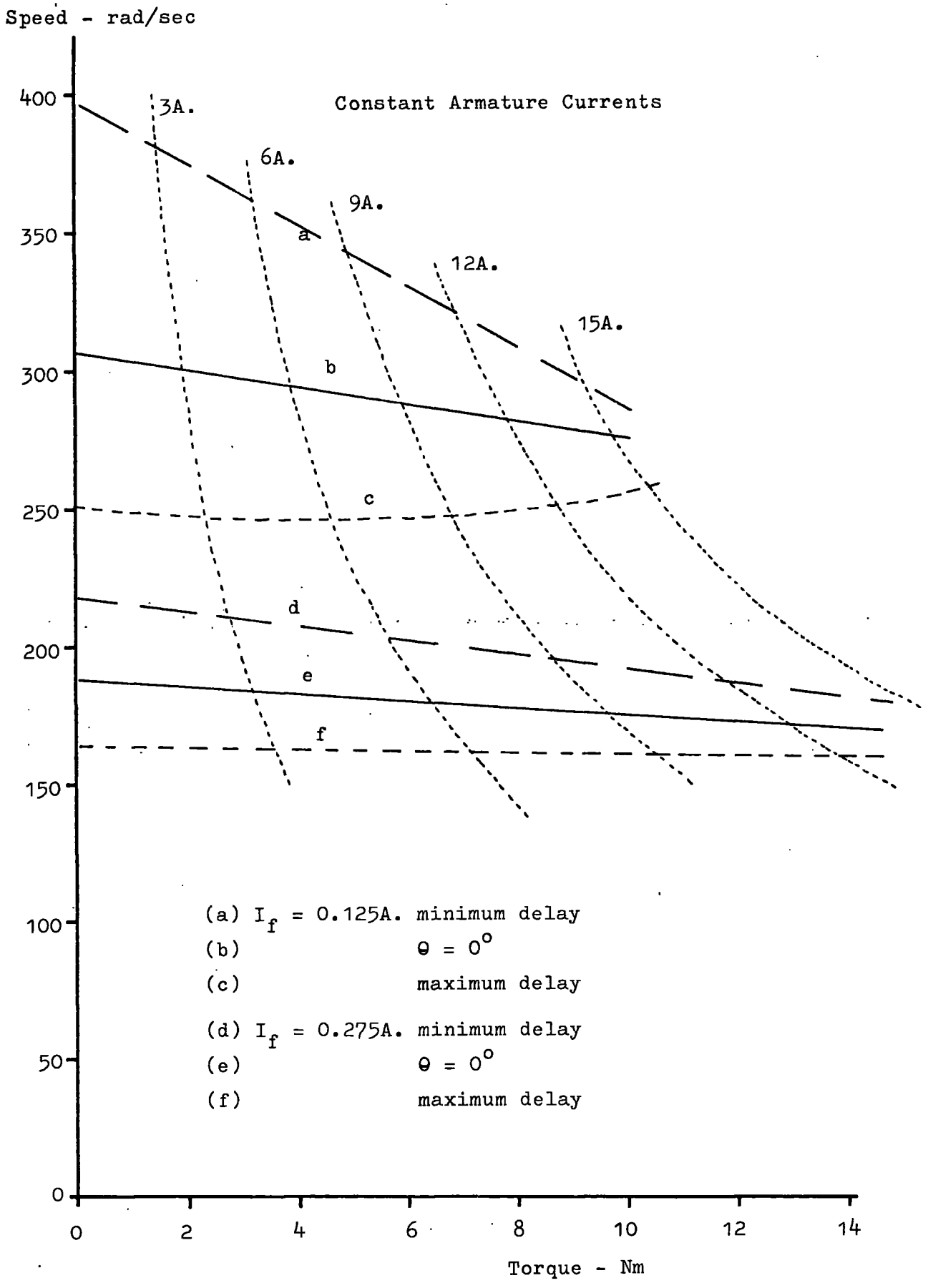

Fig. 7.6 Speed - Torque Characteristics of Motor

(Separate Interpole Excitation)

The range of control of the t.a.c. machine is not constant when using the thyristor delay method. It depends upon the nominal speed torque and speed - field current characteristics and upon the commutating ability of the machine. For the experimental machine only, a range of at least $\pm$7% in the motor speed has been demonstrated for loadings of rated value and below.

7.5 Generator Characteristics

The no load or open circuit characteristic of the t.a.c. generator using a separately excited interpole is shown in Figure 7.7.. The strong interpole acts as an auxiliary field pole and its effect is determined by the relative position of the brushes. With minimum firing delay the interpole assists the main pole to produce a larger output voltage. The converse is true for maximum delay. With series interpole excitation there is no interpole contribution under open circuit conditions and the output voltage is therefore independent of firing delay. The effects of loading are given in Figure 7.8 and, as in the motor, they cause a reduction in the range of control.

7.5.1 Generator Response

The response of the t.a.c. generator to a change in the effective brush positions was compared to an equivalent change in the field current. A constant, separately excited interpole (I_i = 10 A) was used and the desired changes of voltage were

(i) from 0.5 to 0.75 p.u.

and (ii) from 0.5 to 1.0 p.u.

The waveforms of the output voltage are shown in Figure 7.9 . The response using thyristor firing delay was about two orders of magnitude faster than those obtained using field current control. Tests have

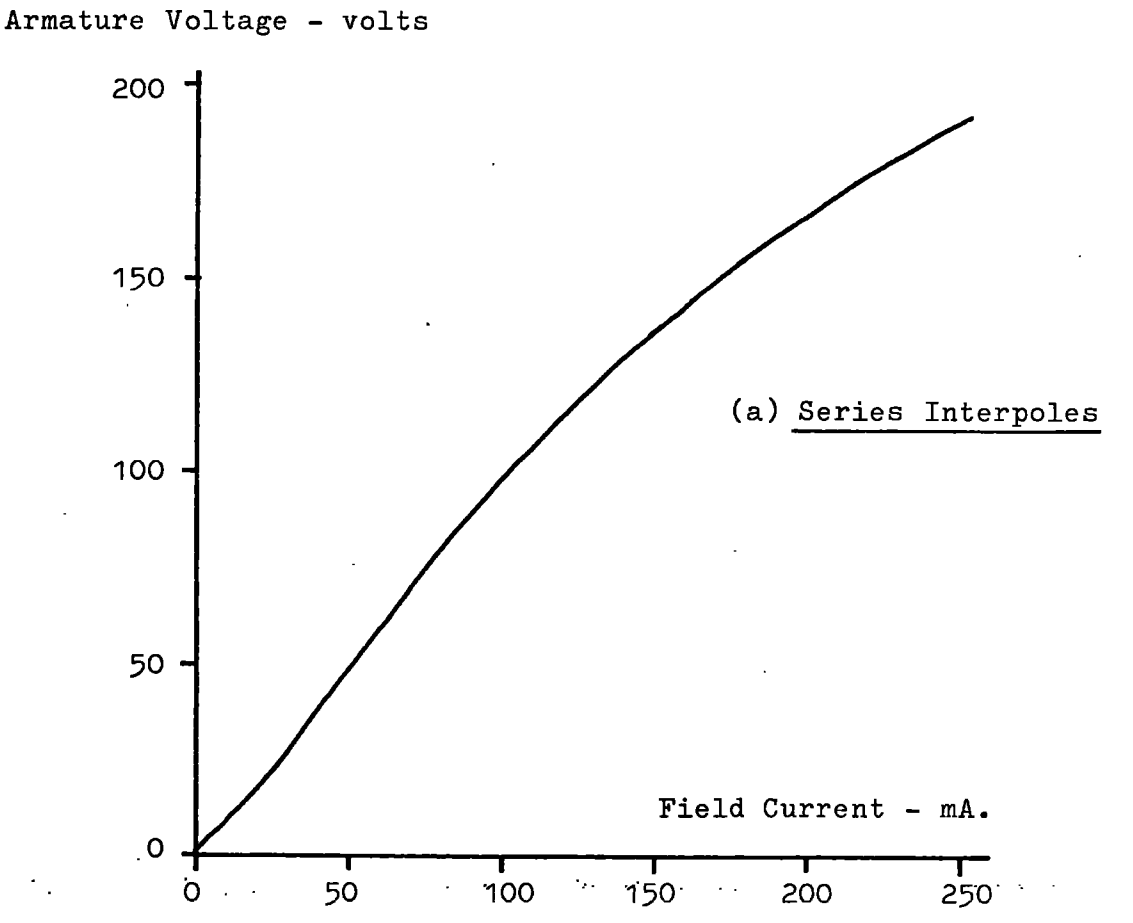

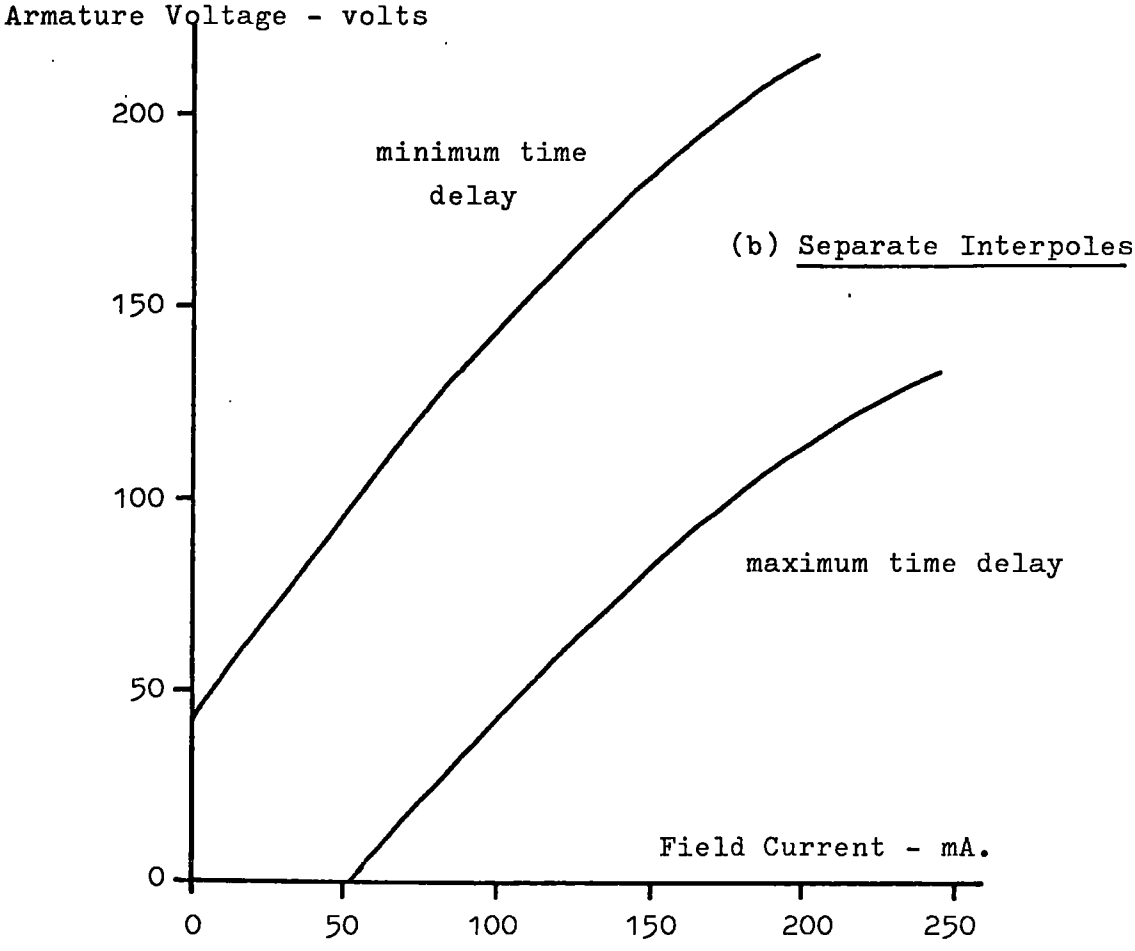

Fig. 7.7 Open Circuit Characteristic of Generator

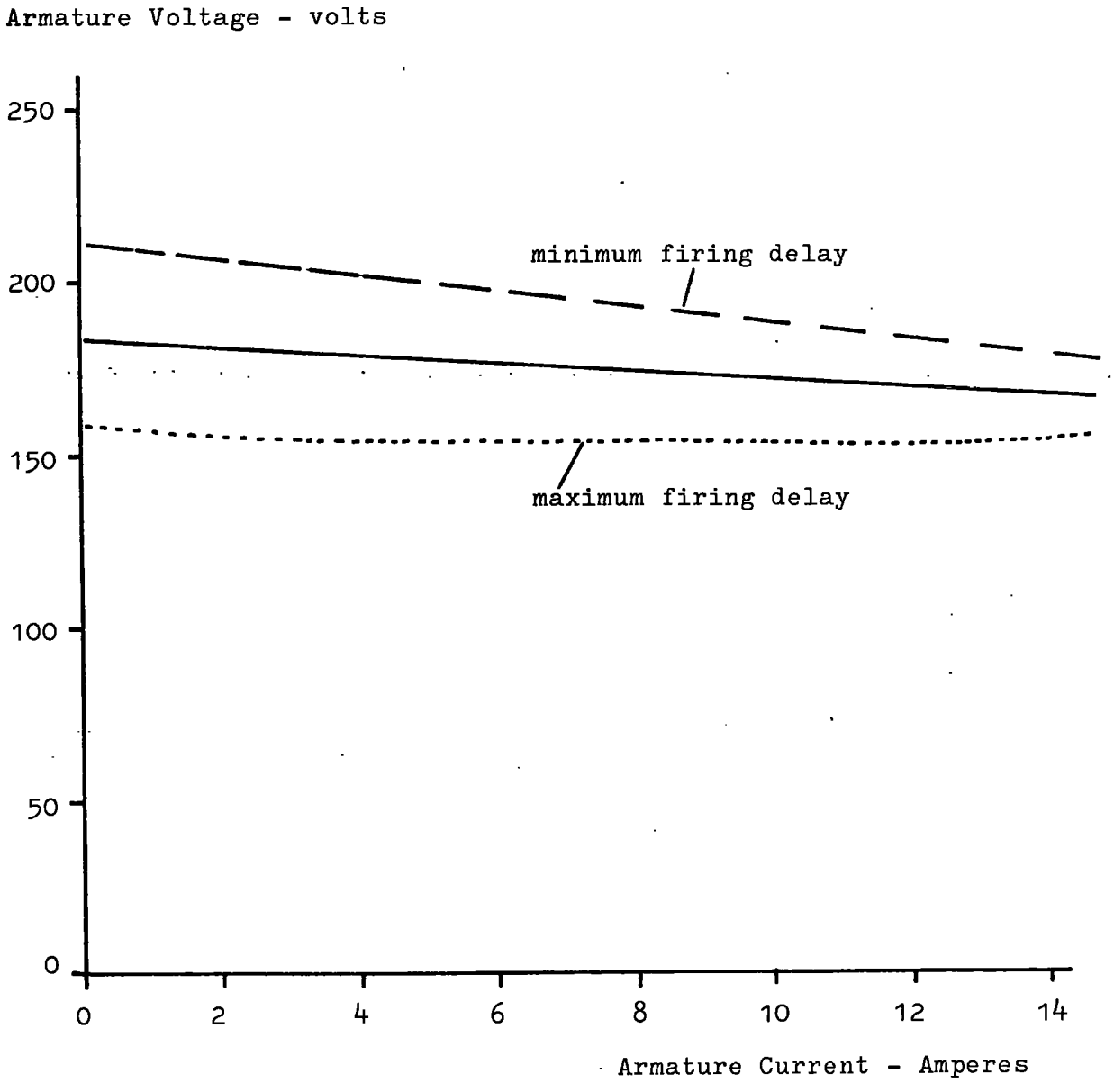

Fig. 7.8 Generator Voltage - Current Characteristics

(separate interpole excitation)

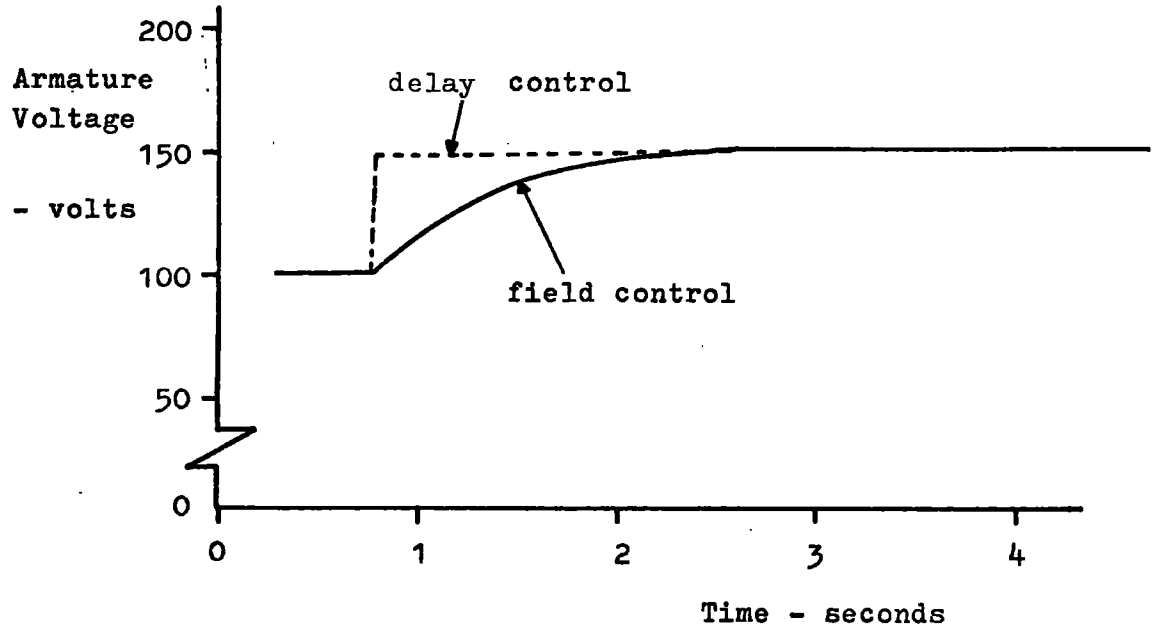

(a) Voltage change from 0.5 to 0.75 p.u.

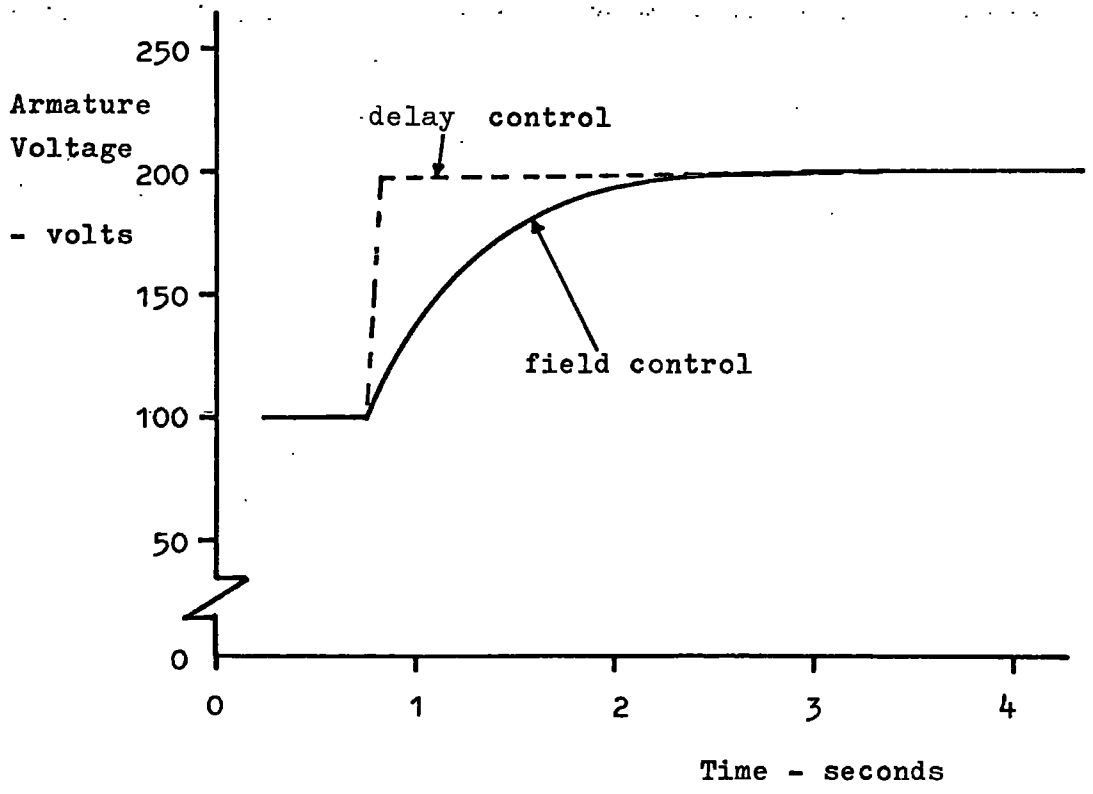

(b) Voltage change from 0.5 to 1.0 p.u.

Fig. 7.9 Control Response of T.A.C. Generator

shown that the electronic method produces a change at the beginning of the next commutation cycle. This is therefore not a time constant but a time delay and on the experimental machine this time delay had a maximum value of 4 mS at 1800 rev/min. The response time of the armature current was limited by the armature time constant (0.03 S) while the response using field current control was limited by the relatively long time constant of 0.7 seconds.

7.5.2 Linearity of Generator Control

The design of the electronic control unit permitted an external a.c. or d.c. signal to modulate the mean time delay set by a manual control. The change in output voltage for a range of input voltages was measured for two values of field current - Figure 7.10 (a) - and within the range indicated there was less than 2% deviation from a straight line. A similar test between output voltage and field current for a constant time delay also gave a linearity of 2% as shown in Figure 7.10 (b).

7.5.3 Gain and Frequency Responses

The response of the generator to a sine wave input to the control unit was recorded for a range of frequencies from 0.003 Hz to 100 Hz. The magnitude of the input sine wave (V_{in}) and the variation of the output voltage (V_{out}) about the mean output voltage (V_A) were measured and the gain of the system calculated as

$$\text{Gain} = 20. \log_{10} (V_{out} / V_{in}) \quad \text{db}$$

The phase displacement between the input and output waveforms was recorded for each frequency. The results are given in Figure 7.11; 7.11 (a) as a gain - frequency and phase-frequency plot and 7.11 (b) as a gain - phase diagram.

A similar test was made using the field current control with a

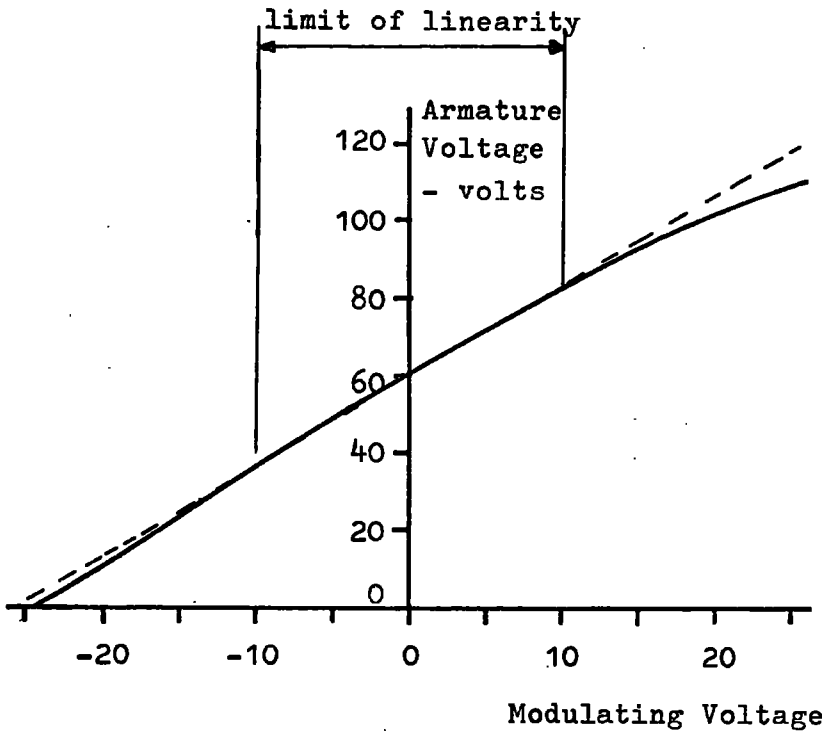

(a) linearity of ‹delay› Control Method

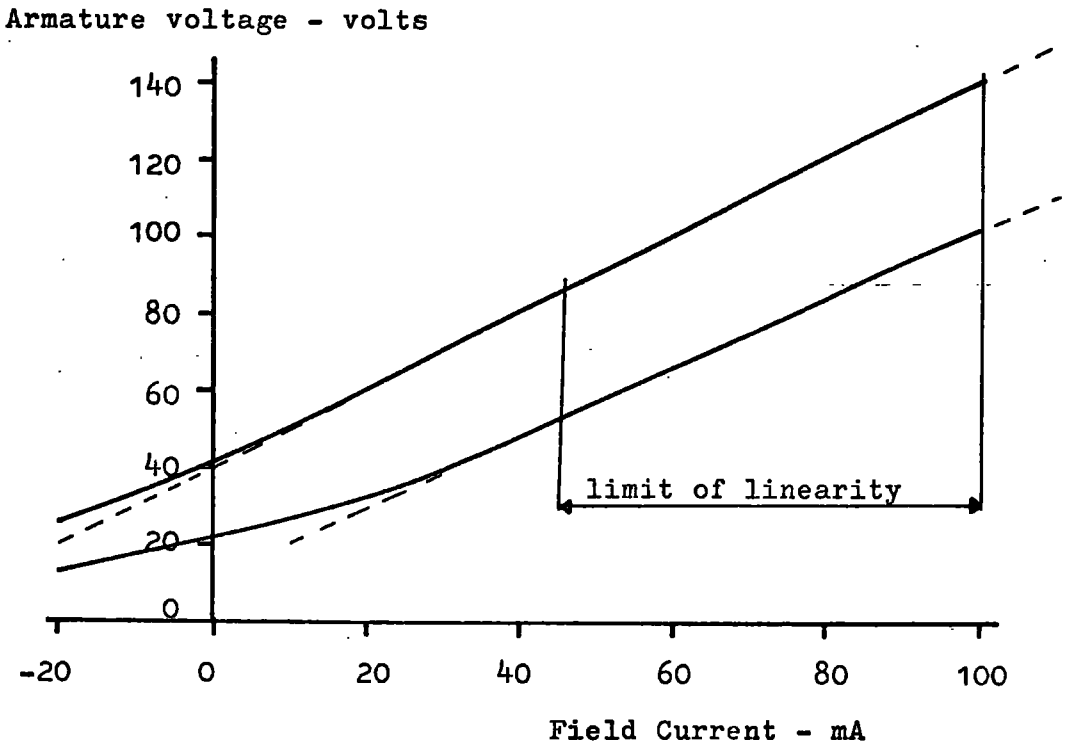

(b) linearity of Field Current Control Method

Fig. 7.10 Linearity of T.A.C. Generator Control Methods

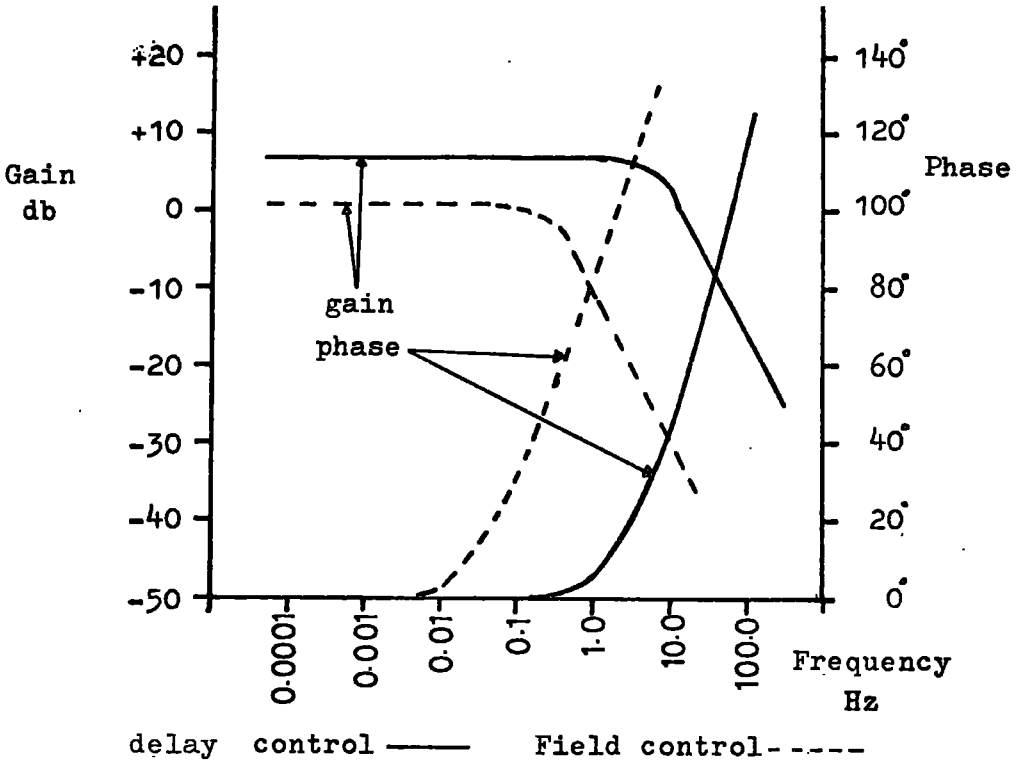

(a) Gain - Frequency, Phase - Frequency Diagram

(b) Gain - Phase Diagram

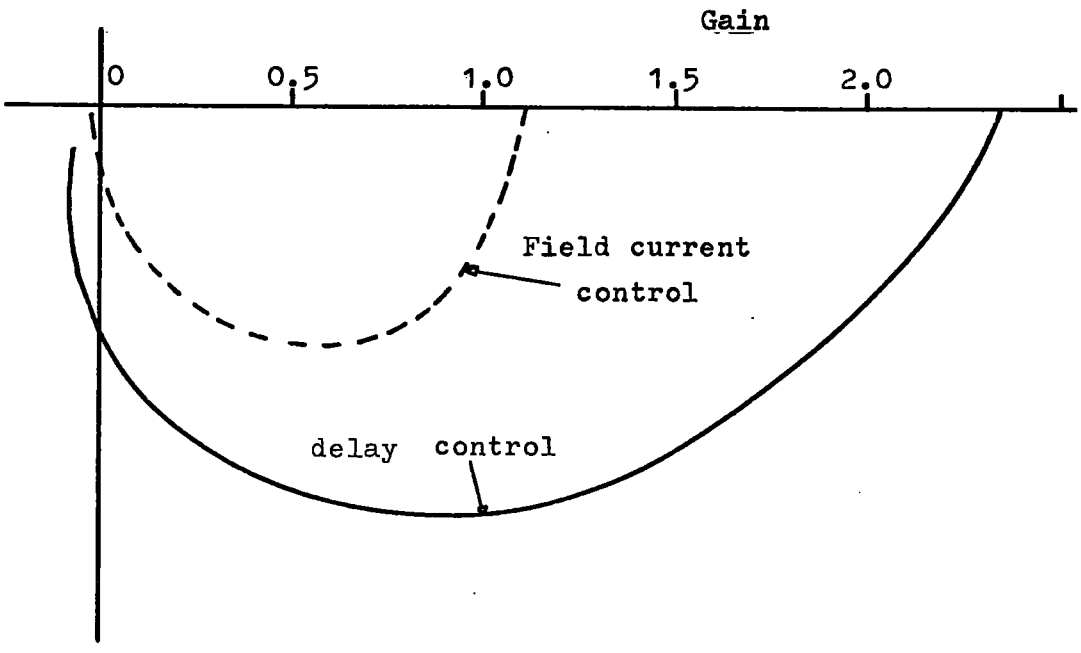

Fig. 7.11 Frequency Response of T.A.C. Generator

constant time delay setting. These results are also shown in Figure 7.11 so that they may be easily compared with the electronic method. The gain-phase diagram shows that both methods of control are second order types but that they contain a dominant first order term. The gain-frequency responses show the electronic method to have a larger bandwidth; the -3db point being at 5 Hz compared to 0.2 Hz for the field control. Calculations confirm that the dominant time constants are that of the armature for the electronic method and of the field for the field current method.

In general, the time constant of the armature circuit is less than that of the field circuit and so the electronic method using thyristor firing delay would produce a faster response time than that of the more conventional field current method.

7.6 Discussion on the Control of D.C. Machines

The controlling parameters of a conventional d.c. machine are the field current, the armature voltage and the speed. With the t.a.c. machine there is the possibility of delayed thyristor firing control which alters the effective positions of the brushes and hence of the armature axis. To determine the relative merits of each method it is instructive to consider three points. First the range over which the method is applicable; secondly, the ease with which the controlling parameter may be changed and thirdly, the response of the machine to a change in this parameter.

As shown and discussed in previous sections, the range of control using thyristor firing delay is dependent upon a number of factors, particularly the armature current. The other methods of control are independent of armature current and generally permit a much wider control range.

The second consideration is ease of control and included with this is the power necessary for that control method. Thyristor methods of control require firing or triggering circuits, the complexity of which depends upon the type of control required. Since the firing circuit is an essential part of the t.a.c. machine the addition of a delay unit involves only a small modification. Power requirements are small - in the order of milliwatts. Control by the more conventional methods of field current or armature voltage control is usually more simple, i.e. a variable resistor in the field circuit, but the power required is higher - typically watts for field current control.

The third consideration is the response time of the system to a change in the control parameter. The thyristor delay method takes effect from the beginning of the next commutation cycle as is illustrated by the increase in armature voltage in Figure 7.12. There is a time delay rather than a time constant with this method and the time delay is given by the time between successive commutation periods. Clearly, this time delay is dependent upon both the speed of rotation and the geometry of the part commutators but at normal operating speeds (i.e. rated value), the time delay will generally be smaller than the time constant (L/R) of the field or armature circuits.

The firing delay method of control has advantages of little power requirements and a fast response time. It is limited by the range over which it is at present applicable. The use of the control method may be in the accurate control of motor speed or generator voltage over a small range (say $\pm$10%) about a mean value.

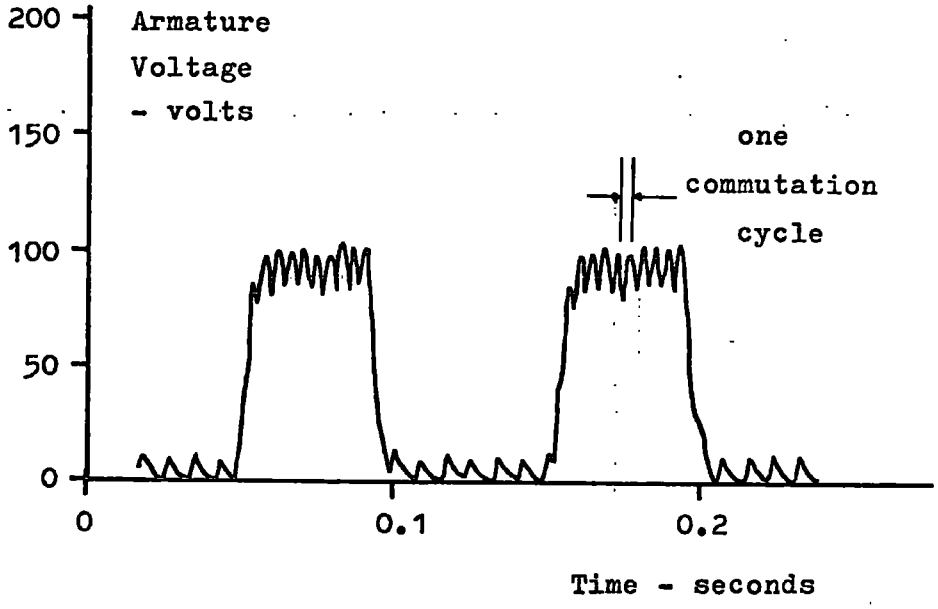

Fig. 7.12 Response time for delay Control of Generator

Chapter 8 The Experimental Machine

8.1 Details of the Experimental Machine

The experimental machine consisted of a specially constructed stator in which a conventional armature from a 2 hp direct current motor was placed. The stator was laminated so that any flux pulsations could be measured and not be damped out by the formation of eddy currents. Moveable field and commutating poles completed the stator iron circuit. Eight tappings from the original motor commutator were taken to alternate segments on a new two part commutator fastened to an extension of the shaft. A dynamometer was also connected to the shaft so that the experimental machine could be tested under motor or generator conditions. Figure 8.1 shows the layout of the machine and details of the magnetic circuit are given in Appendix C.

A schematic diagram of the electrical connections between the original and new commutators is shown in Figure 8.2. Since the original commutator had 57 bars, there were 7 bars between most tappings but eight bars between two tappings. The output voltage of the t.a.c. generator showed no discernable difference between the tappings spaced 7 or 8 bars apart. Figure 8.3 shows the output voltage, the ripple being due to slot effects.

8.2 The Part Commutators

Each part commutator had eight brass segments around its circumference and an air gap separated each segment from its neighbour. Normal carbon brushes were arranged in pairs such that at no time could they bridge more than two segments. The brushes were held in conventional brush holders and were run at average current densities of about one third of their rated values.

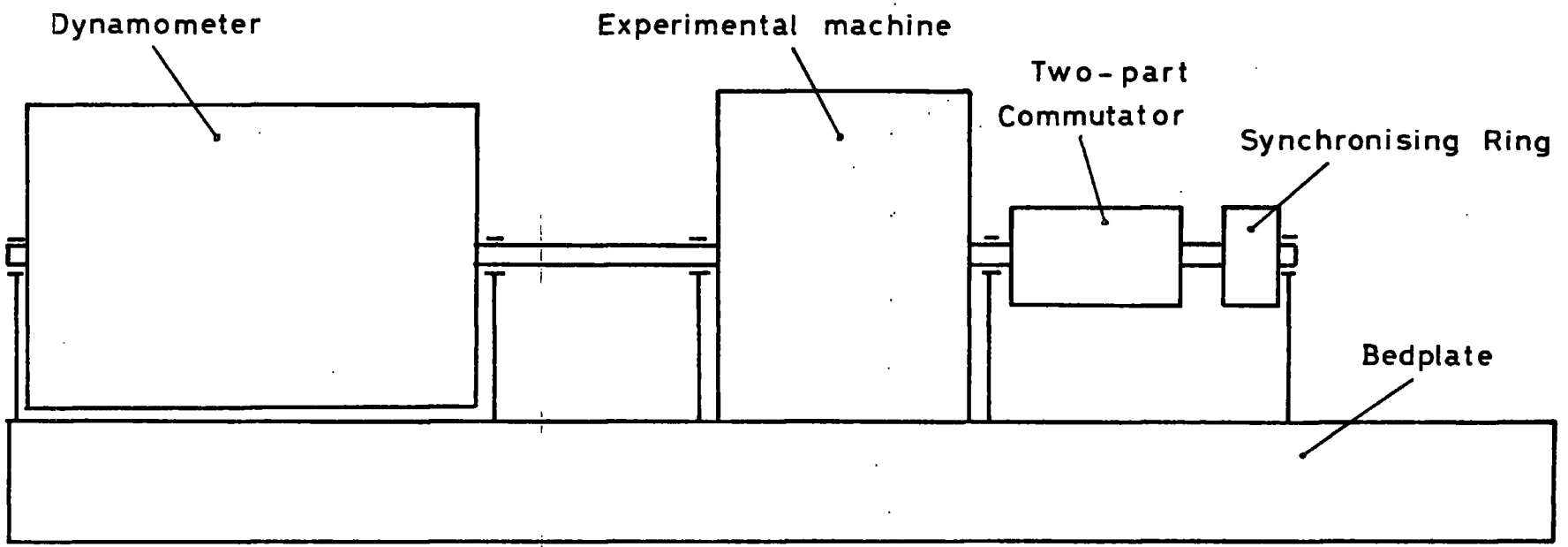

Fig. 8.1 Block Diagram of Experimental Equipment

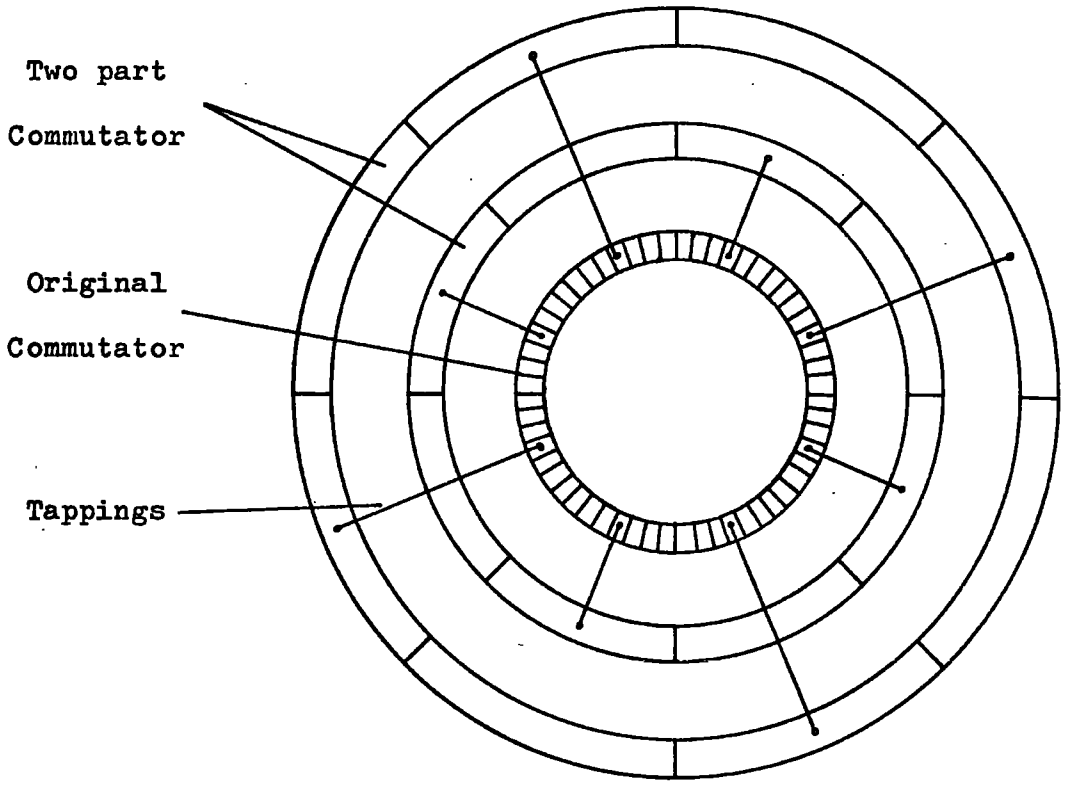

Fig. 8.2 Electrical Connection of Two part Commutator

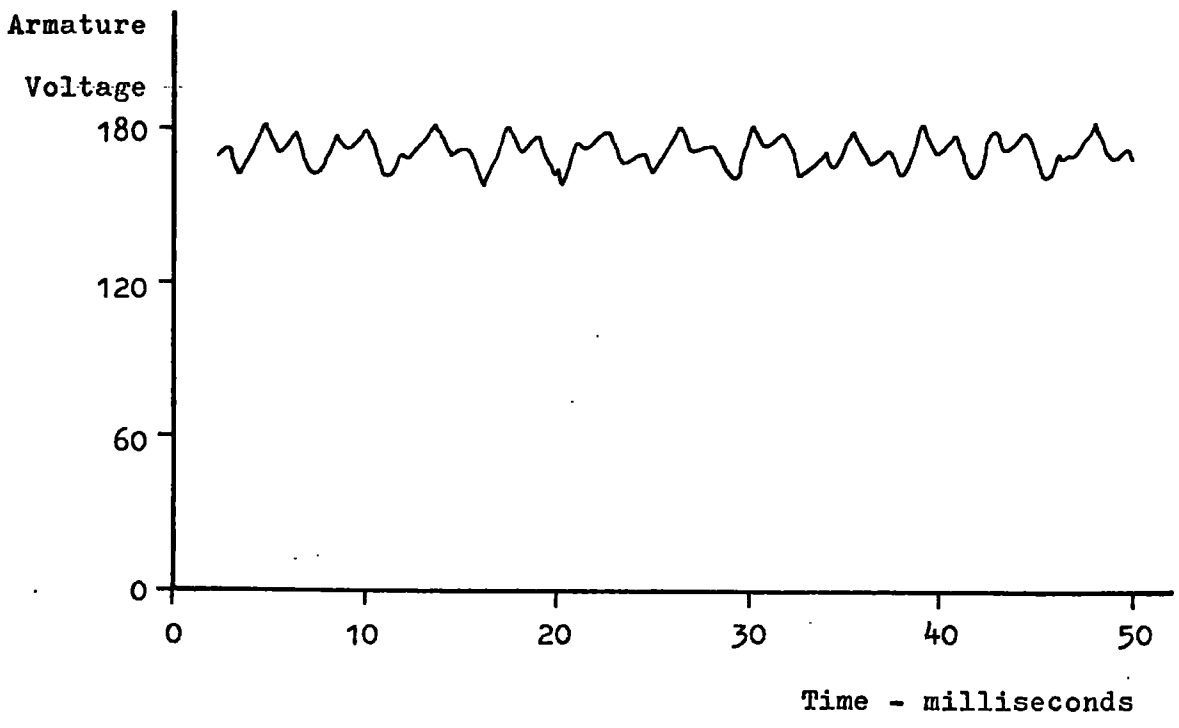

Fig. 8.3 Voltage Waveform of T.A.C. Generator

At speeds greater than 1800 rev/min intermittent sparking was observed under the brushes. Extra pressure on a brush would help to reduce the sparking under that brush and also under the other brush of the same pair. The longer the machine ran, the worse the sparking became and marking of the commutator surface was observed. The waveforms of the currents in the brush circuit were monitored and no irregularity was noticed in the current to the brush pair - Figure 8.4 (a). The waveforms for the leading and trailing brushes showed some very rapid transfers of current - Figure 8.4 (b). When the trailing brush just makes contact with the segment there is an immediate current sharing. In this position, the instantaneous current density along the edge of the brush may be many times (>20) greater than its rated value. A similar situation exists as the leading brush is just about to leave the segment.

To eliminate this transfer, a different design of commutator layout was used [8.1] and the brush pair replaced by a single brush. Figure 8.5 shows the schematic layout of the modified part commutator. Subsequent running of the experimental machine showed no apparent commutator surface damage and no under brush sparking. Further long duration tests are required before any firm conclusions about the relative merits of the two commutator designs may be made. Recent tests by Bates [8.2,8.3] have shown that carbon fibre protecting brushes can be extremely helpful in reducing surface damage. Such brushes may be necessary on large machines with their higher current ratings but, for small machines, the modified commutator may be sufficient to prevent marking and sparking by eliminating the rapid current transfers.

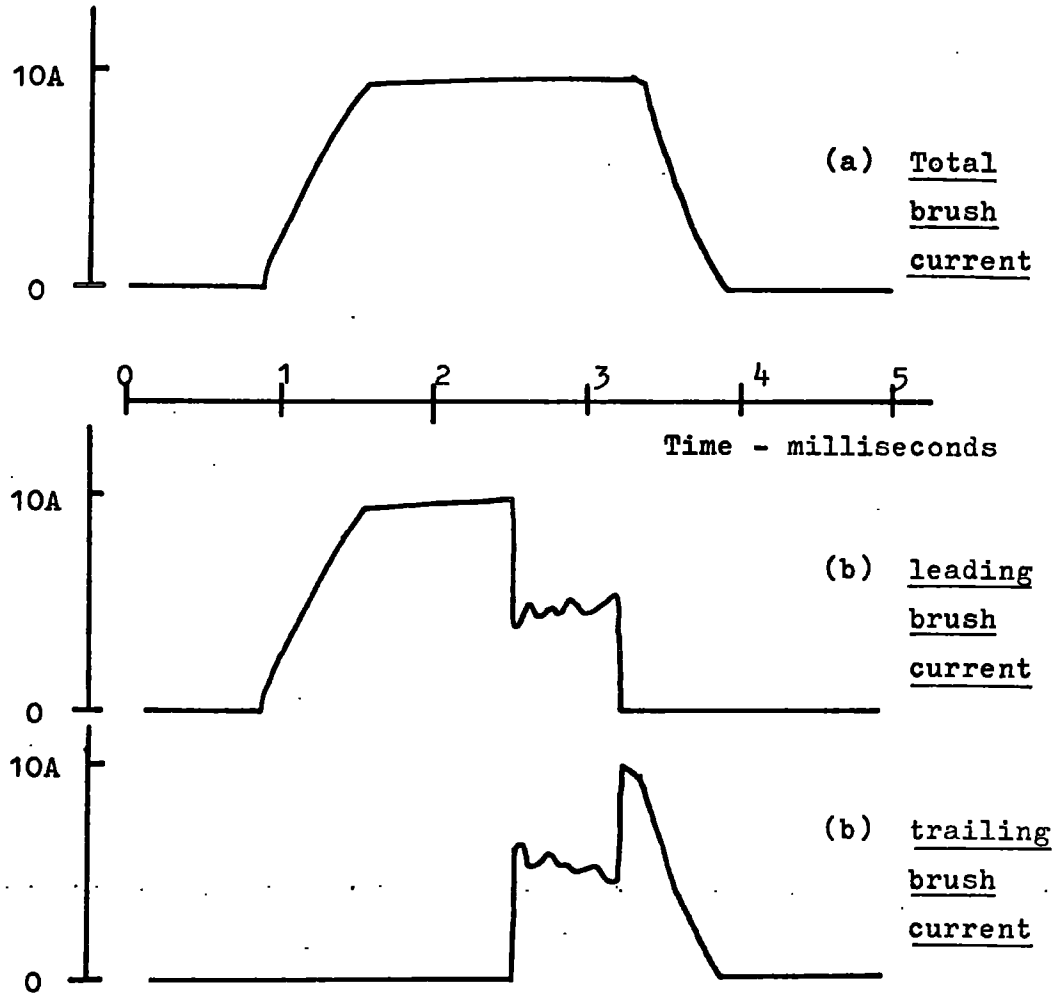

Fig. 8.4 Brush Current Waveforms

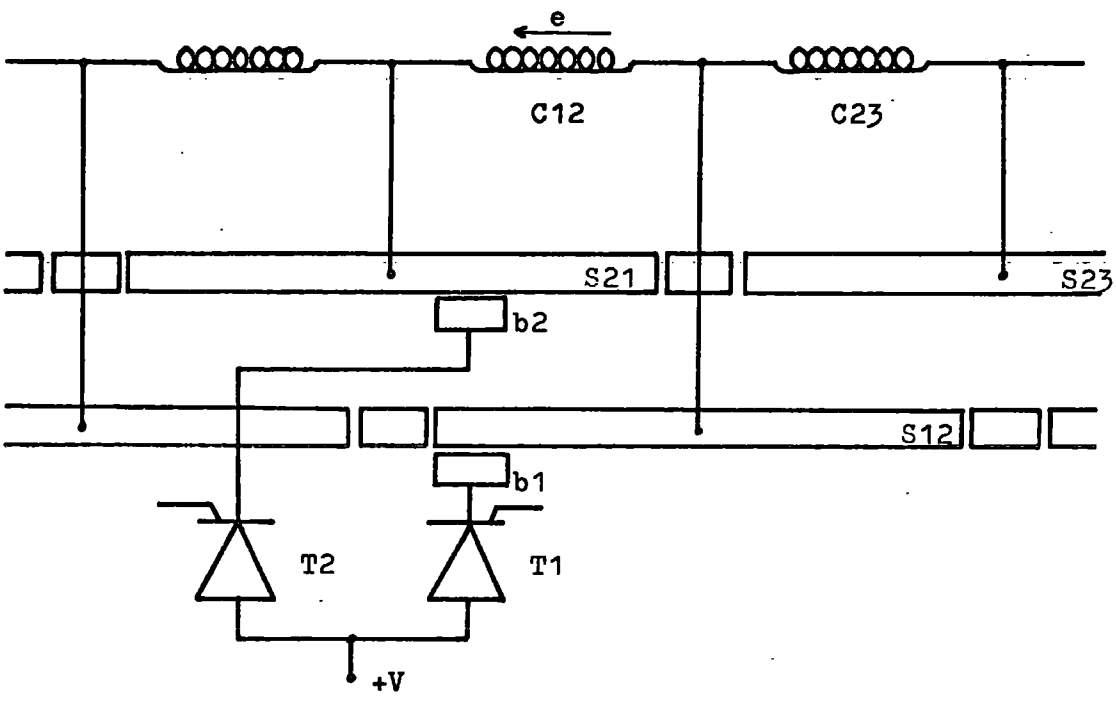

Fig. 8.5 Modified Part Commutator

8.3 Brush Positions and Commutation Angles

In a conventional machine commutation takes place in δ^{o}, beginning at $\frac{1}{2}\delta^{o}$ before the neutral axis and finishing at $\frac{1}{2}\delta^{o}$ after. The mean armature axis position thus lies along the neutral axis. By analogy, the commutation process in the t.a.c. machine is arranged to commence at $\frac{1}{2}(s-2b)^{o}$ before the neutral axis so that if commutation takes all the available angle, the mean axis position is still along the neutral axis. The maximum angle over which commutation can take place is the segment angle less twice the brush arc (8.4). If commutation is completed in a smaller angle the effect will be to move the mean position away from the neutral axis by some angle Θ. This new position will be in front of the neutral axis in the direction of rotation and so Θ is defined to have a negative value. This value will increase in magnitude as the process of commutation becomes quicker for any given speed. It can be shown that the average armature axis position is identical for both commutator and slip ring modes of operation and that the value of Θ will lie between $\frac{1}{2}(s-2b)^{o}$ and 0^{o} for sparkless commutation with no thyristor firing delay.

For the experimental machine the segment arc was 45^{o} and the brush arc $7\frac{1}{2}^{o}$; the maximum commutation angle was 32^{o}. Commutation was arranged to start 16^{o} before the neutral axis in the direction of rotation. The motor was particularly sensitive to small changes of angle and to obtain similar characteristics for reversible running, the starting angle of the commutation process must be accurately set.

8.4 The Triggering Circuits

To fire the thyristors at the correct time, a means of synchronising the triggering circuit with the speed and position of

the shaft was required. A simple way was to gate the triggering circuit by using a contact made with a conducting surface in an extra ring which rotates with the shaft. The need for reliable triggering is emphasised. If a thyristor fails to trigger into conduction either through a fault in the trigger circuit, bad contact with the synchronising ring or by the failure of a thyristor itself, then sparkless commutation will not occur. As the brush leaves an active segment a spark will be drawn from the trailing brush edge back to the segment. Commutation may still occur as the brush establishes itself on the next segment and the reversal of the current done purely by resistance commutation. The arc will extinguish only to reappear at the end of the next segment. A more likely possibility is that of flashover where the arc does not extinguish but is drawn until it reaches the brushes of the opposite polarity. The failure of a thyristor to conduct, from whatever cause, will lead to severe sparking and commutator damage.

The requirements of the trigger circuit are two fold: it must provide an output signal sufficient to initiate conduction and it must do so at a time determined by the synchronising ring. In general, a thyristor will be triggered by a voltage of +3 to +10 volts being applied to the gate. This voltage may be either a d.c. level or it may be in the form of pulses - the minimum pulse width being determined by the time constant of the circuit. Figure 8.6 shows the oscillatory waveform of the series interpole motor with different firing pulse widths. With a narrow pulse, the thyristors need to be more forward biased before the current can reach latching value (about 30 mA) before the pulse is removed. Further information on triggering circuits may be found in References 8.5 and 8.6.

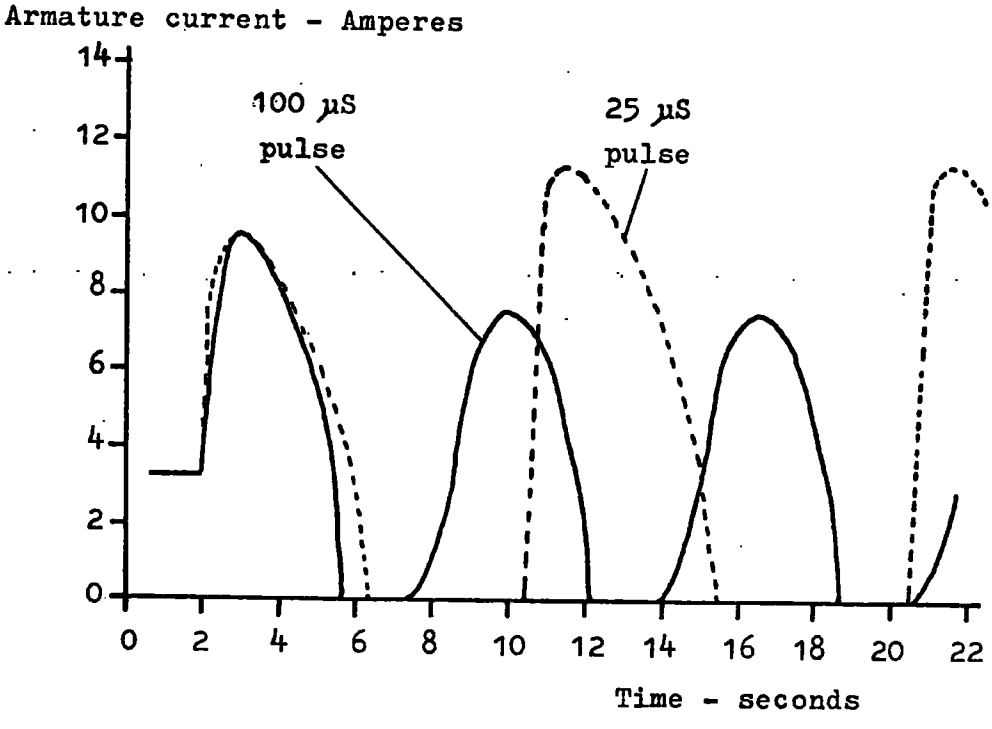

Fig. 8.6 Motor Current Response - Pulse width variation

8.5 The Electronic and Electrical Circuits

The first trigger circuit used a free running, 5 kHz square wave oscillator which produced two anti-phase outputs. These were fed to blocking amplifiers which only transmitted and amplified the signals when a contact was made on the synchronising ring. The amplifier outputs were transformed down to produce isolated +4 volt pulses. The electronic circuit is given in Figure 8.7.

The second trigger circuit incorporated a delay unit which delayed the firing pulses for a variable time after initial contact had been made with the synchronising ring. The time delay could be adjusted manually or 'automatically' by an external a.c. or d.c. signal. The block diagram and circuit details are given in Figure 8.8 and the linearity of the delay time to the external signal in Figure 8.9. The linearity was within 1% over an input range of $\pm$10 volts. Appendix C lists the delay times for the different manual settings of the control unit.

The t.a.c. machine could be used either as a motor or as a generator: the output of the generator being dissipated as heat in a resistor bank. In the former case, the armature was supplied with 200 volts from a direct current source. A unique property of the t.a.c. machine is that a series or a separately excited interpole may be used to induce the commutation voltage. A variable resistor was used to adjust the value of the separate excitation current but it was generally set to 10 amperes. A circuit diagram showing the various switches, meters, resistors and connections is given in Figure 8.10.

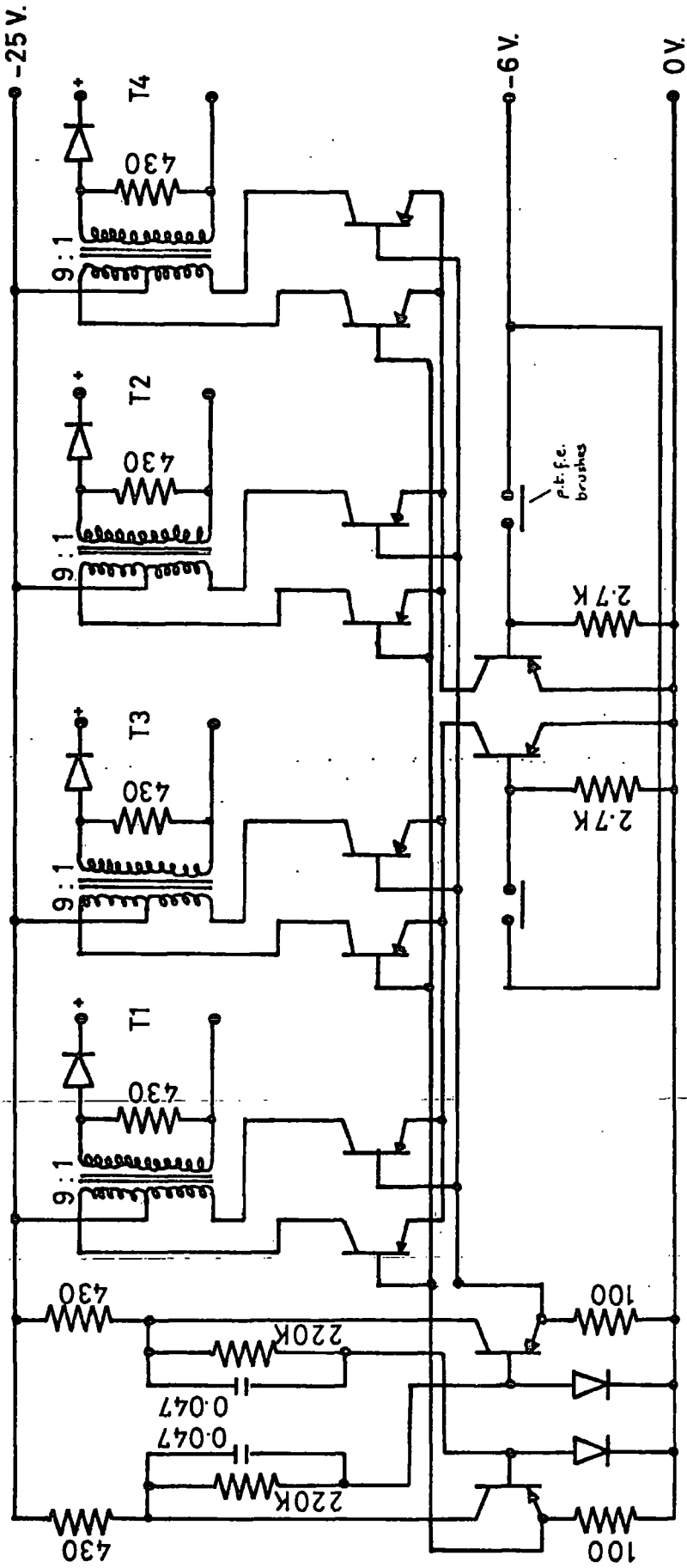

Fig. 8.7 Thyristor Trigger Circuit

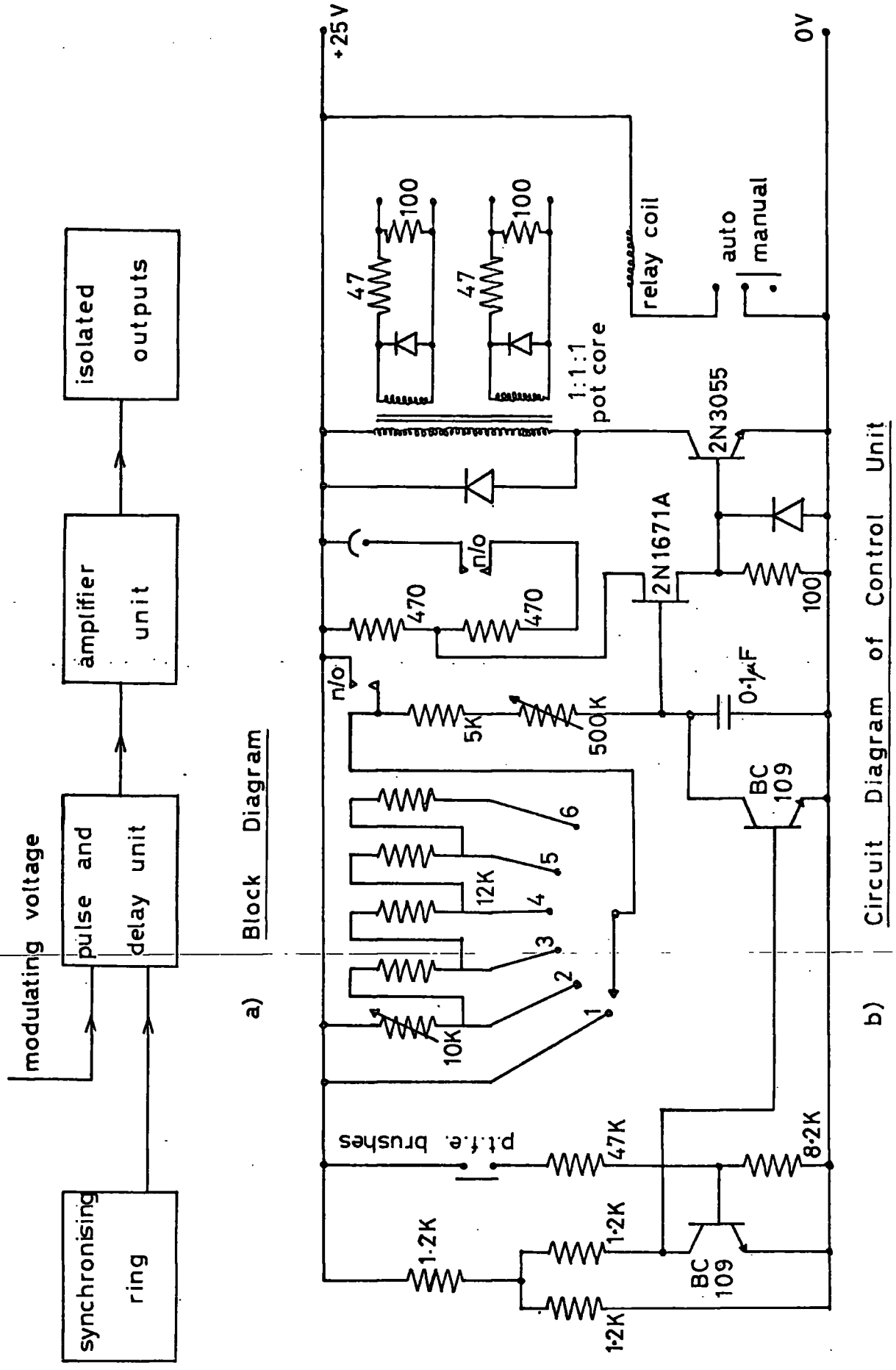

Fig. 8.8 The Variable Delay Control Unit

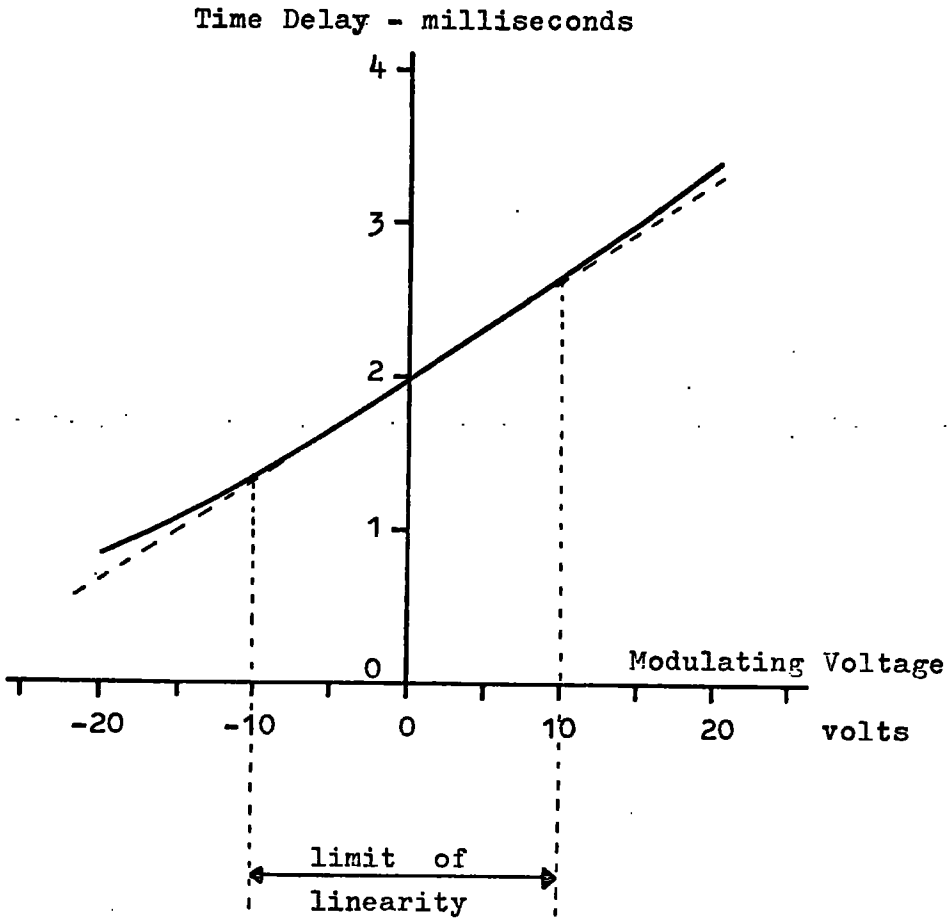

Fig. 8.9 Linearity of Variable Time Delay Control Unit

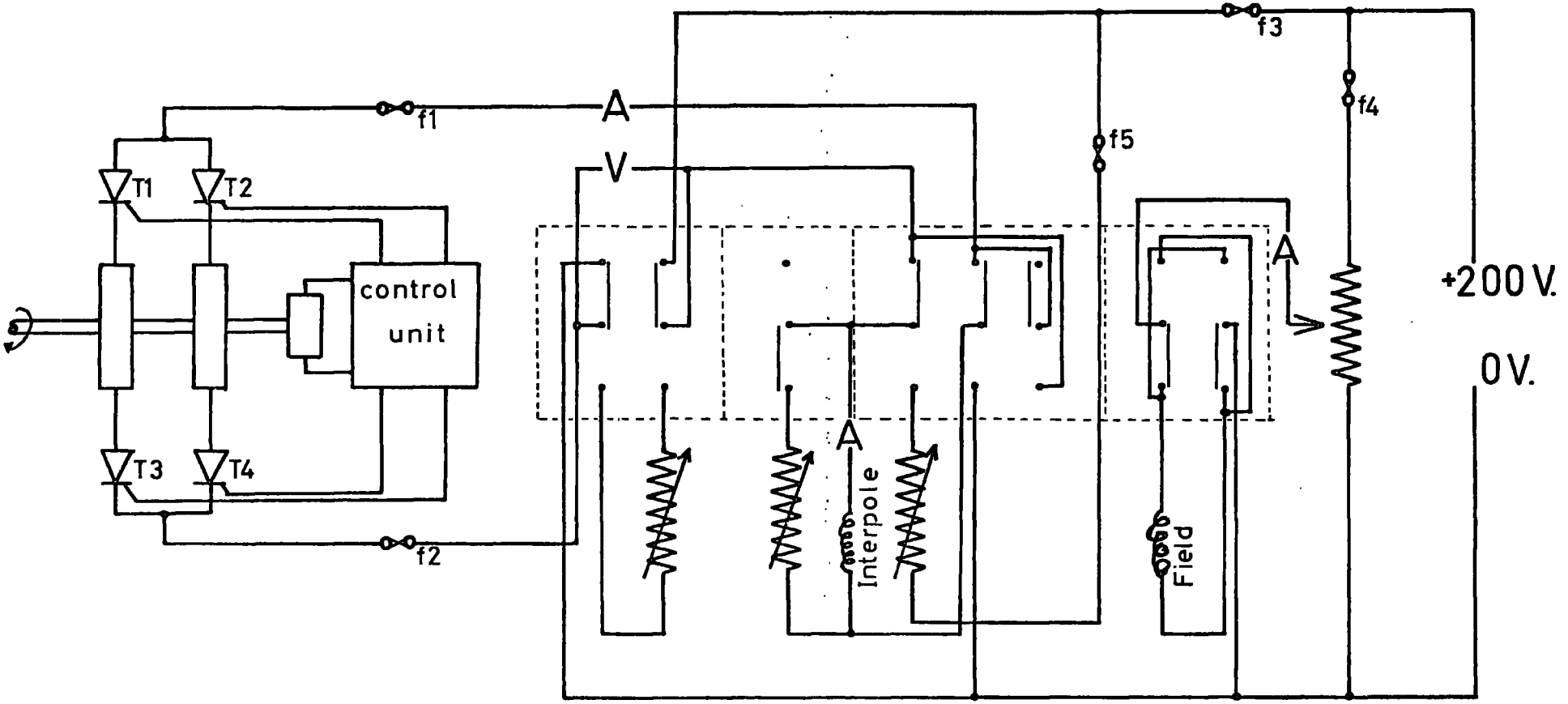

Fig. 8.10 Electrical Circuit Diagram for Experimental Machine

Chapter 9 Conclusions and Recommendations

9.1 Comments and Recommendations

The experimental machine ran for some 1500 hours without failure of any electrical or electronic part. The sparking and marking on the original commutator was absent from the modified commutator but the performance of the machine was unchanged by the modification. The machine proved capable of withstanding overloads of up to four times the rated current without sparking.

One of the advantages of the general theory is that the measurements of inductance may be made under standstill conditions. The study has confirmed this - but only if the exciting currents used in the measurements were of the same order as the normal operating currents. Misleading results are obtained if very small exciting currents are used to minimise heating effects, etc. It is strongly recommended that any standstill results, particularly of inductance, are confirmed if possible by tests made on the machine under normal operating conditions. For example, the open circuit test of the generator can be used to check the value of M_{fa}. The measurements must be accurate because small changes or errors can seriously affect the validity of the computed results. Saturation in the direct and quadrature axes must also be carefully measured. This recommendation is made after personal experience of the need for careful measurement using currents throughout the current range of the windings. This is essential if saturation effects are to be included. Although tedious, time spent in measuring the inductance coefficients accurately will be repaid in the quality of the results.

A valid comment on the programme is that the inductance waveforms were taken as either sine or cosine curves. This has been shown to produce good results but better accuracy may be obtained if the actual waveforms are incorporated into the programme. The computer can be programmed to calculate the values of the inductance and its slope at any desired angle.

9.2 ~~10.2~~ Conclusions

The output of a machine may be controlled over a limited range by a method of electronically rocking the brushes by using delayed thyristor firing. Sufficient experimental results have been presented to show the nature of the method and some of the limitations imposed by loading effects.

The matching of the predicted and experimental characteristics confirm the validity of the method of analysis which was based upon the general machine theory. The fact that the t.a.c. machine differed from conventional machines in having a large commutation angle, two zones of operation (commutator and slip ring) and the inclusion of thyristors in the armature circuit can all be accounted for in the analysis. The differential equation gave an approximate indication of the performance and a more accurate prediction was obtained with the use of a computer programme. Providing suitable numerical values for the parameters were obtained from the measurements, the computer simulation could produce results which matched those obtained experimentally to within 5% of the current and voltage magnitudes, 5% of the frequency of the oscillations and 3% of the machine speed.

The direct current machine with thyristor assisted commutation may be analysed by the general theory. It is essential that the differences between the t.a.c. and conventional machines are kept in mind and allowance made for them. The most important of these factors is that of the armature axis not being restricted to lie about the neutral axis. It may be variable within the range $\pm 20^{o}$ instead of $\pm 2^{o}$. This introduces terms into the equations that would normally be considered zero or negligible in standard d.c. machines. The two zones of operation complicate the analysis in that two sets of equations must be manipulated and combined according to the relative times of each period. The inclusion of the thyristors limits the armature current to zero and positive values only.

The work has provided a satisfactory method of analysing the performance of t.a.c. machines. A computer programme based upon the analysis was developed and this may be used to predict the characteristics of the machine for design changes which may be studied in future developments of direct current machines with thyristor assisted commutation.

9.3 Further Work

The general machine theory has been shown to be able to predict accurately the performance of the t.a.c. machine. By using average values the steady state characteristics may be obtained and also its behaviour under transient conditions. It is an easy step to simplify the dynamic equations to obtain the steady state conditions but it is difficult to obtain dynamic responses from essentially steady state equations. This is a justification for the use of the general theory. The method does however, require the knowledge of certain inductance parameters and to prove the method the inductances were measured on an experimental machine. The values may be calculated by considering the flux (ϕ) produced by a current (i) in a (n) turn winding. Since inductance (L) is given by

$$L = n.\phi / i$$

an estimate of the inductance may be obtained. Problems do exist in the calculations and, in particular, the effects of saturation are complex.

A study into the calculation of these inductances from the design data, i.e. the electrical and mechanical details, would enable the behaviour of t.a.c. machines to be calculated at the design stage.

Appendices

Appendix A The Measurement of Inductance

A.1 The D.C. Inductance Bridge

The bridge used to measure the variation of the inductance coefficients is based upon that described by Prescott and El-Karashi. Jones compares his inductance bridge which uses a ballistic galvanometer [A.1] with that of Prescott's in which a fluxmeter is used as the detecting instrument. He concludes that, although the galvanometer is more sensitive, readings must be taken in a time which is small compared to the time required for a quarter swing of the galvanometer. The fluxmeter would record even minute changes of voltage quite faithfully. More recently, Barton and Dunfield [A.2] have used operational amplifiers as the detector.

The basic circuit is shown in Figure A.1 and consists ideally of a constant current source, a switch, a non inductive resistor, a non resistive inductor and a voltage integrator. Initially the switch is closed and the current (I) flows through it. The switch is then opened and the current redistributes itself into a current (i_1) through the resistor and current (i_2) through the inductor. The voltage across the integrator is

$$v = L.d(i_2)/dt = R.i_1$$

and, since $I = i_1 + i_2$,

$$R.I = R.i_2 + L.d(i_2)/dt$$

The solution of this equation is

$$i_2 = I.(1-e^{-(R/L).t})$$

The voltage across the integrator is therefore

$$v = L.d(i_2)/dt = R.I.e^{-(R/L).t}$$

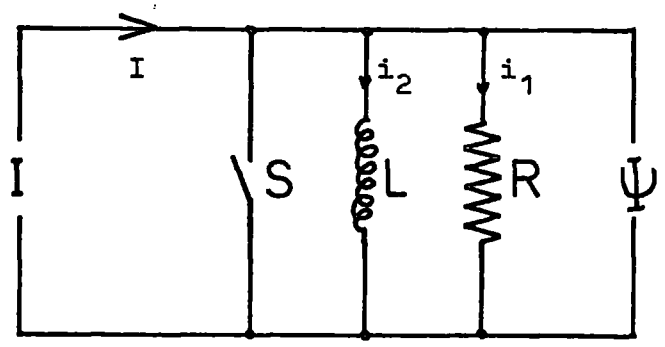

Fig. A.1 Basic Circuit for Inductance Measurement

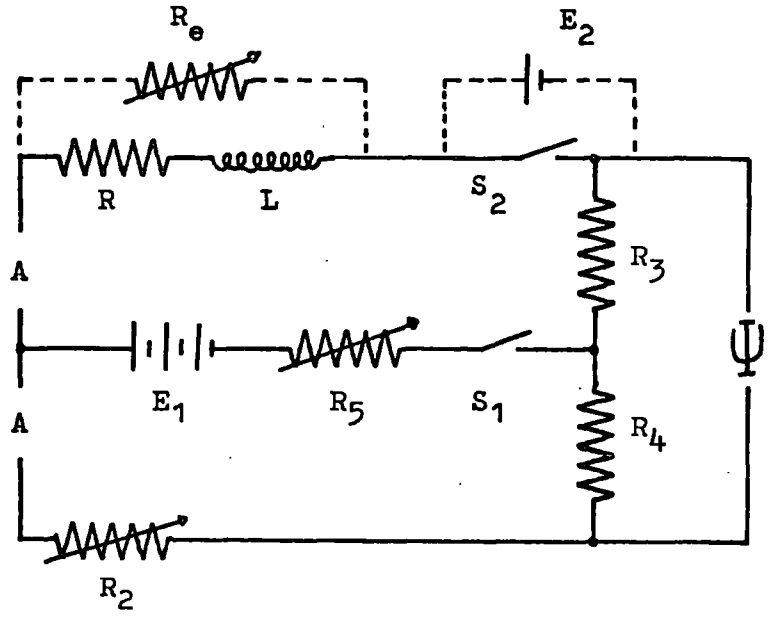

Fig. A.2 The Direct Current Inductance Bridge

and the integral of this voltage with respect to time is

$$\psi = \int_0^\infty v.\,dt = L \cdot I$$

The voltage integrator reads ψ and the inductance is given by

$$L = \Psi / I$$

Practically, an inductor will have resistance and the voltage across the integrator will not be zero but will be r.i where r is the resistance of the inductor and i the current through it. Since the fluxmeter integrates the voltage across its terminals there will be no steady state result. To overcome these difficulties the inductance bridge is used to compensate for the resistance of the coil.

A.2 Calibration and Use of Bridge

The circuit of the bridge is given in Figure A.2. Resistors R_3 and R_4 are equal in value and small compared to the fluxmeter resistance. Resistance R_2 is variable so that it could be set equal to the resistance of the coil under test. Resistor R_5 sets the magnitude of the exciting current.

To calibrate, a resistance R_e equivalent in value to that of the coil was substituted for the coil. The resistor R_2 was adjusted to balance the bridge. Switches S_1 and S_2 were opened and a known voltage E_2 placed across switch S_2 for a known time t seconds. The deflection of the fluxmeter (Ψ) was recorded. The constant of proportionality (K) is given by

$$K = E_2 . t/\psi$$

and has the units of volt-seconds per weber turn.

Since inductance is defined as volt-seconds per ampere, it is only necessary to note the fluxmeter deflection (ψ) for a change of

current (i). The inductance is, therefore

$$L = K.\Psi / i \quad \text{Henry}$$

A simple modification allows the mutual inductance between two coils to be measured - Figure A.3. By analogy with the self inductance circuit, the mutual inductance is

$$M_{2.1} = K.\Psi / i_1 \quad \text{Henry}$$

This circuit may also be used to measure the values at different levels of saturation by adjusting the value of the current (i_2).

A.3 Practical Difficulties with the Bridge

With small currents (less than 0.01 A) the heating effect of the current was negligible and the bridge could be quickly balanced. At higher current levels the bridge took a considerable time to reach equilibrium and the only accurate way of obtaining results was by switching off the current. An estimate of hysteris effects was done by taking the average of two readings; one as the current changed from +I to 0, the second as the current changed from -I to 0. The average of these readings was used as the value of the inductance.

To enable higher currents to flow, it was necessary to shunt the fluxmeter with external resistors. Figure A.4 shows the arrangement. The value of the shunt resistor R_p was 1 ohm while that of R_s was adjusted to give as large a deflection as possible. Calibration was necessary each time R_s was adjusted. By setting R_s to a large value, any imbalance of the bridge does not cause the fluxmeter to deflect wildly. As the balance point is approached the value of R_s can be reduced to the required value.

The introduction of ammeters can seriously affect the validity of the results. Some instruments, in particular microammeters, had

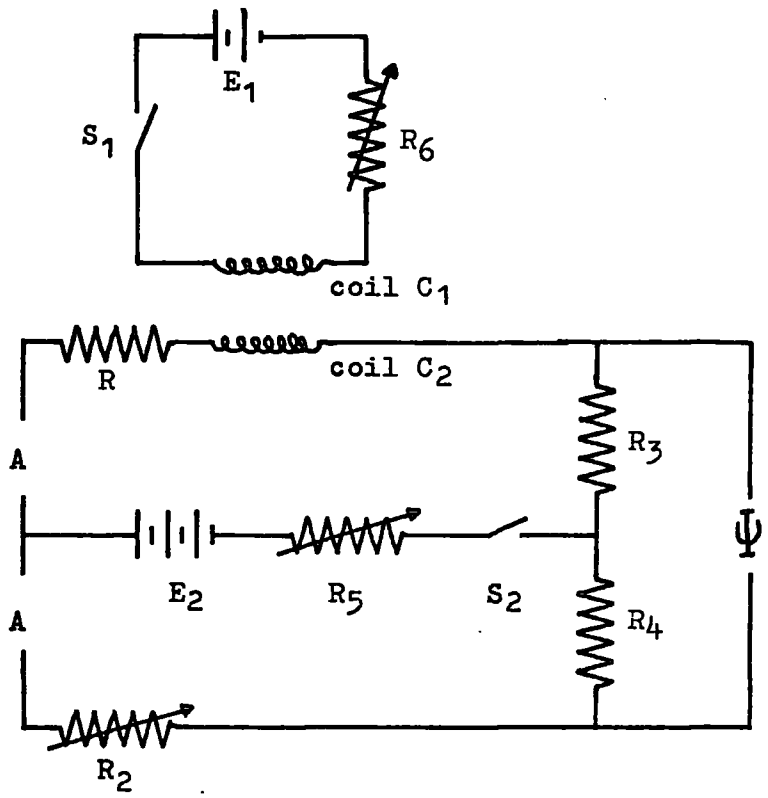

Fig. A.3 Mutual Inductance Bridge

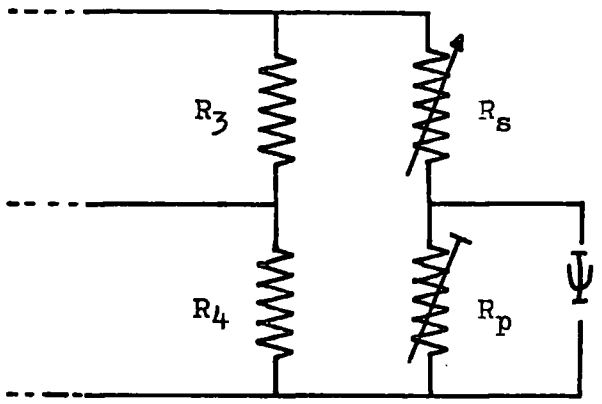

Fig. A.4 The Shunted Fluxmeter

a large inductance which could be many times that of the coil under test. By using two ammeters of the same rating, one in each arm of the bridge, the overall effect of the meters could be made small. During the calibration checks, the only inductance in the circuit is that of the meters and their effects can be calculated. Corrections were made to the inductance coefficients only if the meter contribution was more than 1-2% of the fluxmeter reading.

Appendix B The Computer Programme

B.1 Flowchart and Computer Programme

The flowchart for the simulation is given in Figure B.1. The computer programme follows closely the layout of the flowchart and is shown in Figure B.2. The programme contains no comment statements and so a brief description is now presented.

Lines 1 to 17 provide numerical values for the simulation and enables the input data to be changed without altering the statements themselves. CSMP accepts data in the 'graphical form' as (x,y) coordinates. The saturation criteria has been entered as the FUNCTION FLUX in this form (lines 13 - 17). The computer interpolates between the given points for any intermediate value. In the INITIAL section approximate values of current and speed are calculated (lines 20 - 36) and the simulation ran for a simulated time of 10 -15 seconds to allow the speed and currents to reach steady state values.

The DYNAMIC section follows in lines 37 to 79 and the calculations performed in this section are those that determine the dynamics of the machine. The programme first tests for armature current flow and then adjusts the saturation criteria according to the value of the current. Using the short circuited voltage equation, lines 52 to 54, the rate of change of current in these turns can be calculated. Since the armature current is known, the time taken for the current in these turns to reverse from $-\frac{1}{2}I$ to $+\frac{1}{2}I$ can be evaluated. Strictly, this should be done by integrating over the above range. To do this for every change in speed or current would involve a prohibitive amount of computing time. The time of commutation was therefore calculated from the expression -

$$t_{comm} = I_{ia} / pI_c$$

This expression assumes that the initial rate of increase is maintained and this is practically true for speeds around the normal operating values. At starting and slow speeds this method gives optimistic values for the time of commutation. Above 200 rev/min there is less than 4% error between the integration method and the method using the initial rate of increase. Around the normal operating value of 2000 rev/min, the error is less than 1%.

The relative times of the commutation period and the slip ring period allow the average value of to be calculated (lines 57,62,63). The rates of change of current and speed are then computed for each period and combined according to the relative times of each period, lines 64 to 76 refer. The dynamic section is then repeated until the simulation time is equal to that specified on the TIMER card, (line 88). After each run through the dynamic section the rates of change of current and speed are fed into an integration routine. New values are computed from the old values and the rates of change and the new values are fed back into the dynamic section. By this process the performance of the machine can be determined.

B.2 Introduction of Step Changes

The introduction of a step change is performed by a Fortran IF statement in the DYNAMIC section. Up to a certain specified time, the simulation uses a particular value for one of the machine's parameters. At and after this time another value is used. In the programme, the machine is simulating the effect of a change in the delay time of the firing pulses. Up to 10 seconds, a time delay of 1.44 mS is used; at and after 10 seconds, the time delay is 0.36 mS.

Further information on CSMP may be obtained from Reference B.1 and on Fortran IV from Reference B.2

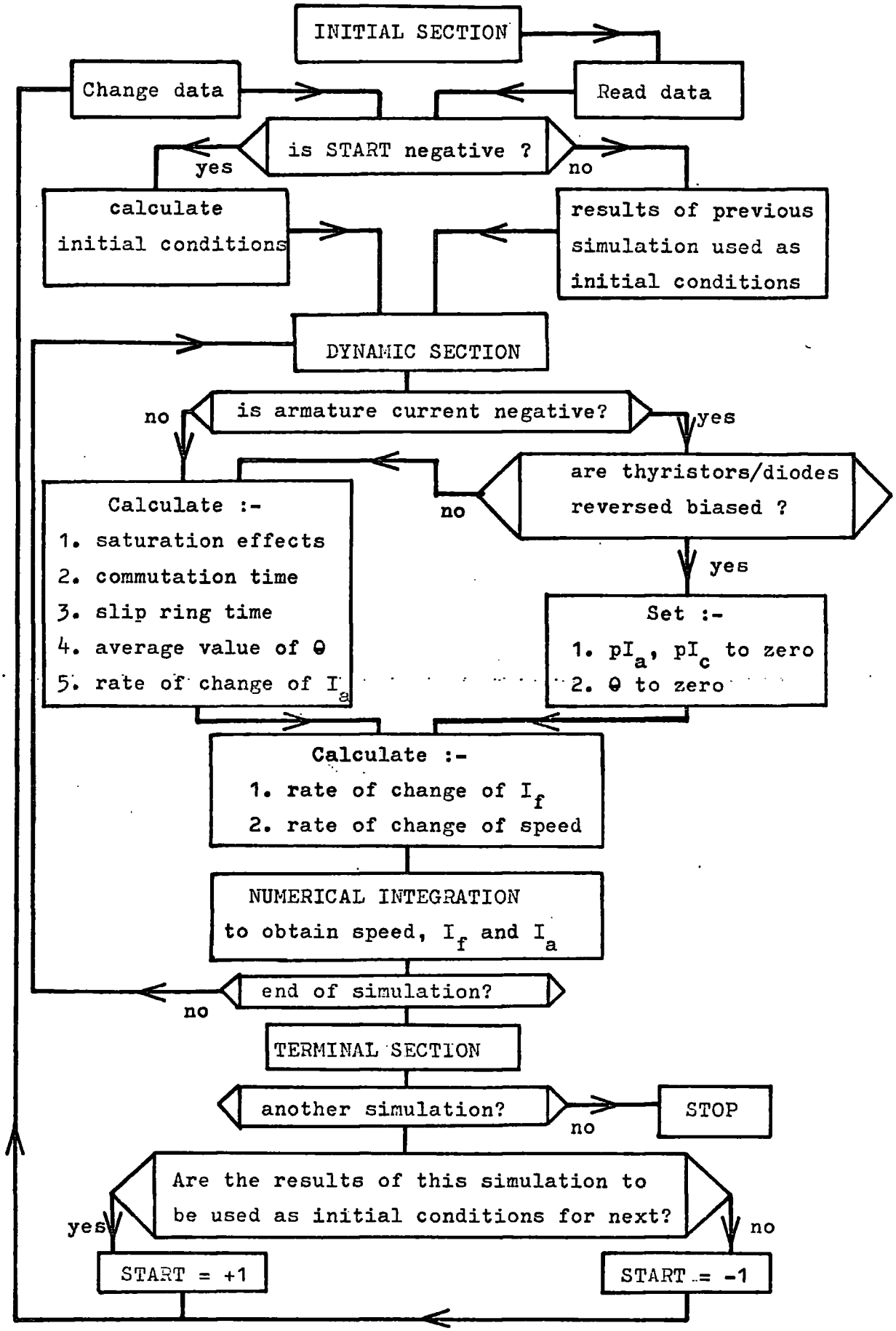

Fig. B.1 The Computer Programme Flowchart

```
>      1      *      ****************** Program for Thyristor assisted d.c. Machine *******
>      2      PARAM PHI= (-10.0, -12.0, -14.0, -16.0, -18.0, -20.0)
>      3      PARAM T1=0.36,  T2=1.44
>      4      PARAM VIA=200.0,  VF=-140.0
>      5      PARAM TF=3.0,  J=0.5
>      6      PARAM FACTOR=1.0
>      7      PARAM RF=800.0,  RIA=2.6,  RIAC=2.9,  RC=0.3
>      8      PARAM LF=500.0,  LIA=0.1,  LIAC=0.1,  LC=0.007
>      9      PARAM MFA=5.1,  MFAC=5.1,  MFC=1.0
>     10      PARAM MIA=0.1,  MIAC=0.11,  MIC=0.040
>     11      PARAM MAC=0.0
>     12      PARAM START=-1.0
>     13      FUNCTION FLUX= (-1.0,1.060), ( 0.0,1.010), ( 1.0,0.960), ( 2.0,0.910)...
>     14                   , ( 3.0,0.860), ( 4.0,0.810), ( 5.0,0.760), ( 6.0,0.715)...
>     15                   , ( 7.0,0.665), ( 8.0,0.620), ( 9.0,0.575), (10.0,0.530)...
>     16                   , (11.0,0.495), (12.0,0.465), (13.0,0.435), (14.0,0.415)...
>     17                   , (15.0,0.400), (20.0,0.370), (25.0,0.350), (30.0,0.335)
>     18      INIT
>     19      NOSORT
>     20            TIMDLY=T2
>     21            IF(START) 100,100,101
>     22        100 X1=TF
>     23            X2=VF/RF
>     24            IF(X2.EQ.0.0) X3=0.0
>     25            IF(X2.NE.0.0) X3=VIA/(-MFA*X2)
>     26            THETA=-0.12
>     27            SAT=1.0
>     28        101 CONTINUE
>     29            IIA=X1
>     30            IFF=X2
>     31            SPEED=X3
>     32            IC1=X2
>     33            IC2=X1
>     34            IC3=X3
>     35            PIF=0.0
>     36            PIIA=0.0
```

Figure B.2

```
>     37      DYNAM
>     38      NOSORT
>     39            IF(TIME-10.0) 298,299,299
>     40        299 TIMDLY=T1
>     41        298 CONTINUE
>     42            IF(IIA) 200,200,201
>     43        200 CUTOFF=VIA+MFAC*SPEED*IFF
>     44            IF(CUTOFF) 202,201,201
>     45        202 IIA=0.0
>     46            PIIA=0.0
>     47            PIC=0.0
>     48            RATIO = 0.712
>     49            GOTO 206
>     50        201 CUTOFF=0.0
>     51            SAT=AFGEN(FLUX,IIA)
>     52            PIC=( 0.5*RC*IIA -MFC*PIF -(MAC*SIN(2.0*THETA)-MIC*FACTOR...
>     53                *SIN(THETA))*0.5*(1.0+SAT)*PIIA -(2.0*MAC-MIC)*0.5*...
>     54                (1.0+SAT)*FACTOR*SPEED*IIA) / LC
>     55            TPEROD=3.1416/(4.0*SPEED)
>     56            IF(PIC) 204,204,203
>     57        203 TCOM=IIA/PIC
>     58            RATIO = TCOM/TPEROD
>     59            GOTO 205
>     60        204 RATIO=0.712
>     61        205 IF(RATIO.GT.0.75) RATIO=0.75
>     62        206 ANGLE=PHI+0.0573*SPEED*TIMDLY+22.5*RATIO
>     63            THETA = ANGLE*3.1416/180.0
>     64            PIFC=(+VF -RF*IFF +MFA*SIN(THETA)*PIIA )/LF
>     65            PIFS=( +VF -RF*IFF +MFAC*SIN(THETA)*PIIA ) / LF
>     66            PIIAC=( VIA +MFA*SPEED*IFF +MFA*SIN(THETA)*PIF -RIA*IIA...
>     67              -IIA*(1.0+FACTOR)*SPEED*MIA*SIN(THETA)*SAT -(MAC*SIN(...
>     68              2.0*THETA)-MIC*SIN(THETA))*PIC*0.5*(1.0+SAT))/(LIA*SAT)
>     69            PIIAS=( VIA +MFAC*SIN(THETA)*PIF +MFAC*SPEED*IFF -RIAC*IIA...
>     70              -(1.0+FACTOR)*SPEED*MIAC*SIN(THETA)*IIA*SAT)/(LIAC*SAT)
>     71            PIF  = RATIO*PIFC  + (1.0-RATIO)*PIFS
>     72            PIIA = RATIO*PIIAC + (1.0-RATIO)*PIIAS
>     73            IF(CUTOFF.LT.0.0) PIIA=0.0
```

Figure B.2

```
>     74            DWDTC=( -TF -IIA*IFF*MFA +IIA*IIA*MIA*SAT*SIN(THETA) ) /J
>     75            DWDTS=( -TF -IIA*IFF*MFAC +IIA*IIA*MIAC*SAT*SIN(THETA) ) /J
>     76            DWDT = RATIO*DWDTC +(1.0-RATIO)*DWDTS
>     77            IFF=INTGRL(IC1,PIF)
>     78            IIA=INTGRL(IC2,PIIA)
>     79            SPEED=INTGRL(IC3,DWDT)
>     80      TERMIN
>     81      NOSORT
>     82            START=1.0
>     83            X1=IIA
>     84            X2=IFF
>     85            X3=SPEED
>     86
>     87      METHOD MILNE
>     88      TIMER PRDEL=0.1,  DELT=0.001,  FINTIM=25.0
>     89      PRINT IIA, SPEED, IFF, ANGLE, PIIA, DWDT, PIF
>     90      TITLE       MACHINE SPEED AND LINE CURRENT VARIATIONS
>     91      TITLE
>     92      END
>     93      STOP
>     94      ENDJOB
#END OF FILE
#
```

Figure B.2

Appendix C Experimental Details

C.1 Machine Details

General 2 pole d.c. generator fitted with interpoles

Dimensions

Field Pole Core	square section	7.62 cm sq.
	length	7.26 cm
Field Pole Shoe	length	10.00 cm.
	breadth	7.60 cm
	thickness	1.27 cm
Air Gap	length	0.03 cm
Armature	outside diameter	12.45 cm
	axial length	7.60 cm
Teeth	width	1.13 cm.
Slot	width	0.84 cm
	depth	2.00 cm
Yoke	periphery	151.20 cm
	breadth	20.00 cm
	thickness	7.50 cm
Interpole Core	length	7.26 cm
	width	7.62 cm
	thickness	2.80 cm
Interpole Shce	length	7.60 cm
	width	2.80 cm
	thickness	1.27 cm

C.2 Electrical Details

Rotor

Number of slots	19	
Conductors per slot	72	
Total conductors	1368	
Commutator bars	57	

Field

Number of coils	2	
Turns per coil	8333	
Wire thickness	26	swg
Resistance	350	ohms
Current rating	0.3	ampere

Interpole

Number of coils	2	
Turns per coil	300	
Wire thickness	14	swg
Resistance	0.5	ohms
Current rating	10	ampere

Thyristors

Type	BTY 99	
Rating	70	ampere

C.3 Magnetic Circuit Details

Part	Area	Length	Flux density (relative to that in air gap)
Yoke	0.0240 m^2	1.512 m	0.31
Pole core	0.0046 m^2	0.145 m	1.56
Air gap	0.0072 m^2	0.006 m	1.00
Teeth	0.0025 m^2	0.040 m	2.83
Armature core	0.0030 m^2	0.076 m	2.42

Relationship between parts of magnetic circuit

Part	Flux Density	MMF	Ampere Turns
Yoke	0.207 Tesla	37 AT/m	56 AT
Pole core	1.04 T	222 AT/m	32 AT
Air gap	0.67 T	533099 AT/m	3198 AT
Teeth	1.89 T	22012 AT/m	880 AT
Armature core	1.62 T	7354 AT/m	559 AT

Ampere Turns for Polar Flux of 0.0049 Weber

C.4 Delay Times of Control Unit

'master' control	minimum delay	0.3 mS
	maximum delay	4.0 mS

'coarse/fine' control

Coarse	Fine	
	min	max
'off'	0.36 mS	
1	0.36 mS	1.08 mS
2	1.44 mS	2.08 mS
3	2.36 mS	3.08 mS
4	3.24 mS	4.00 mS
5	4.10 mS	4.82 mS

References

1.1 'Commutation in rotating machines', I.E.E. Conf. Publ. 11, 1964

1.2 Bates J.J., Sridhar T.V. & Tustin A. 'Possibility of compensation of commutating emfs by voltages in external circuits using separation of alternate tappings', I.E.E. Conf. Publ. 11, 1964, p87.

1.3 Bates J.J. & Sridhar T.V. 'Thyristor assisted sliding contact commutation', Proc. I.E.E., 1966, 113, (2), p339.

1.4 Bates J.J., Stanway J. & Sansum R.F. 'Contact problems in machines using thyristor assisted commutation' Proc. I.E.E., 1970,117, (2), p387-397.

1.5 Andrews H.I. 'Development of an electronically commutated motor with laminated brushes' Proc. I.E.E., 1969, 116, (5), pp763-768.

1.6 Wilson T.G. & Trickey P.H. 'D.C. machines with solid state commutation' A.I.E.E. Conf. Paper, CP62-1372, 1962.

3.1 Jones C.V. 'An analysis of commutation for the unified machine theory' Proc. I.E.E., 1958, 105C, (4), p476.

3.2 Prescott J.C. & El-Karashi A.K. 'A method of measuring self inductances applicable to large electrical machines' Proc. I.E.E., 1959, 106A, (4), p169.

6.1 Moullin E.B. 'Electromagnetic Principles of the Dynamo' Oxford, 1955.

8.1 Moore J.R. 'Discussion on "Contact problems in machines using thyristor assisted commutation"' Proc. I.E.E., 1970, 117, (12), pp2266-2267.

8.2 Bates J.J., Stanway J. & Sansum R.F. 'Contact problems in machines using thyristor assisted commutation' Proc. I.E.E., 1970, 117, (2), pp387-397.

8.3 Bates J.J. 'Correspondence on "Diode assisted commutation"' Proc. I.E.E., 1970, 117, (5), pp1017-1019.

8.4 Bates J.J. 'Thyristor assisted commutation in electrical machines' Proc. I.E.E., 1968, 115, (6), pp791-801.

8.5 General Electric 'S.C.R. Manual' New York, U.S.A., 1964, Chapter 4.

8.6 General Electric 'Transistor Manual' New York, U.S.A., 1964, Chapter 13.

9.1 Jones C.V. 'The Unified Theory of Electrical Machines' Butterworth, London, 1967, pp349-352.

A.1 Jones C.V. 'The Unified Theory of Electrical Machines' Butterworth, London, 1967, chapter 21.

A.2 Barton T.H. & Dunfield J.C. 'Inductances of a practical slip ring primitive' Trans. A.I.E.E., PAS85, 1966,(2), pp140-151.

B.1 IBM 'Continuous Systems Modelling Program' 4th edition, 1969.

B.2 McCracken D.D. 'A guide to Fortran IV programming' Wiley, New York, 1965.

Acknowledgements

The author is indebted to the following -

Dr. C. Preece for his continued encouragement and discussion of the work.

The acedemic staff of the Department of Engineering Science for their interest in the work.

The technical staff of the Department of Engineering Science for their assistance in the preparation of the experimental equipment.

The University of Durham for the use of library, computer and laboratory facilities.

The County Borough of Hartlepool.